



INSTITUTO
SUPERIOR
TÉCNICO

Pedro Bicudo
IST, Lisboa

*work partly done with Orlando Oliveira, Marco
Cardoso, Nuno Cardoso and Gonçalo Marques*



INSTITUTO
SUPERIOR
TÉCNICO

Pedro Bicudo
IST, Lisboa

- o Motivation
- o Confinement of exotics in Lattice QCD
- o The hybrid flux tube in Lattice QCD
- o Scalar confinement and Schwinger Dyson Eqs

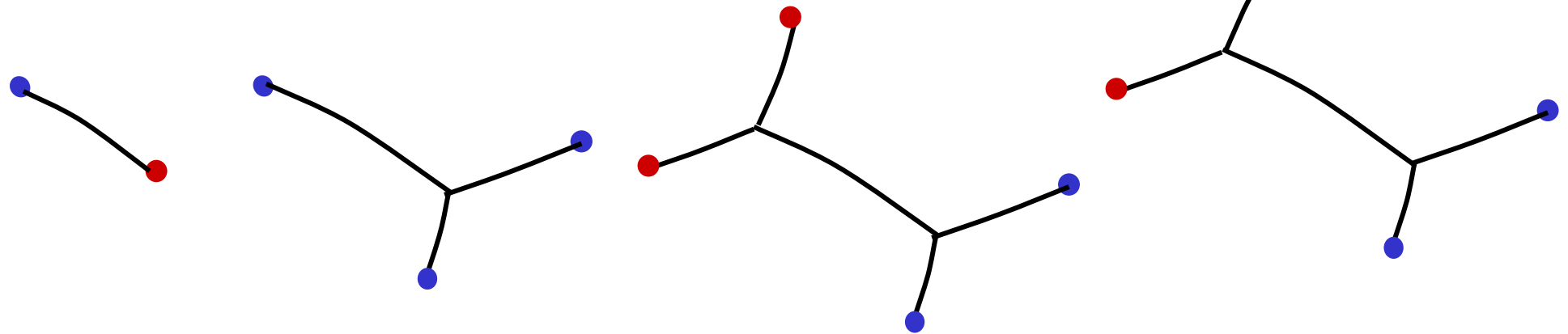
Motivation

(to study static potentials
for hybrids and glueballs)

Motivation

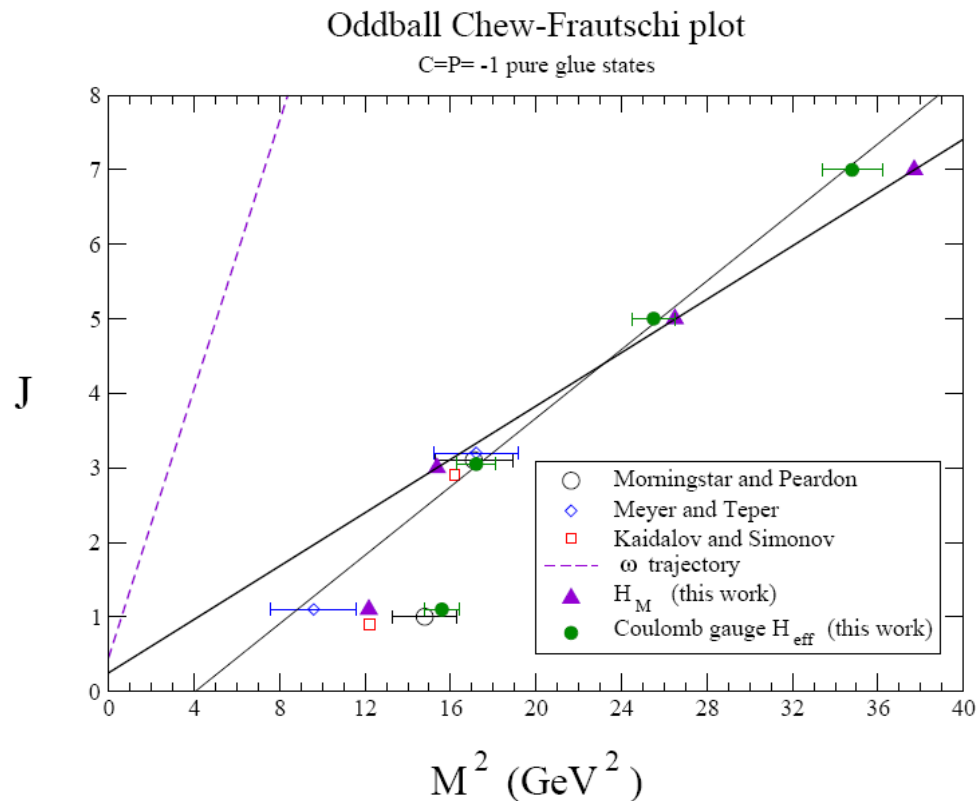
Previously, Static potentials have been studied in Lattice QCD to

- be applied in constituent quark-gluon models
- understand confinement
- *mostly for mesons, some for 2-gluon glueballs, baryons, for tetraquarks, pentaquarks, see many Suganuma papers including F. Okiharu, H. Suganuma, T. T. Takahashi, P. R. D 72, 014505 (2005)*
- **but not** for GQQ hybrids and GGG glueballs



Motivation

The **experiments** BESIII at IHEP in Beijing, LHC at CERN, GLUEX at JLab and PANDA at GSI in Darmstadt, will scan the mass range of GQQ hybrids and GGG glueballs. The odderon might also depend on GGG glueballs...



F. Llanes-Estrada, P. Bicudo
and S. Cotanch,
Phys.Rev.Lett.96, 081601(2006).

Motivation

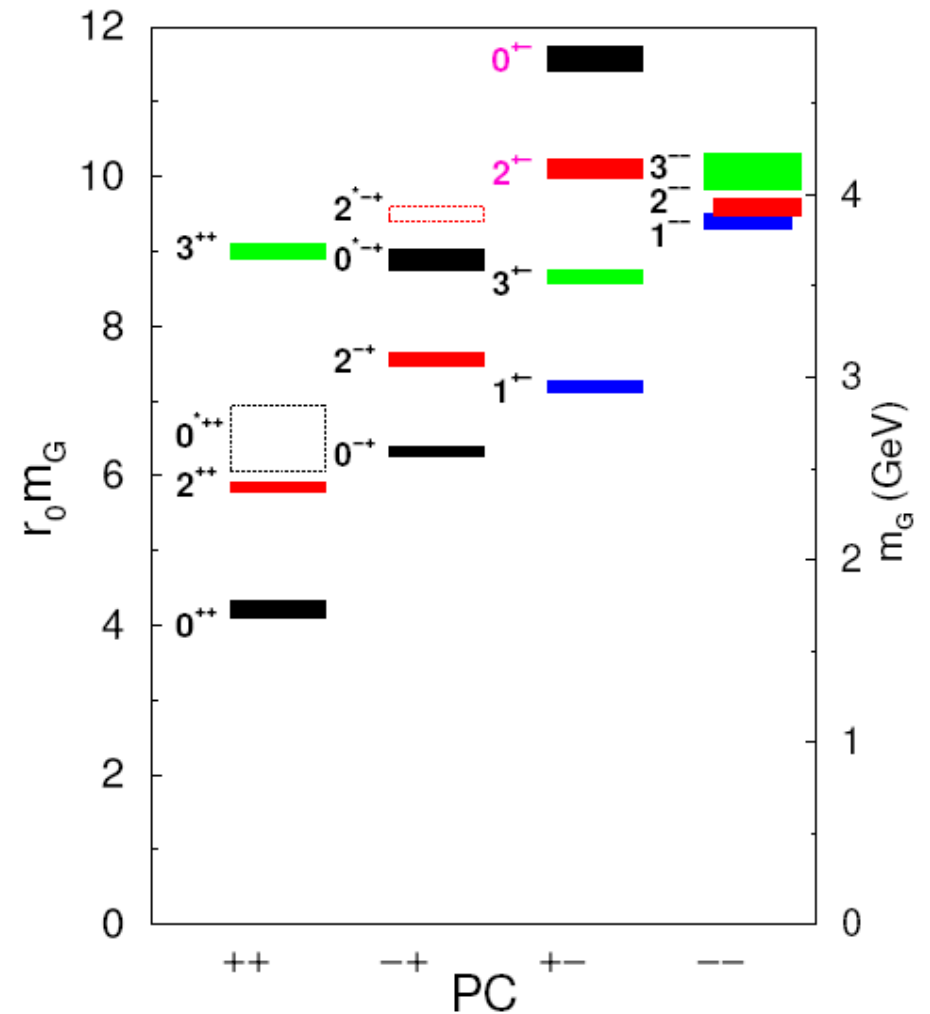
The **computations** of GQQ hybrids and GGG glueballs are performed,

- in Lattice QCD,

C. Morningstar and M. Peardon,
 Phys. Rev. D **60**, 034509 (1999)

- or with constituent quark-gluon models,

V. Mathieu, C. Semay, B. Silvestre-Brac
 Phys.Rev. D**74**, 054002 (2006)

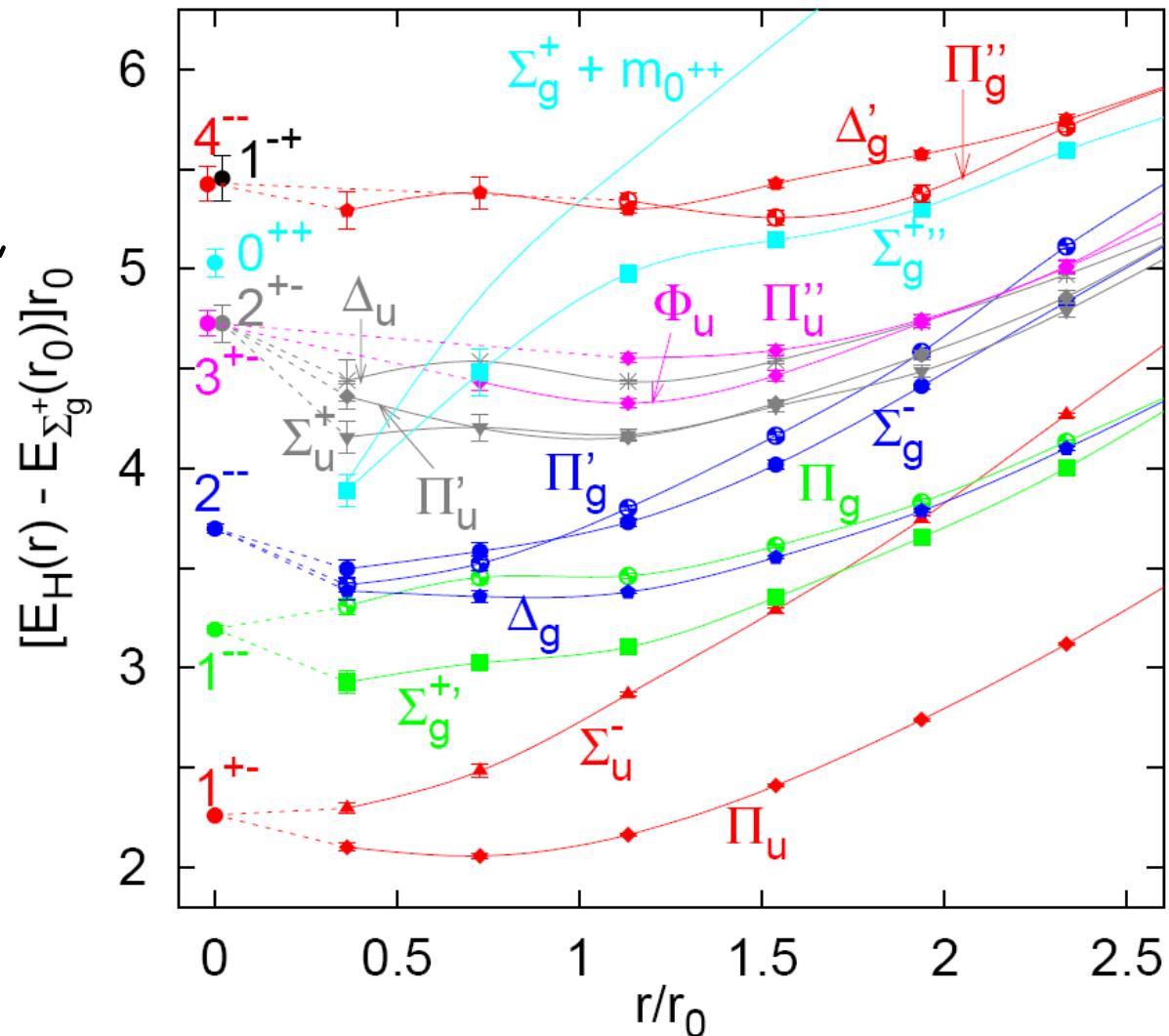


mass spectrum of glueballs in the pure SU(3)

Motivation

In what concerns excitations of the static quark potential, they are studied in lattice QCD

K.J. Juge, J. Kuti,
C.J. Morningstar
Nucl.Phys.Proc.Suppl.
63, 326 (1998)



hybrid potentials (Juge et al., 2003) at a lattice spacing $a_\sigma \approx 0.2$ fm

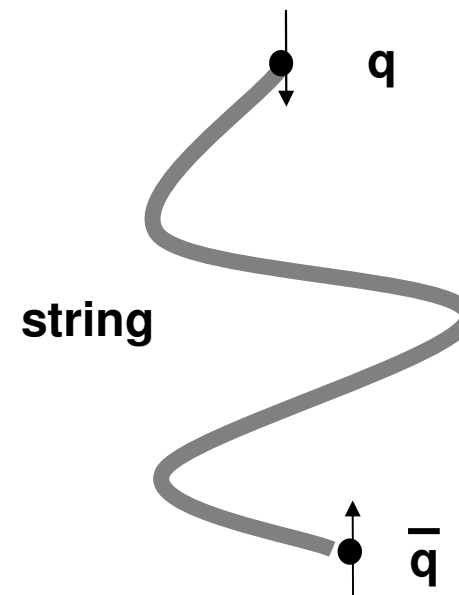
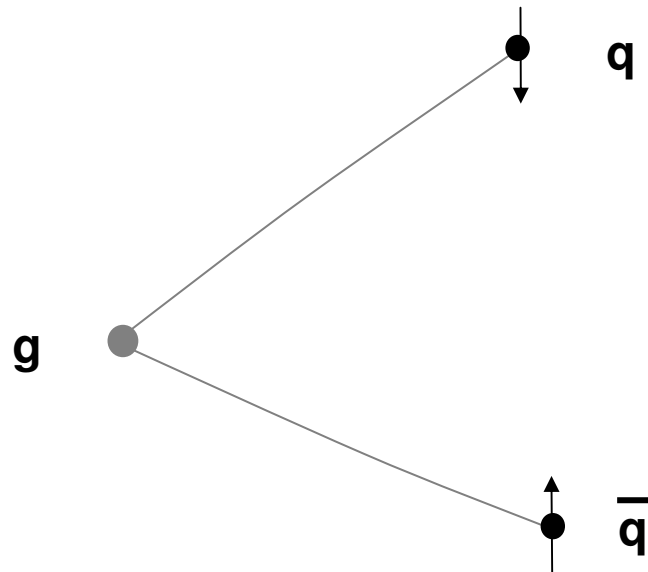
Motivation

The hybrid excitations may either be understood with string fluctuations

M. Lüscher, Nucl. Phys. B190, 317 (1981)

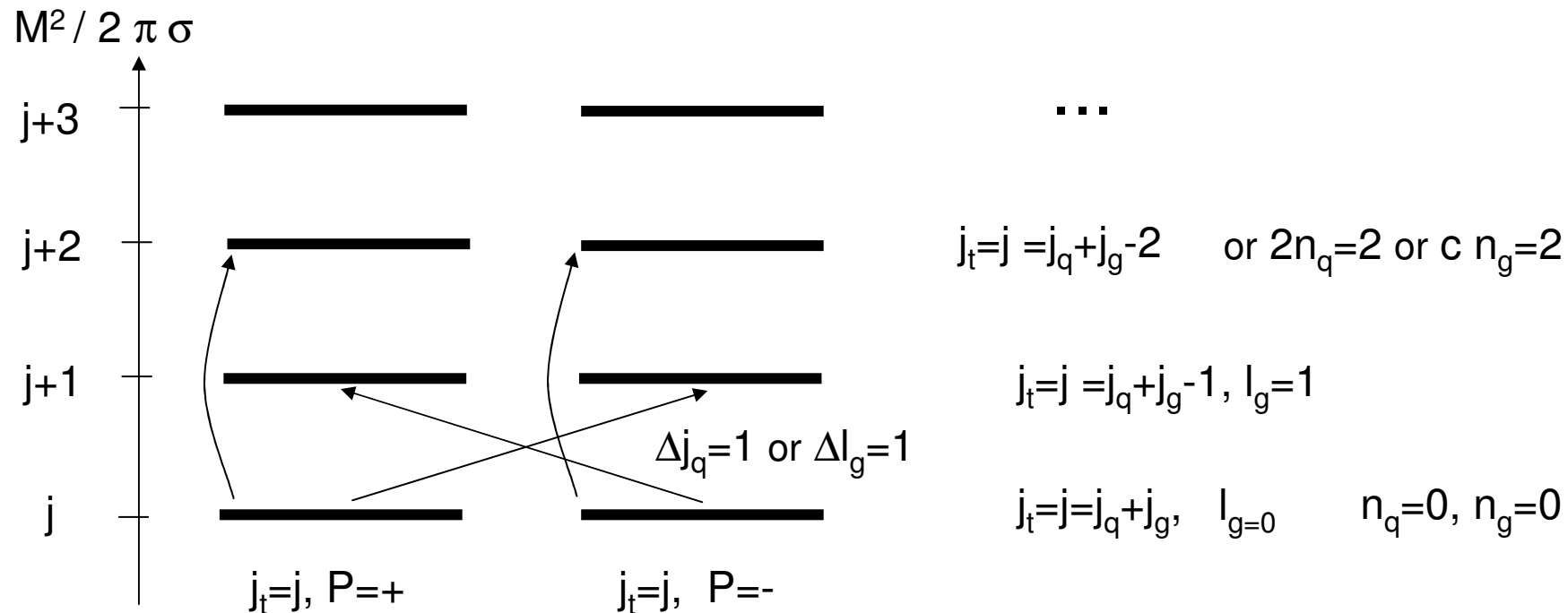
or with an extra constituent gluon

F. Buisseret, V. Mathieu Eur.Phys.J.A29, 343 (2006)



Motivation

and possibly the excited meson spectrum Large Degeneracy Problem can only be understood including **Gluon Excitations and Quark Chiral Symmetry in the Meson Spectrum**, P. Bicudo, arXiv:0904.0030, P. Bicudo, M. Cardoso, T. Van Cauteren, F. Llanes-Estrada, P. R. L. **103**, 092003 (2009)



Motivation

and finally we would like to understand confinement, in analogy with type II superconductors M. Cardoso, P. Bicudo, P. Sacramento A. Phys. 323, 337 (2008)

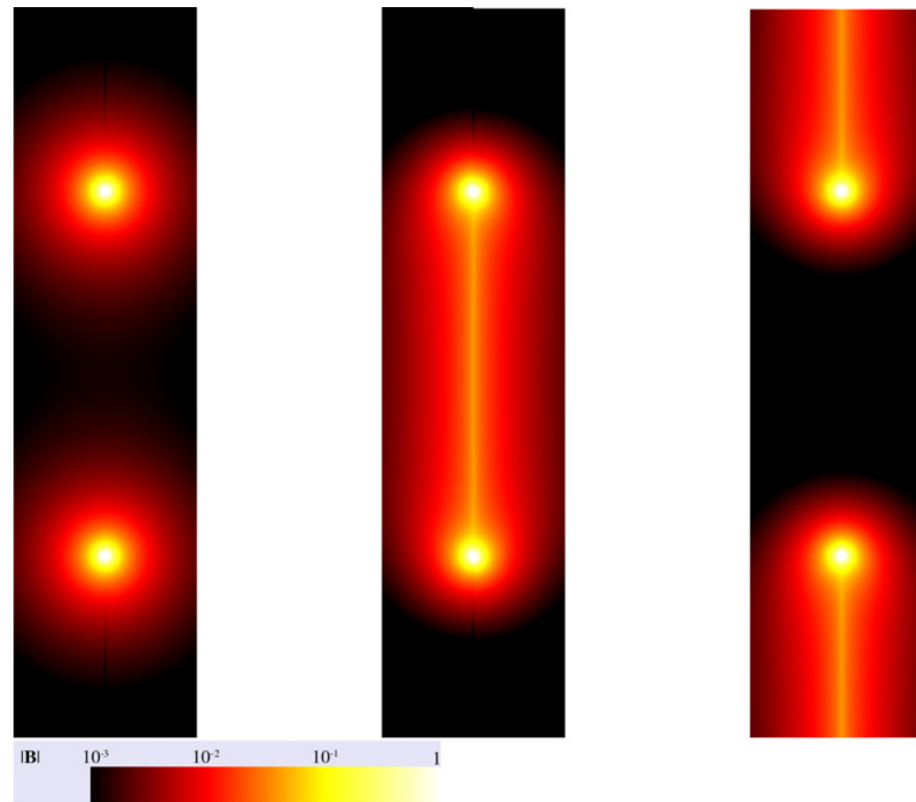
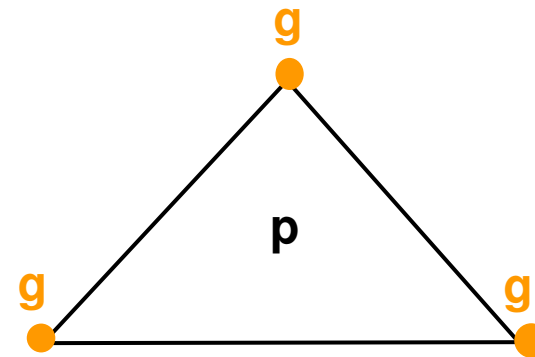
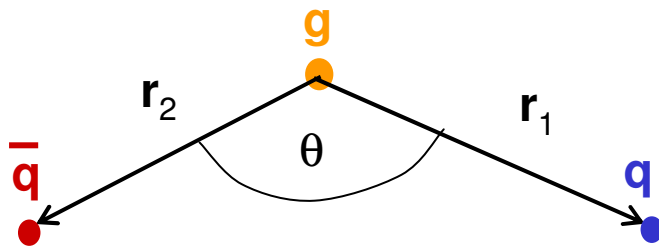


Fig. 3. Density plot for the total magnetic field $|\mathbf{B} = \mathbf{B}^{\text{ext}} + \mathbf{B}^{\text{sup}}|$ when the monopole and the antimonopole are separated by a distance $d = 2z_0 = 480$. The panels correspond from left to right to: no superconductor, superconductor with topological charge $n = 1$ and superconductor with topological charge $n = 0$, respectively.

Confinement in Static Exotic Potentials for QGQ and GGG

Confinement in Static Exotic Potentials for GQQ and GGG

Utilizing Wilson Loops, we study the static potentials of $Q\bar{Q}Q$ and GGG



P. Bicudo, M. Cardoso and O. Oliveira, Phys. Rev. D **77**, 091504 (2008)

M. Cardoso, P. Bicudo Phys. Rev. D **78**:074508 (2008)

Confinement in Static Exotic Potentials for GQQ and GGG

We utilize **Wilson loops** to measure the **static** potentials in Lattice QCD. The positions of the quarks are connected by gauge paths composed of fundamental links, to maintain gauge invariance, while the positions of gluons are connected by adjoint paths,

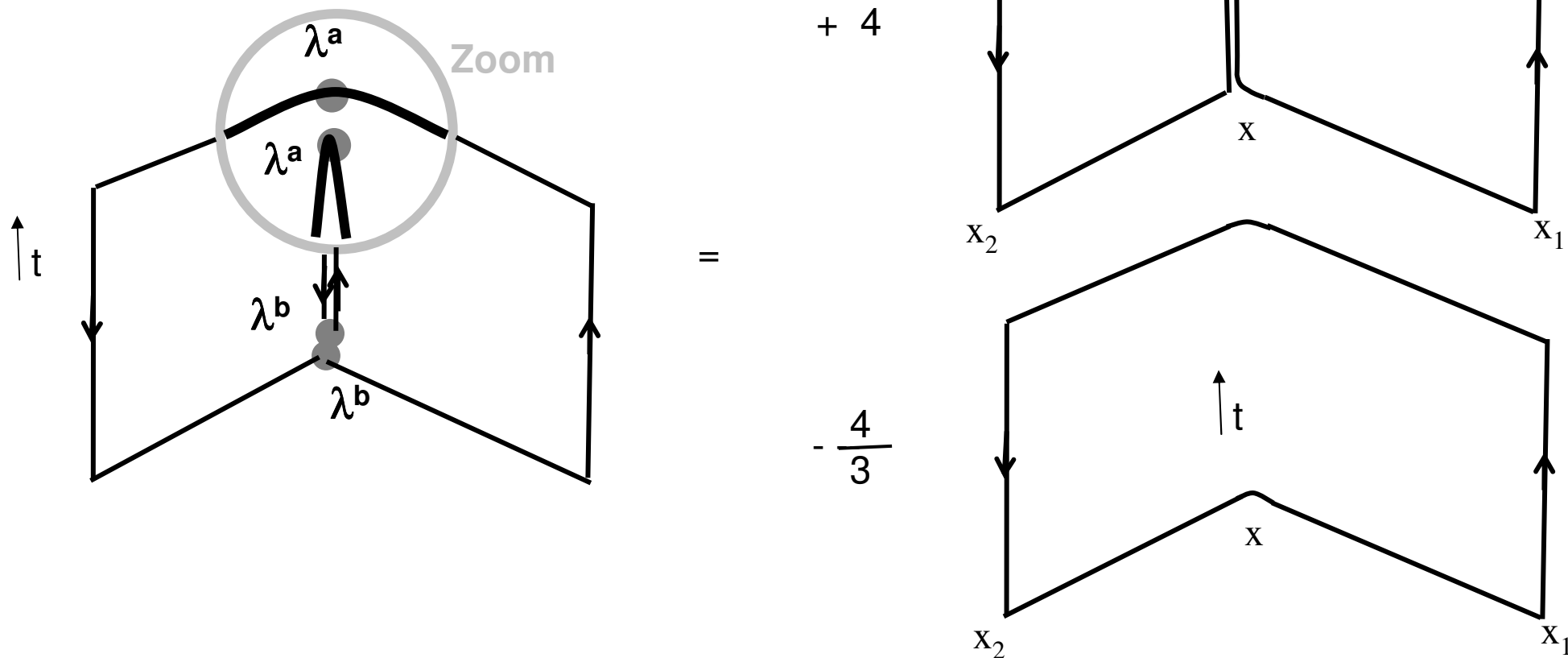
$$\tilde{U}^{ab} = \lambda^a \begin{array}{c} \leftarrow U^+ \\ \rightleftarrows \\ \rightarrow U \end{array} \lambda^b$$

The Fierz relation can be used to re-write the adjoint paths with fundamental paths.

$$\Sigma_a \begin{array}{c} \nearrow \\ \lambda^a \\ \bullet \\ \lambda^a \\ \searrow \end{array} = 2 \begin{array}{c} \nearrow \\ \curvearrowright \\ \searrow \end{array} - (2/3) \begin{array}{c} \searrow \\ \curvearrowleft \\ \nearrow \end{array}$$

Confinement in Static Exotic Potentials for GQQ and GGG

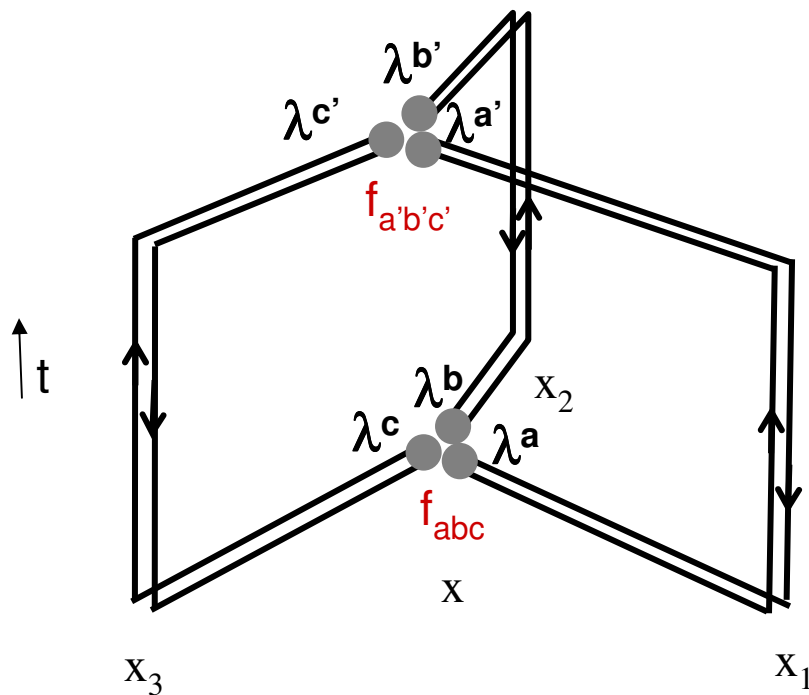
For instance, for the **hybrid GQQ** Wilson loop we get,



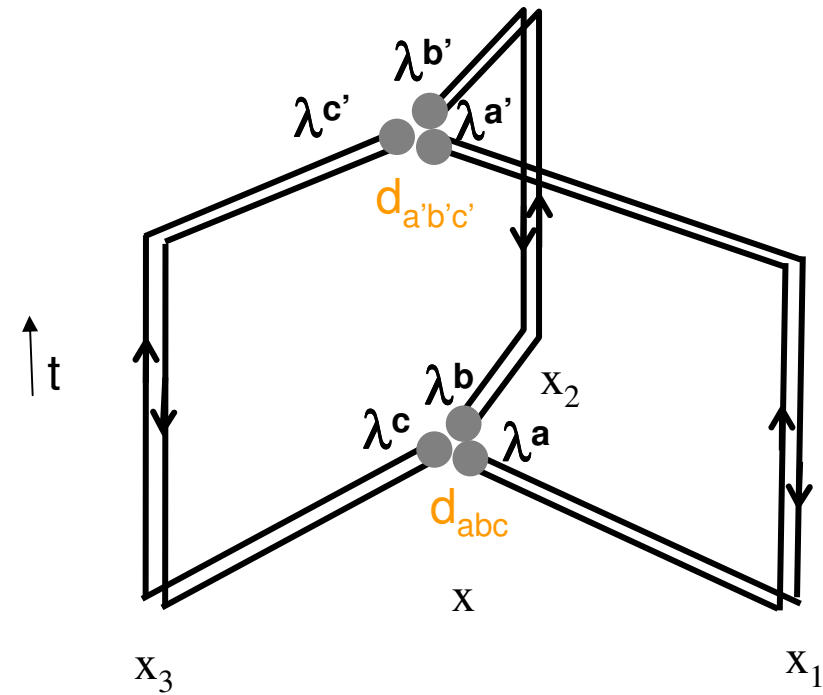
Confinement in Static Exotic Potentials for GQQ and $G\bar{Q}\bar{Q}$

Whereas for the glueball $G\bar{G}\bar{G}$, we have two possible wavefunctions, **antisymmetric** or **symmetric**, with Wilson loops,

antisym.

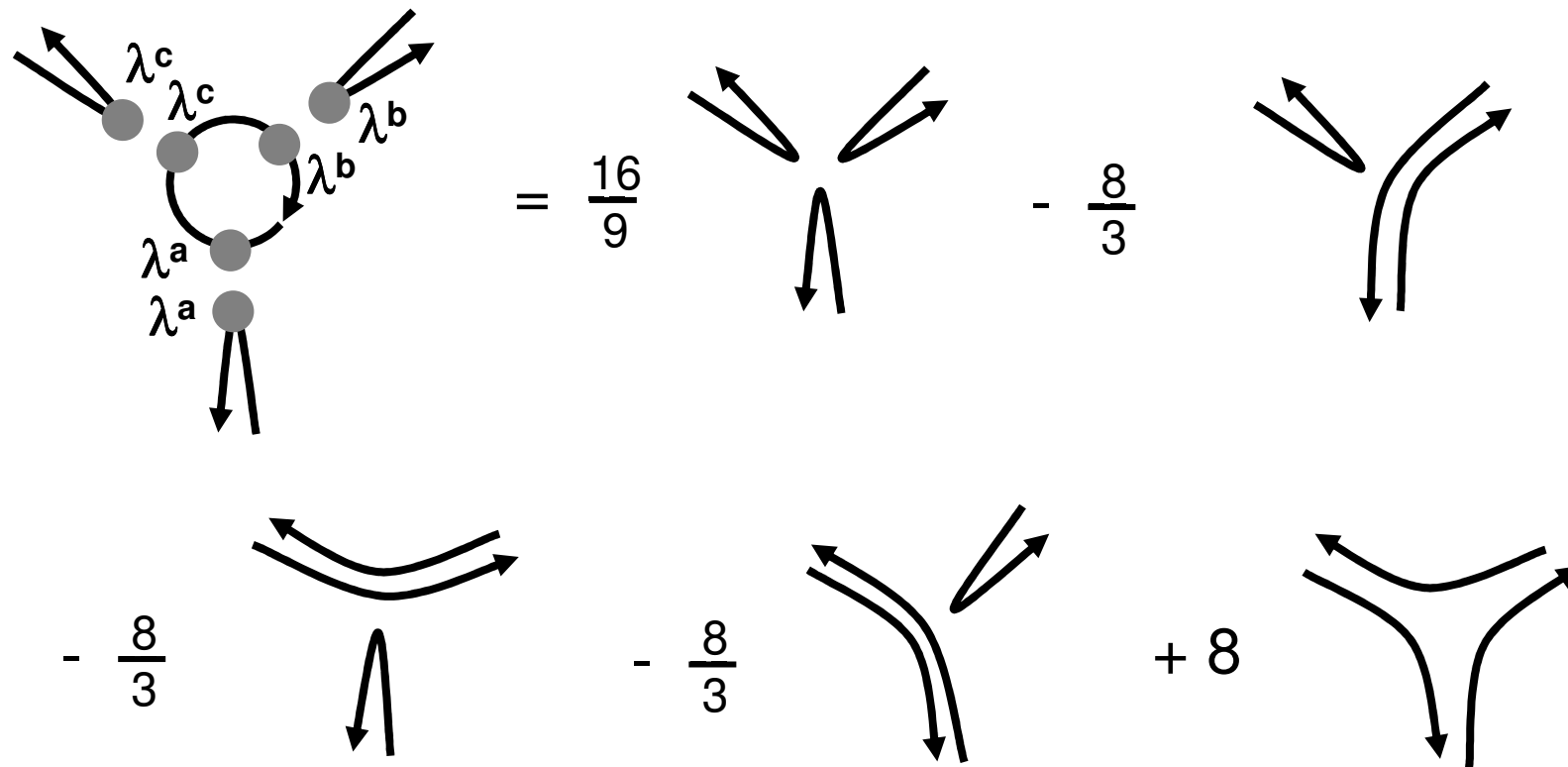


symmetric



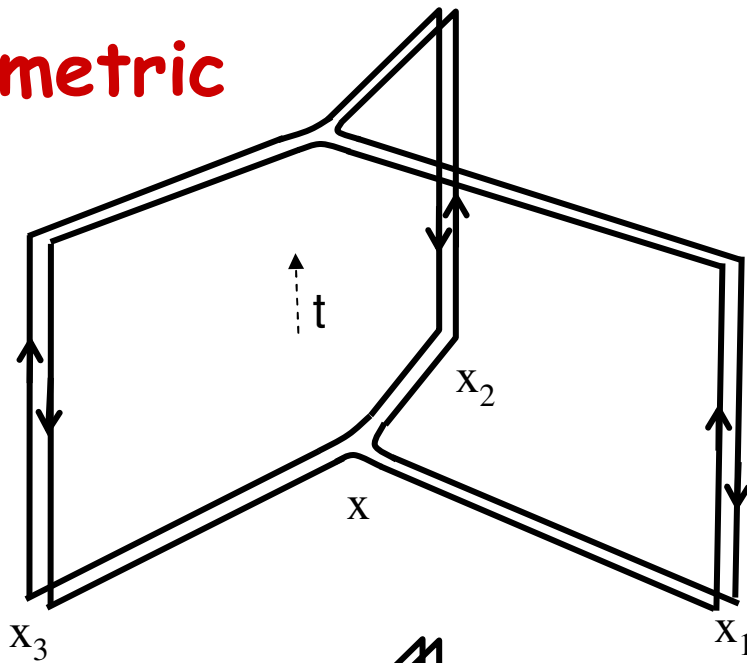
Confinement in Static Exotic Potentials for GQQ and GGG

The two GGG Wilson loops can be rewritten with the Fierz relation,

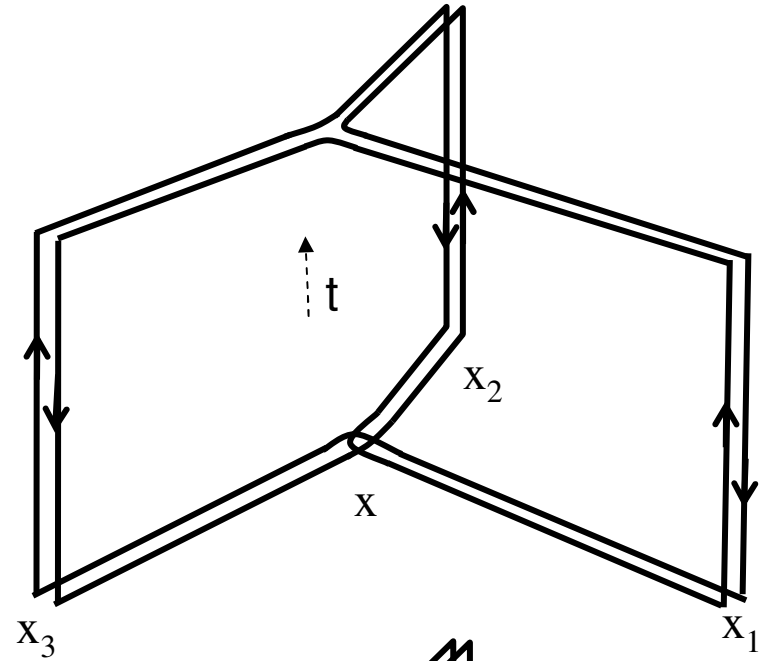


antisymmetric

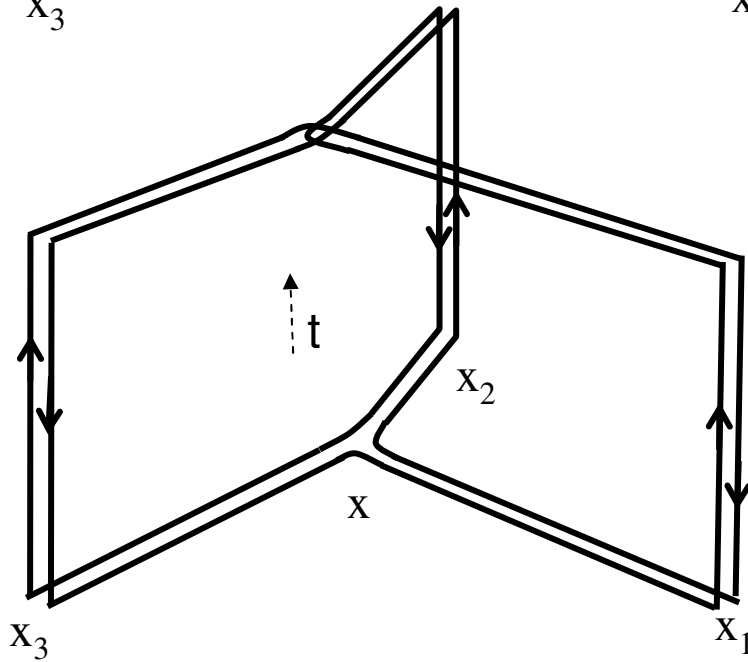
$$W_{3g}^A = 4$$



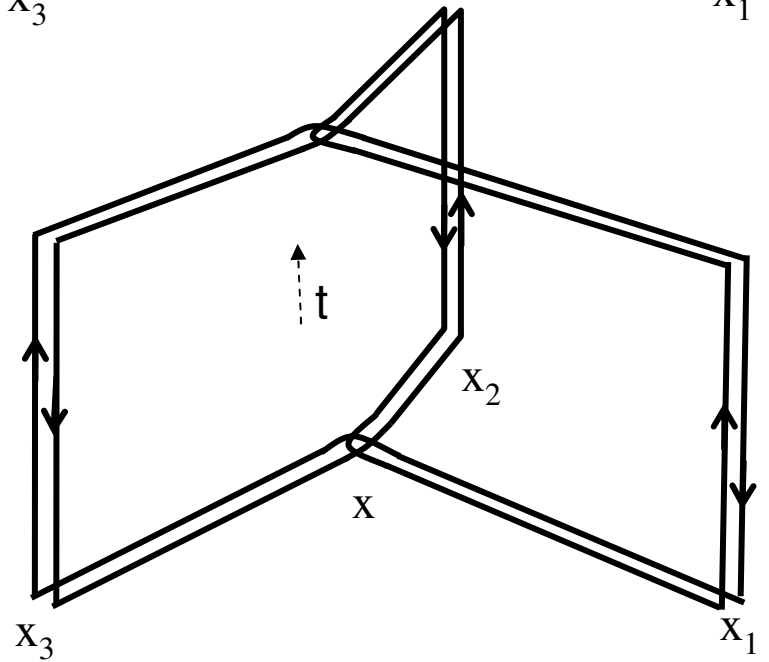
$$- 4$$



$$- 4$$

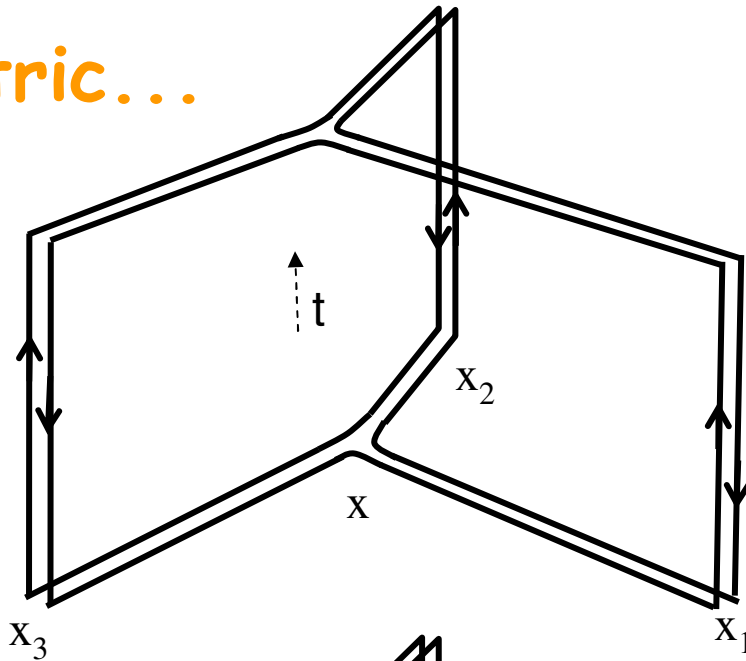


$$+ 4$$

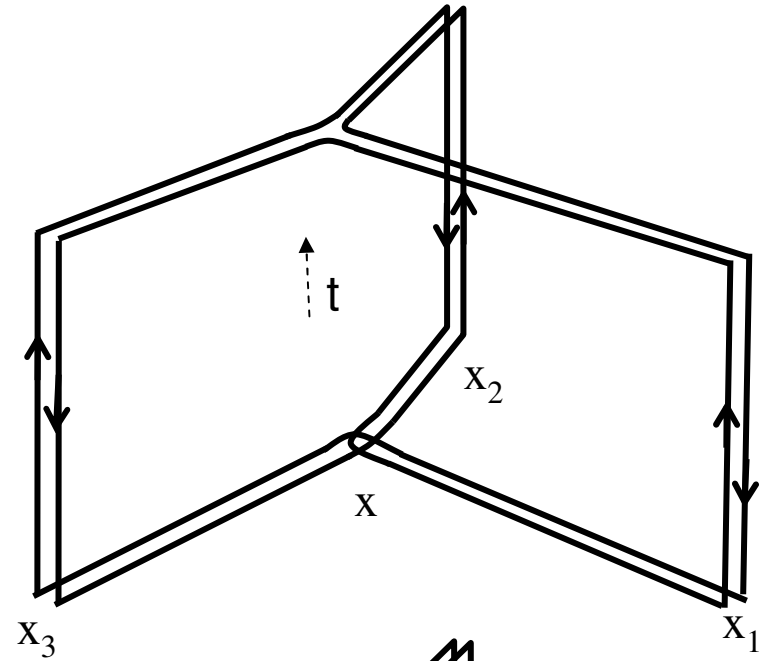


symmetric...

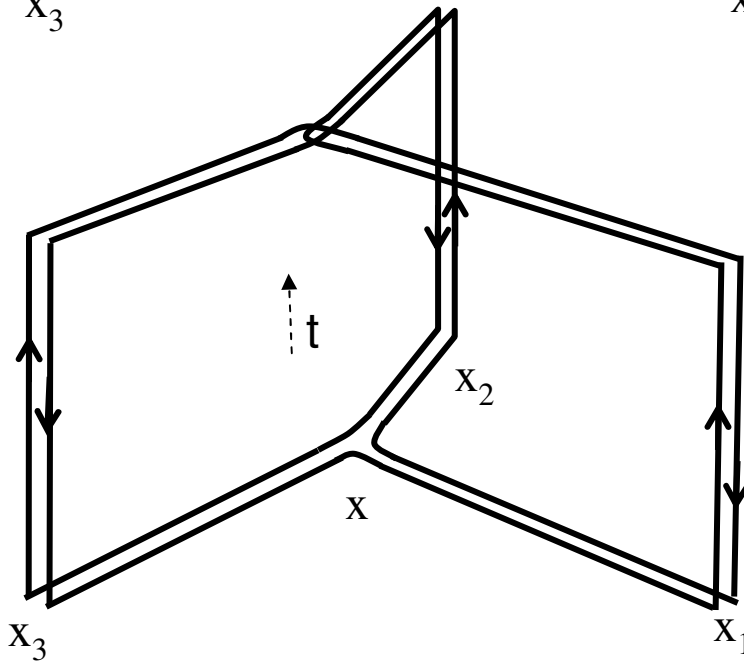
$$W_{3g}^S = 4$$



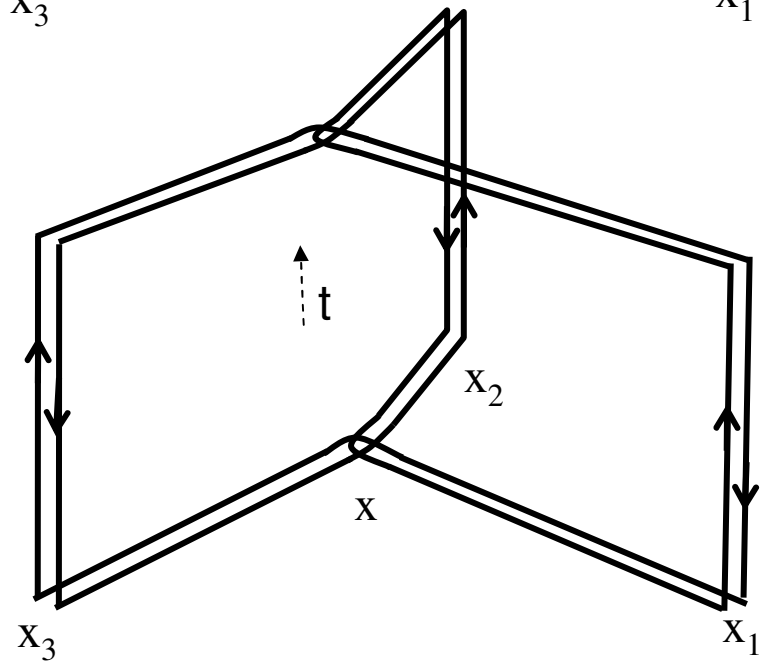
+ 4



+ 4

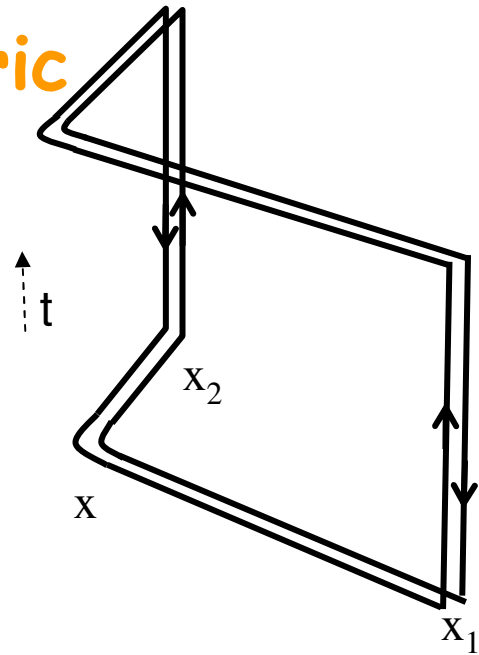


+ 4

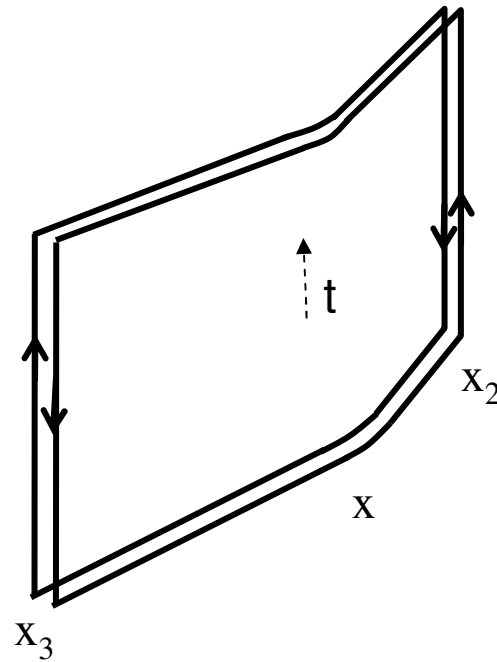


...symmetric

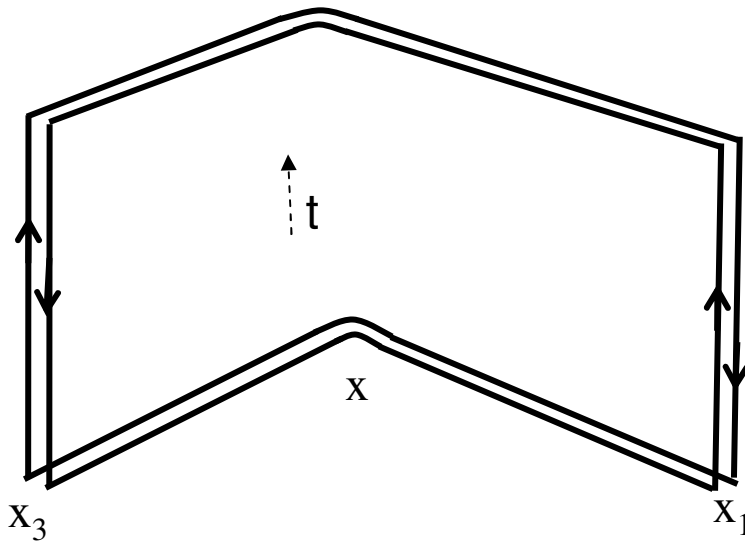
$$-\frac{16}{3}$$



$$-\frac{16}{3}$$



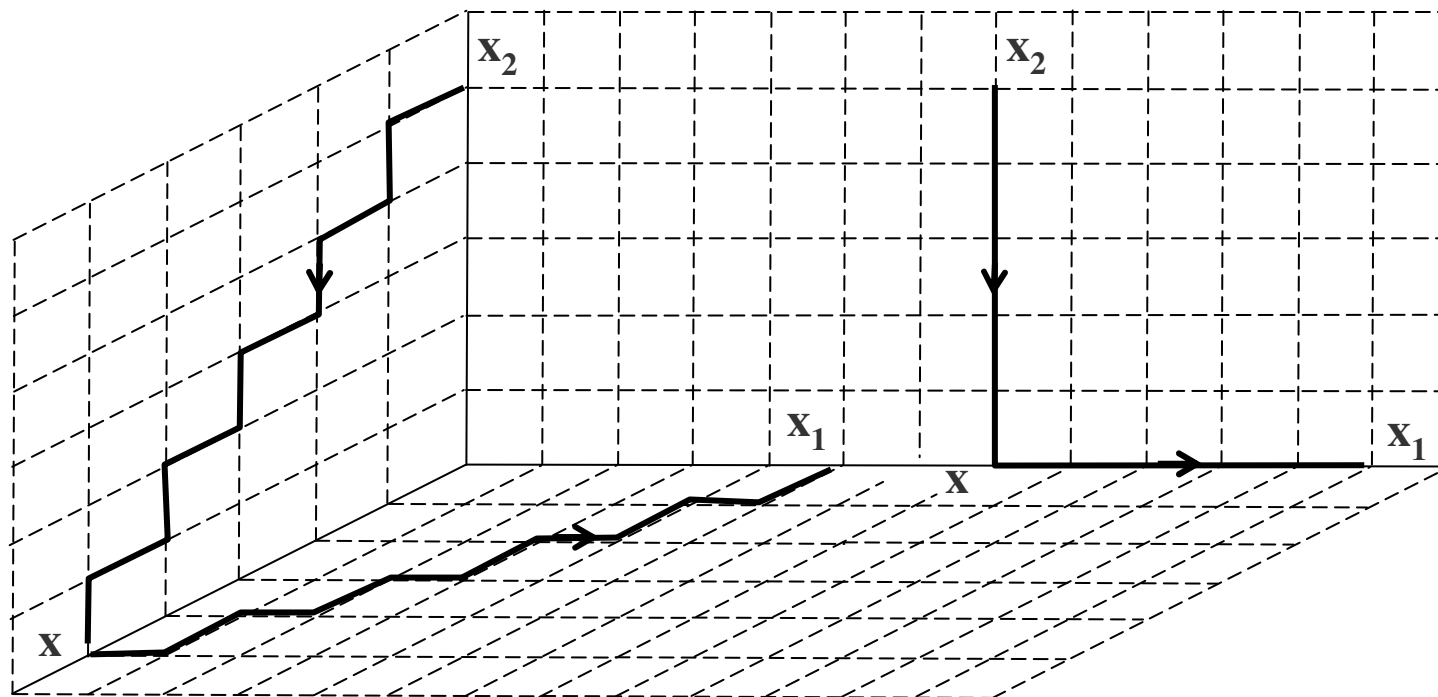
$$-\frac{16}{3}$$



$$+\frac{32}{3}$$

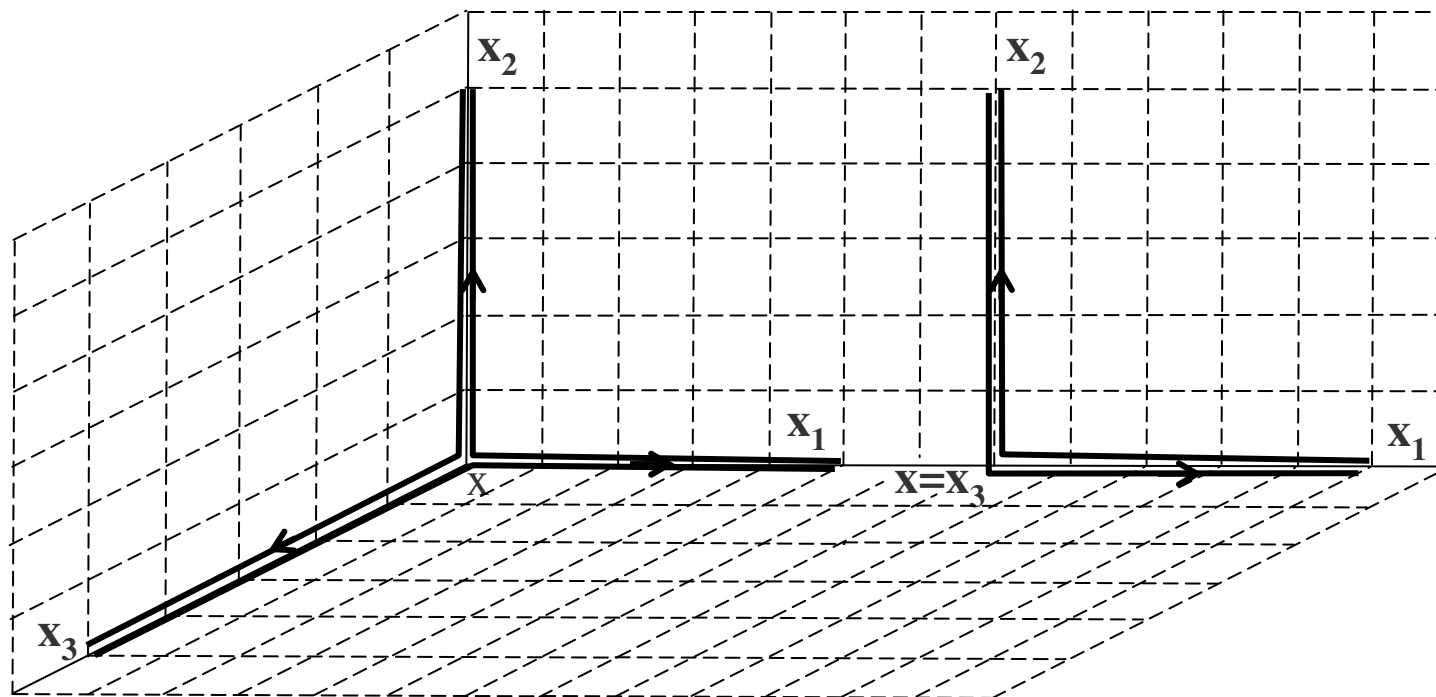
Confinement in Static Exotic Potentials for GQQ and GGG

The **spatial paths** we use for the GQQ include of-axis geometries,



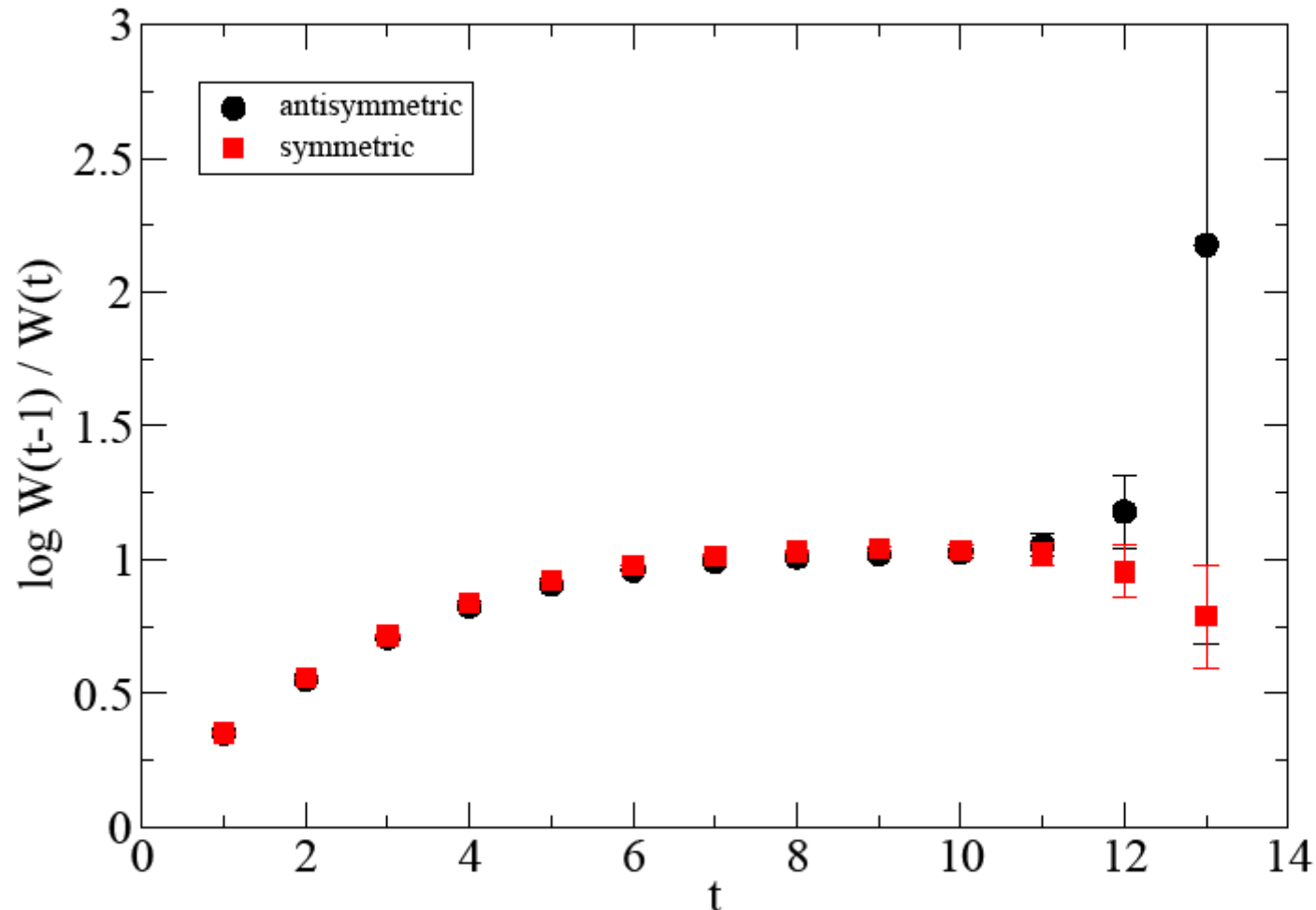
Confinement in Static Exotic Potentials for GQQ and GGG

In what concerns the spatial geometry of the GQG we first use the simplest spatial paths



Confinement in Static Exotic Potentials for GQQ and $G\bar{Q}Q$

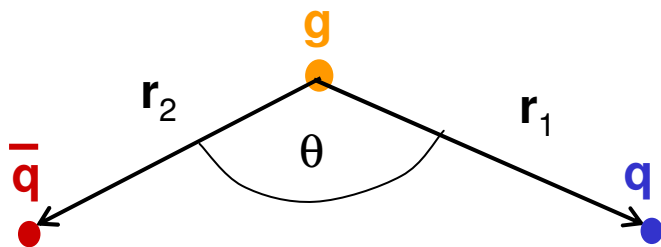
Then the **static potential** V is obtained fitting the exponential euclidian time t decay of the Wilson loop W , $W = cst. \text{Exp} (- V t)$



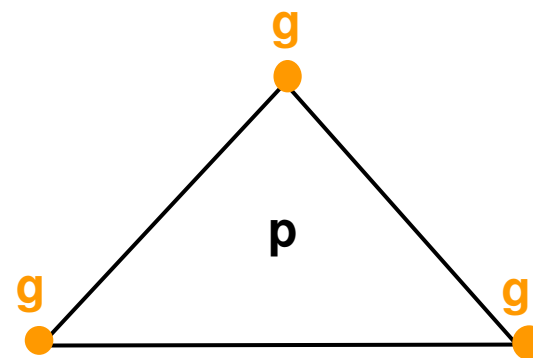
Confinement in Static Exotic Potentials for GQQ and GGG

We compute the static potentials as a function of the **variables**,

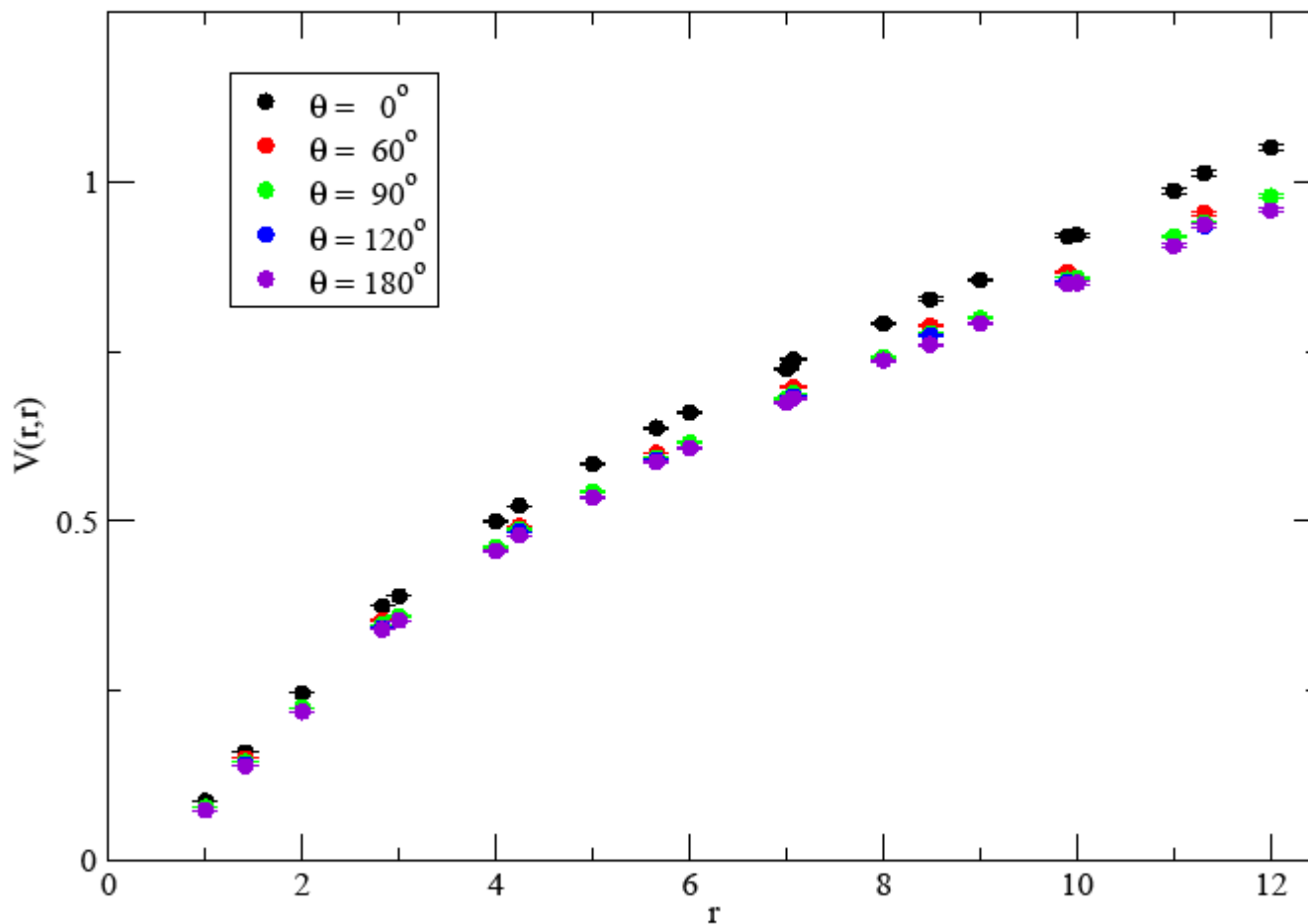
for the hybrid GQQ
distance r_1 , distance r_2 and angle θ



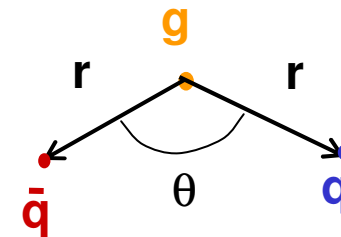
for the glueball GGG
perimeter p



Confinement in Static Exotic Potentials for GQQ and GGG

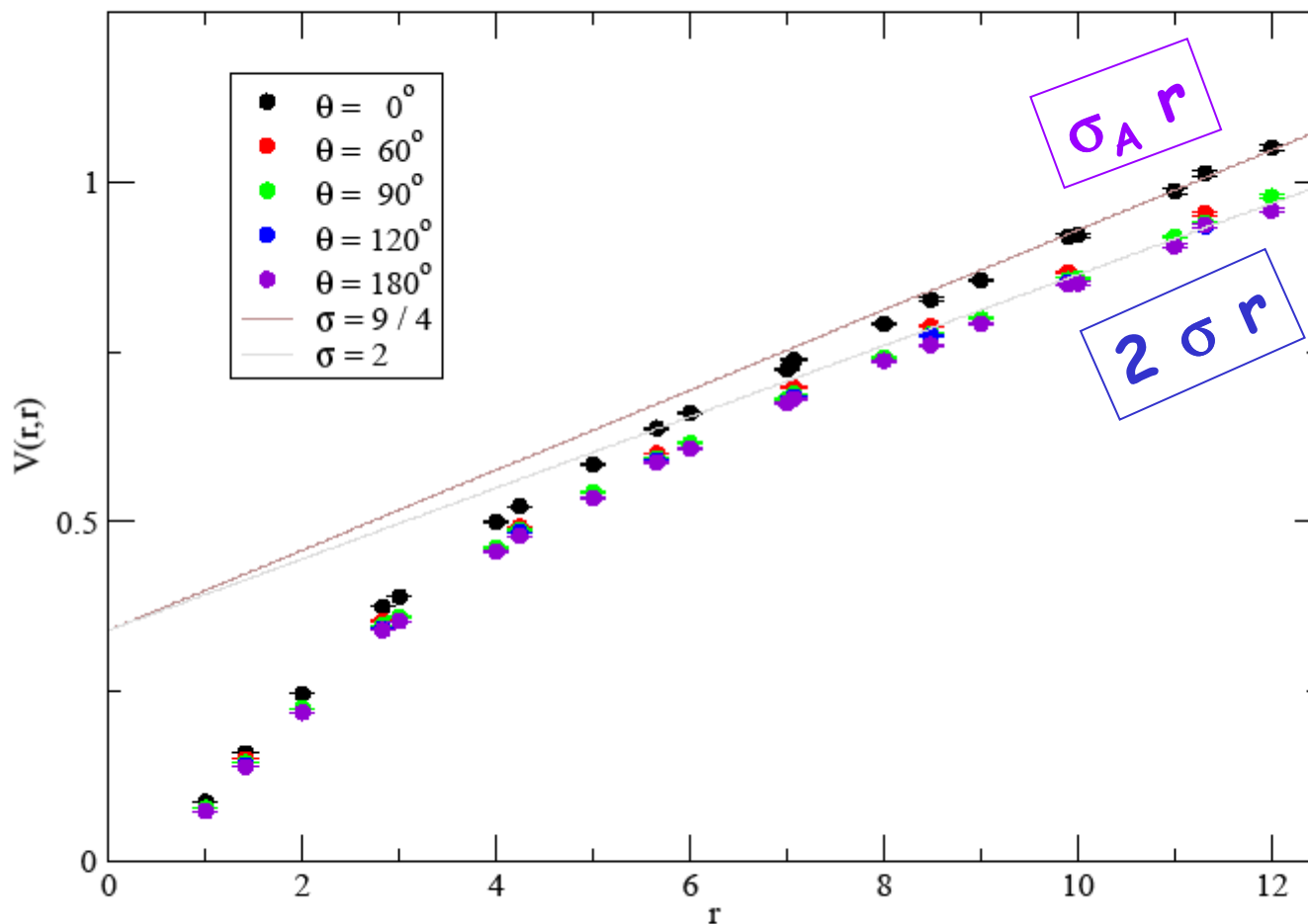


variables:

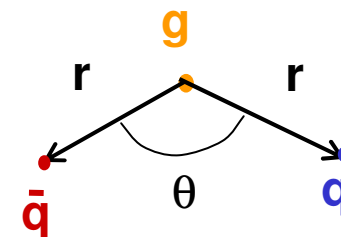


units: $a = 0.072$ fm ($24^3 \times 48$, $\beta = 6.2$, 141 config.)

Confinement in Static Exotic Potentials for GQQ and GGG

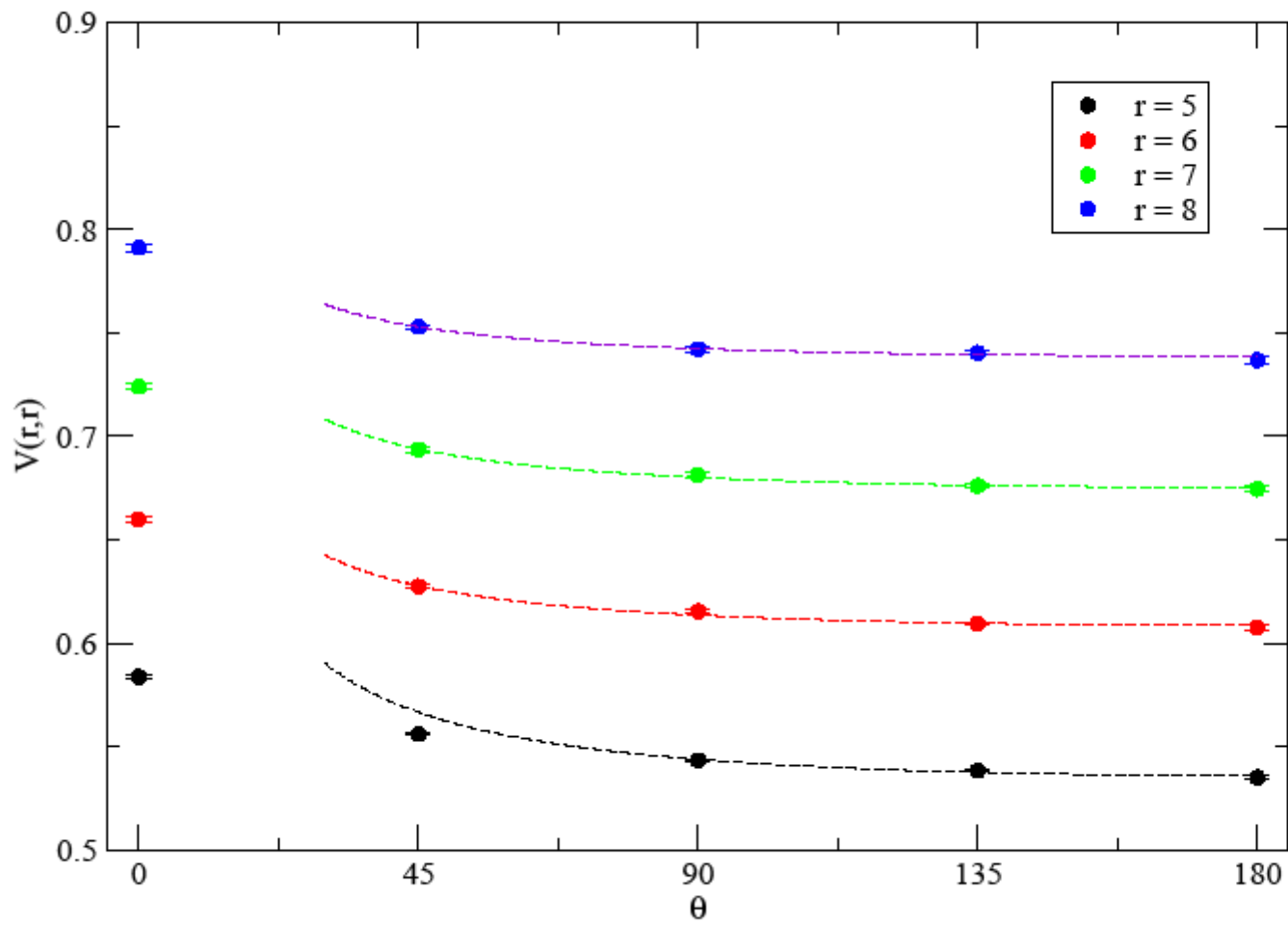


variables:

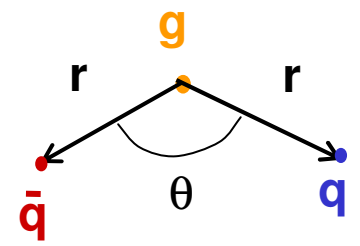


units: $a = 0.072$ fm ($24^3 \times 48$, $\beta = 6.2$, 141 config.)

Confinement in Static Exotic Potentials for GQQ and GGG

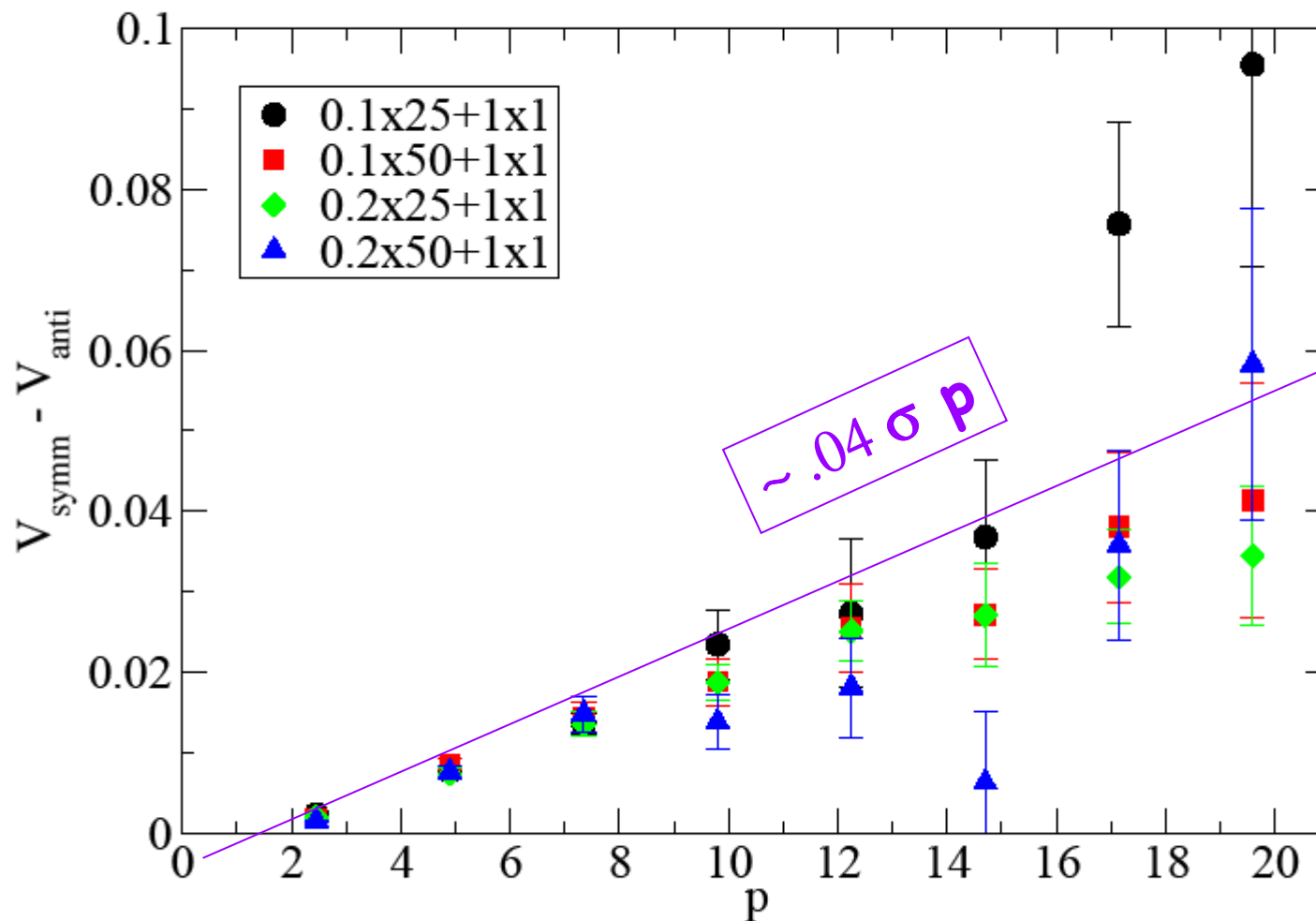


variables:

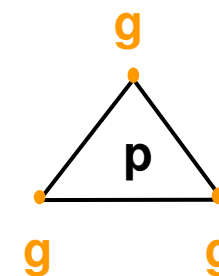


units: $a = 0.072$ fm ($24^3 \times 48, \beta = 6.2, 141$ config.)

Confinement in Static Exotic Potentials for GQQ and $G\bar{G}\bar{G}$

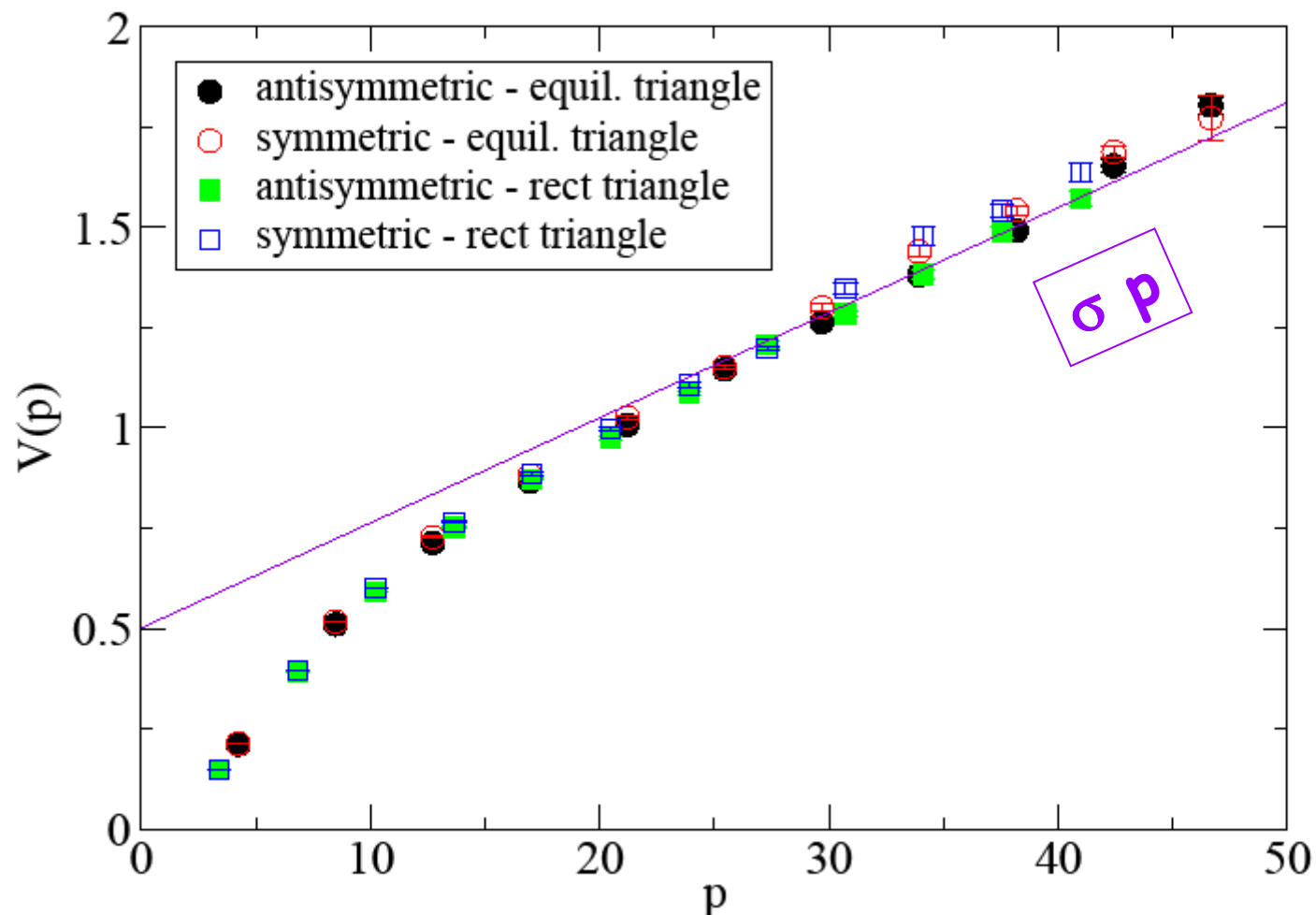


variables:



units: $a = 0.072 \text{ fm}$ ($24^3 \times 48, \beta = 6.2, 141 \text{ config.}$)

Confinement in Static Exotic Potentials for GQQ and GGG



units: $a = 0.072$ fm ($24^3 \times 48$, $\beta = 6.2$, 141 config.)

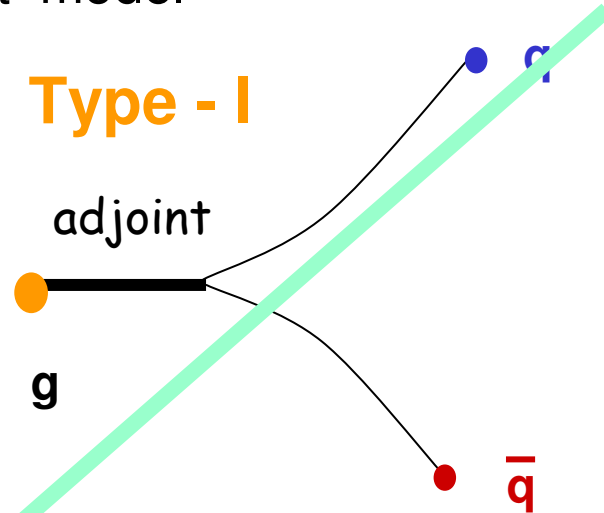
Comparing different **paradigms of confinement**, the **fundamental string dominance** is the best model

Casimir

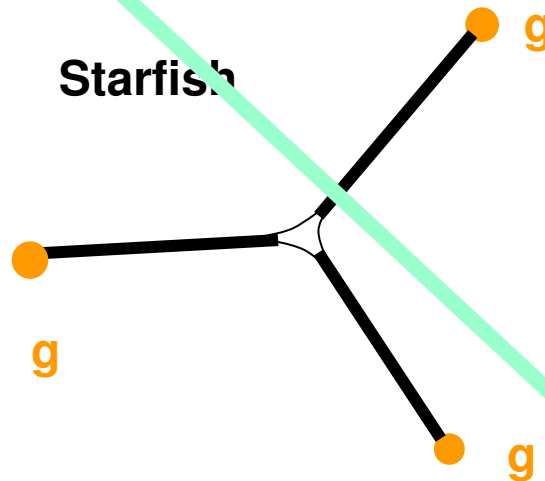
The potentials are a sum of 2- body potentials,

$$V_{ij} \propto \lambda_i \cdot \lambda_j$$

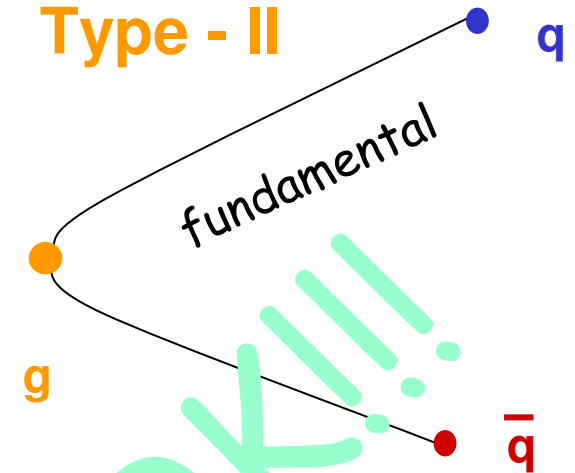
Type - I



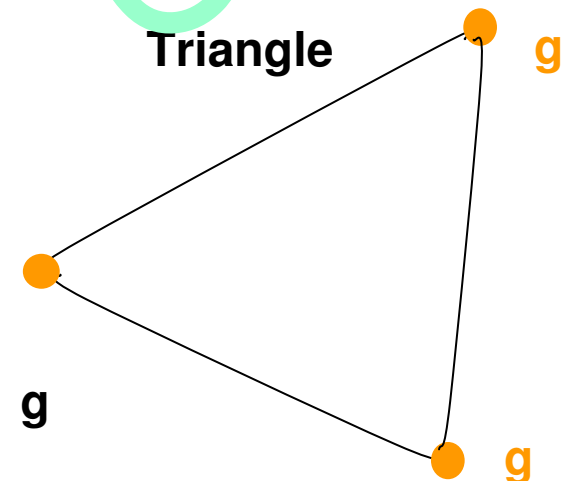
Starfish



Type - II



Triangle

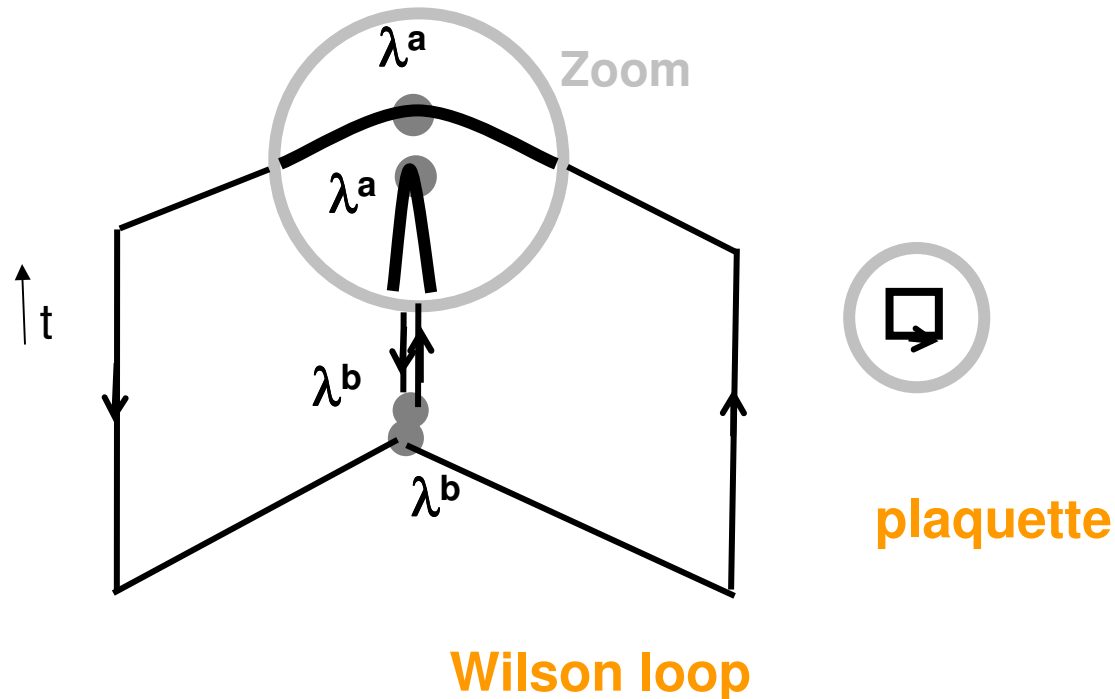


OK!!!

The hybrid $Q\bar{G}Q$ flux tube in lattice QCD

The hybrid $QG\bar{Q}$ flux tube in lattice QCD

For a confirmation of the **fundamental string picture** of confinement in exotic hadrons, we proceed with the study of the flux tubes in the static hybrid system $QG\bar{Q}$.



The hybrid QGQ flux tube in lattice QCD

This is performed simply computing the E_i and B_i chromoelectric and chromomagnetic fields with the **plaquette**, who discretizes the $F^{\mu\nu}$

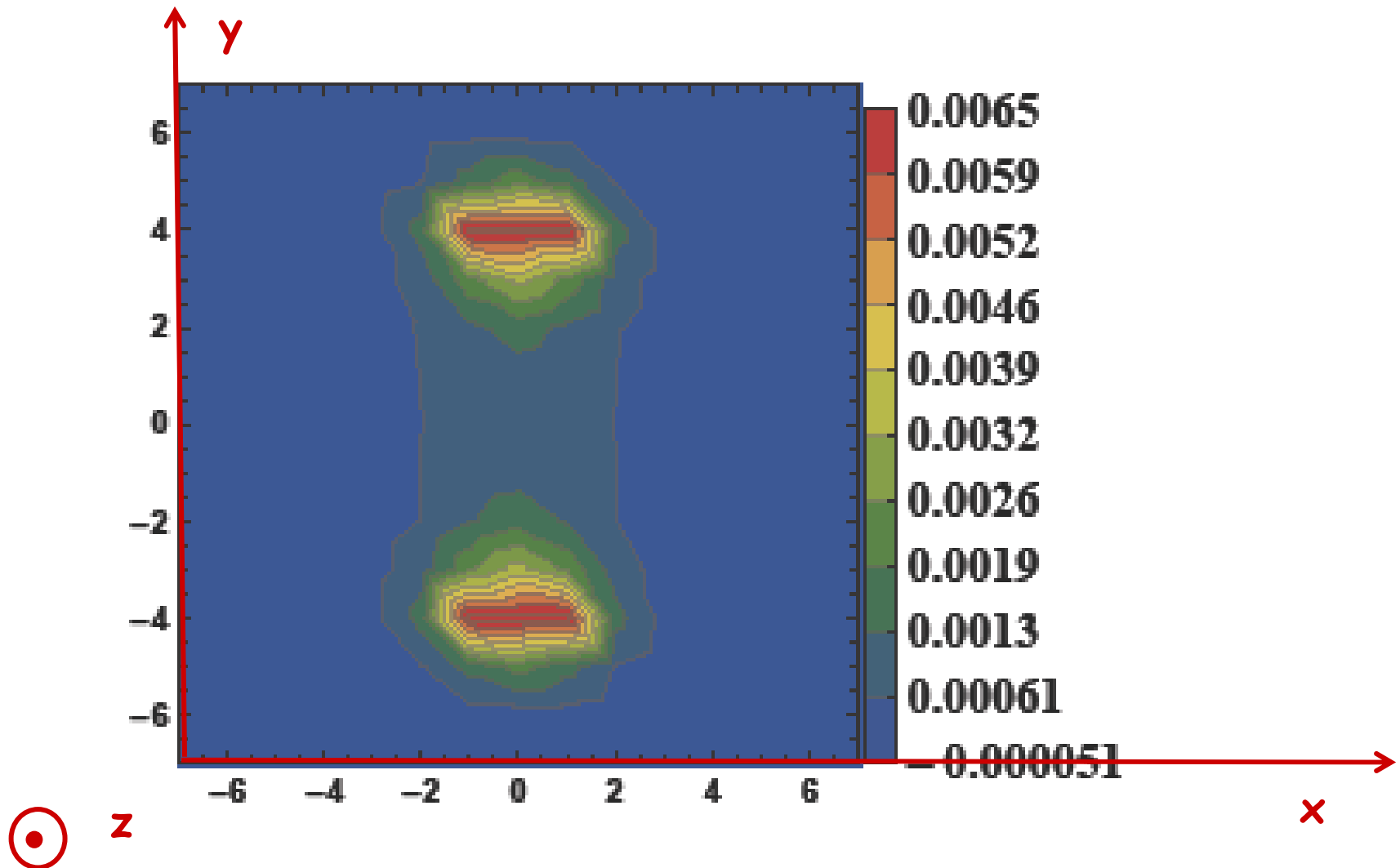
component	plaquette
E_x	P_{xt}
E_y	P_{yt}
E_z	P_{zt}
B_x	P_{yz}
B_y	P_{zx}
B_z	P_{xy}

$$\langle E^2 \rangle = P_{0i} - \frac{\langle W P_{0i} \rangle}{W}$$

$$\langle B^2 \rangle = \frac{\langle W P_{ij} \rangle}{W} - P_{ij}$$

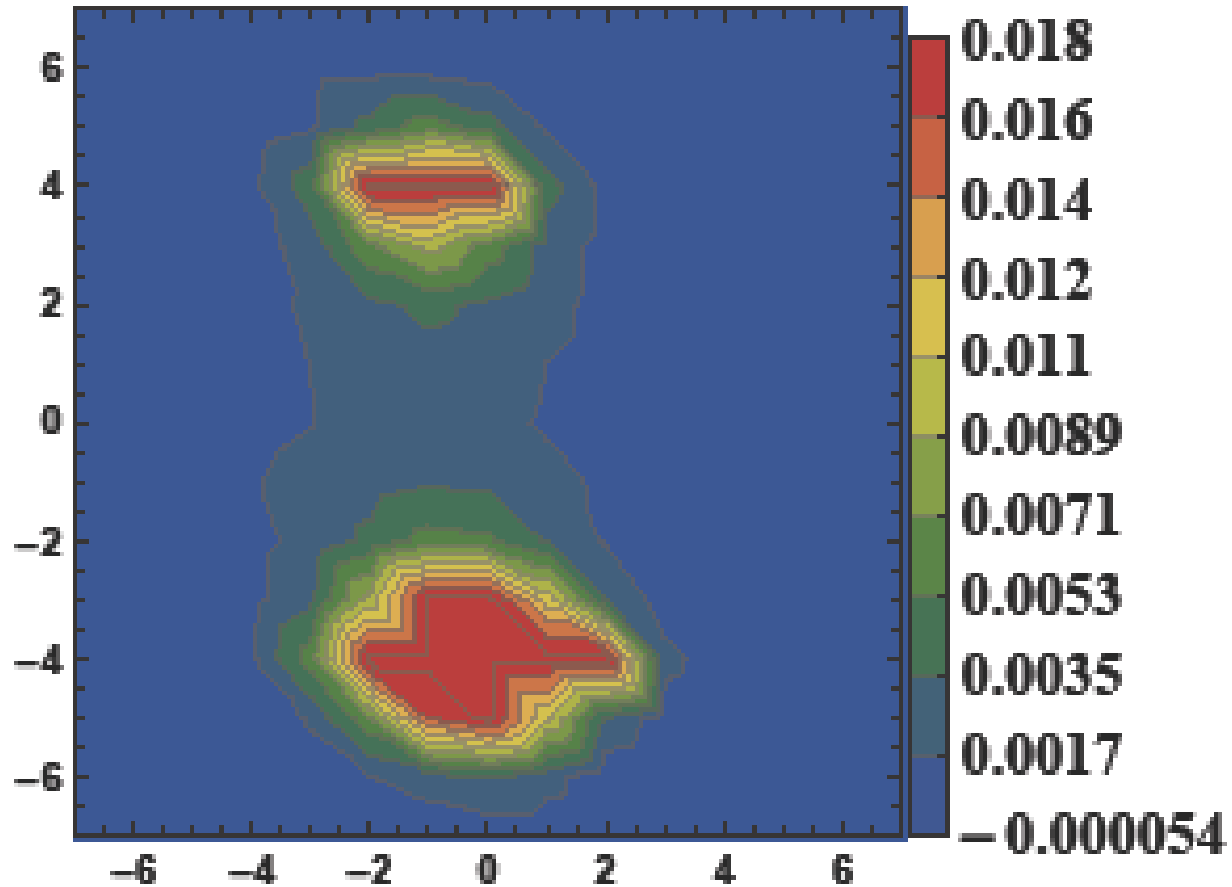
The hybrid flux tube $QG\bar{Q}$ in lattice QCD

Ex



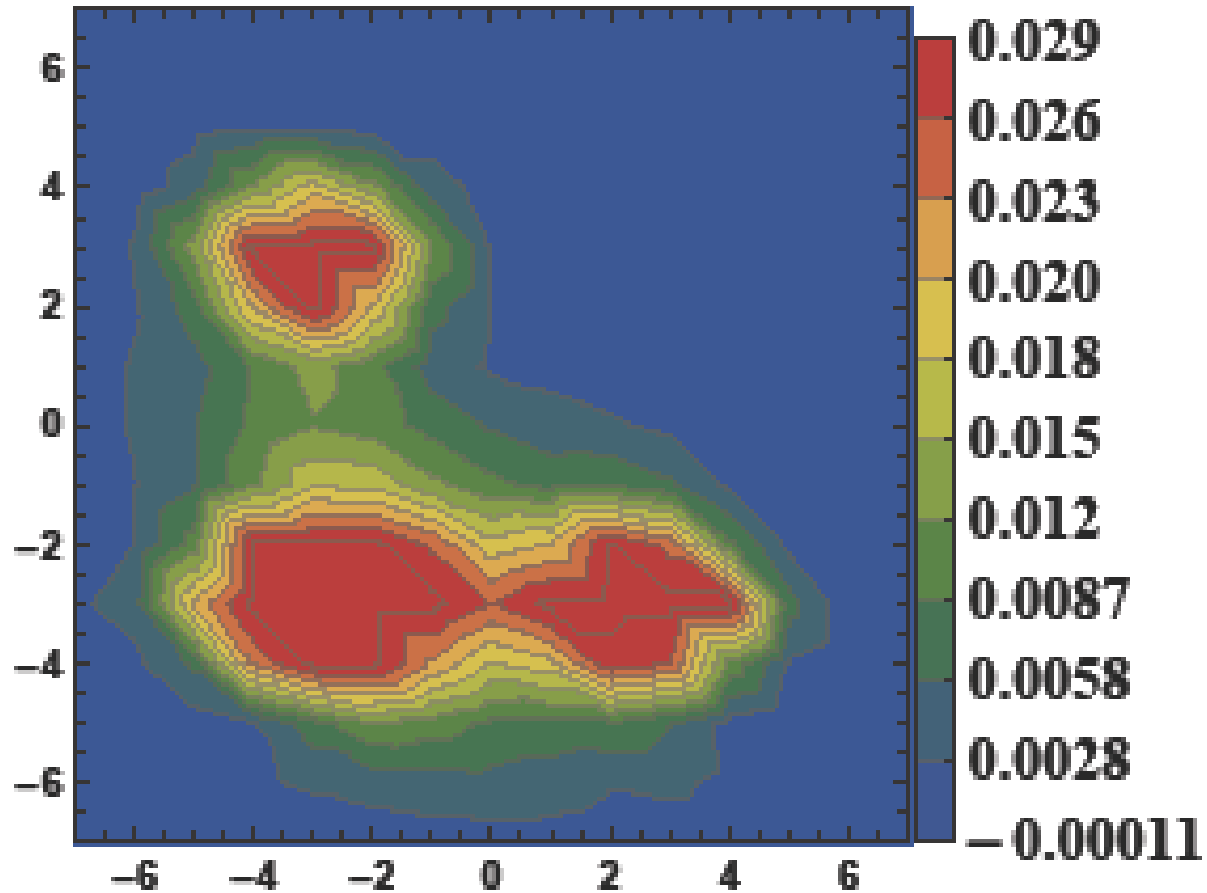
The hybrid QGQ flux tube in lattice QCD

Ex



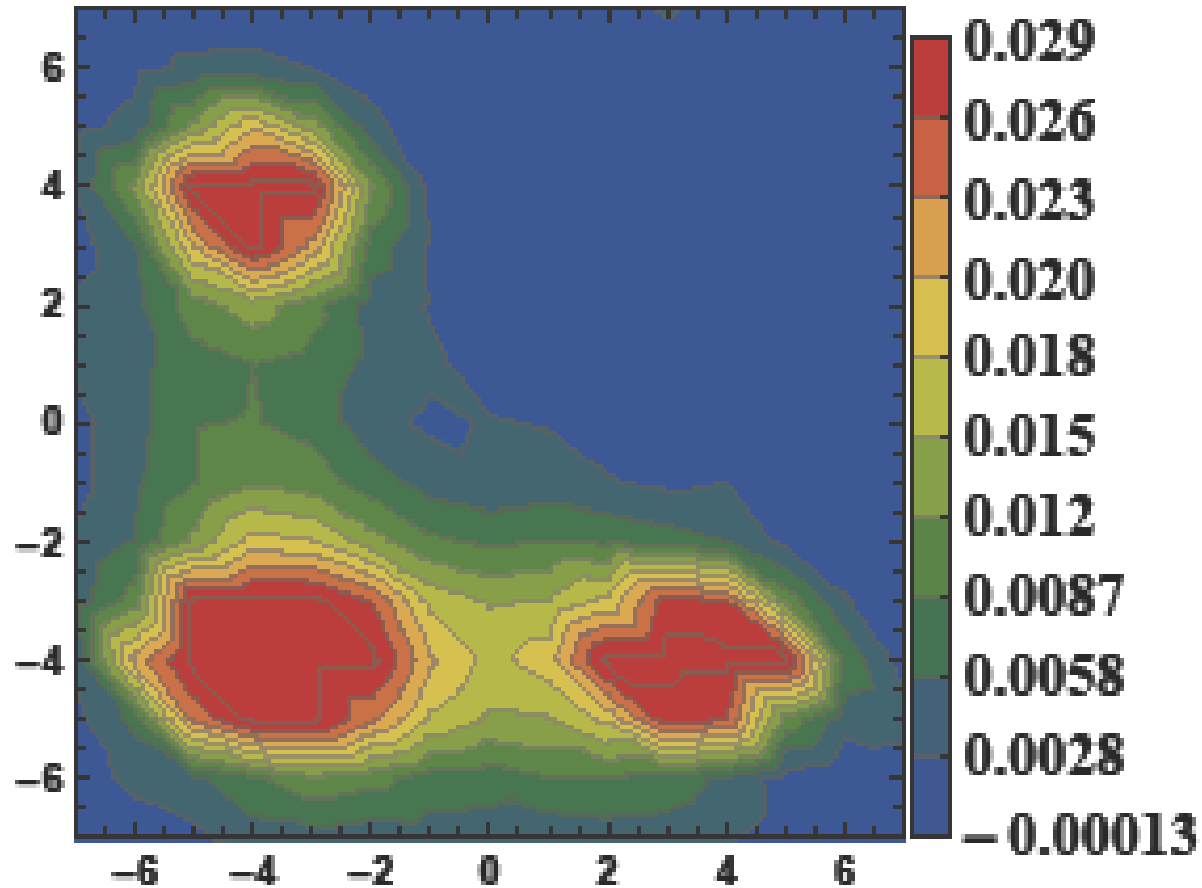
The hybrid $QG\bar{Q}$ flux tube in lattice QCD

Ex



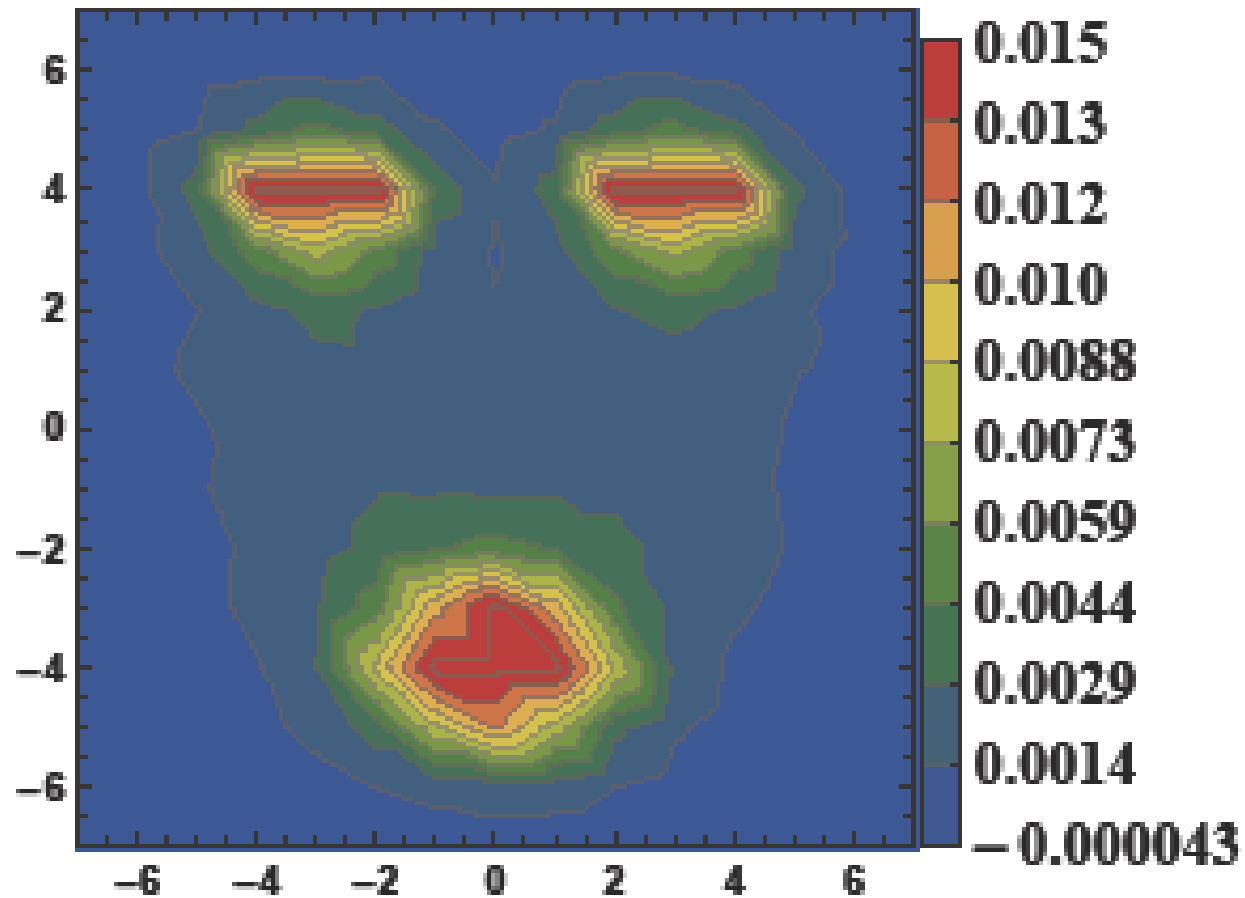
The hybrid $Q\bar{Q}$ flux tube in lattice QCD

Ex



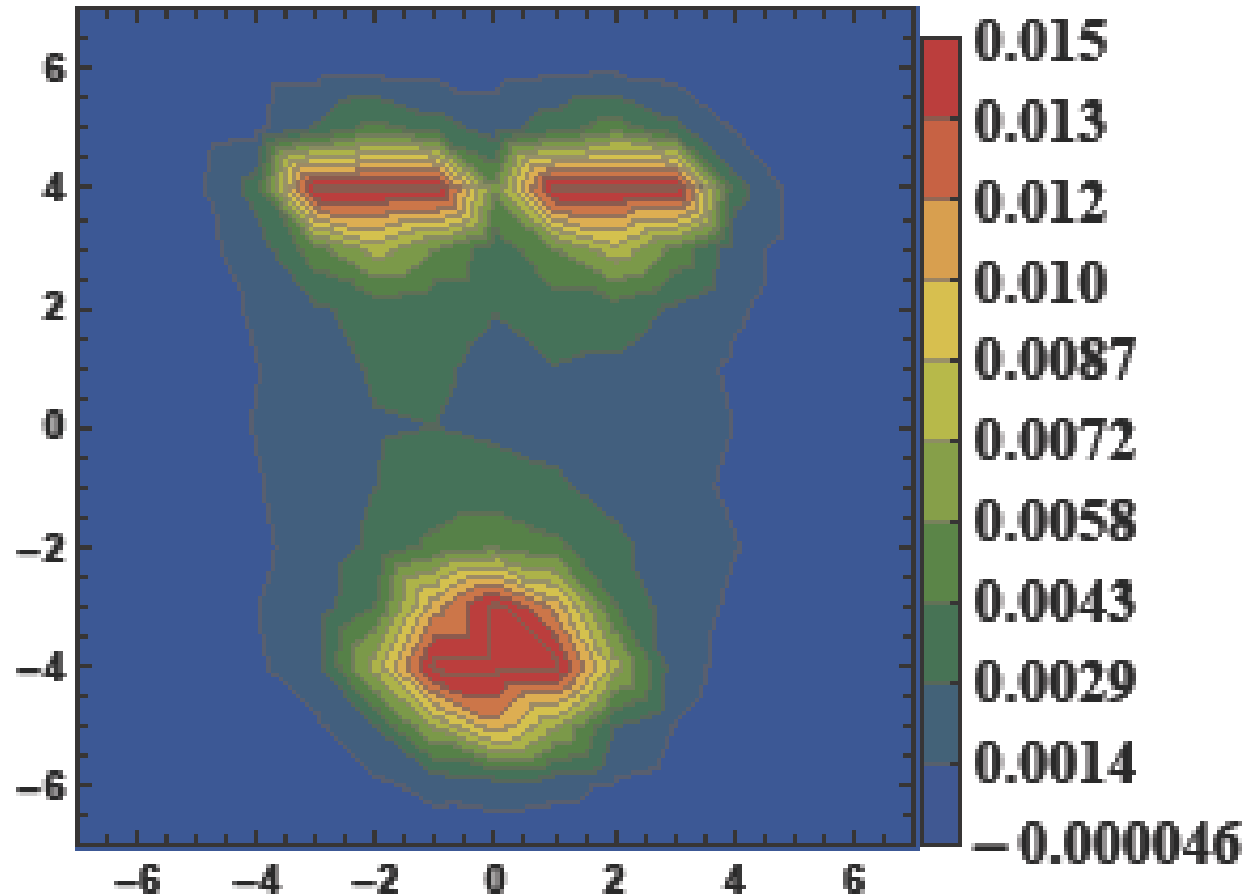
The hybrid QGQ flux tube in lattice QCD

Ex



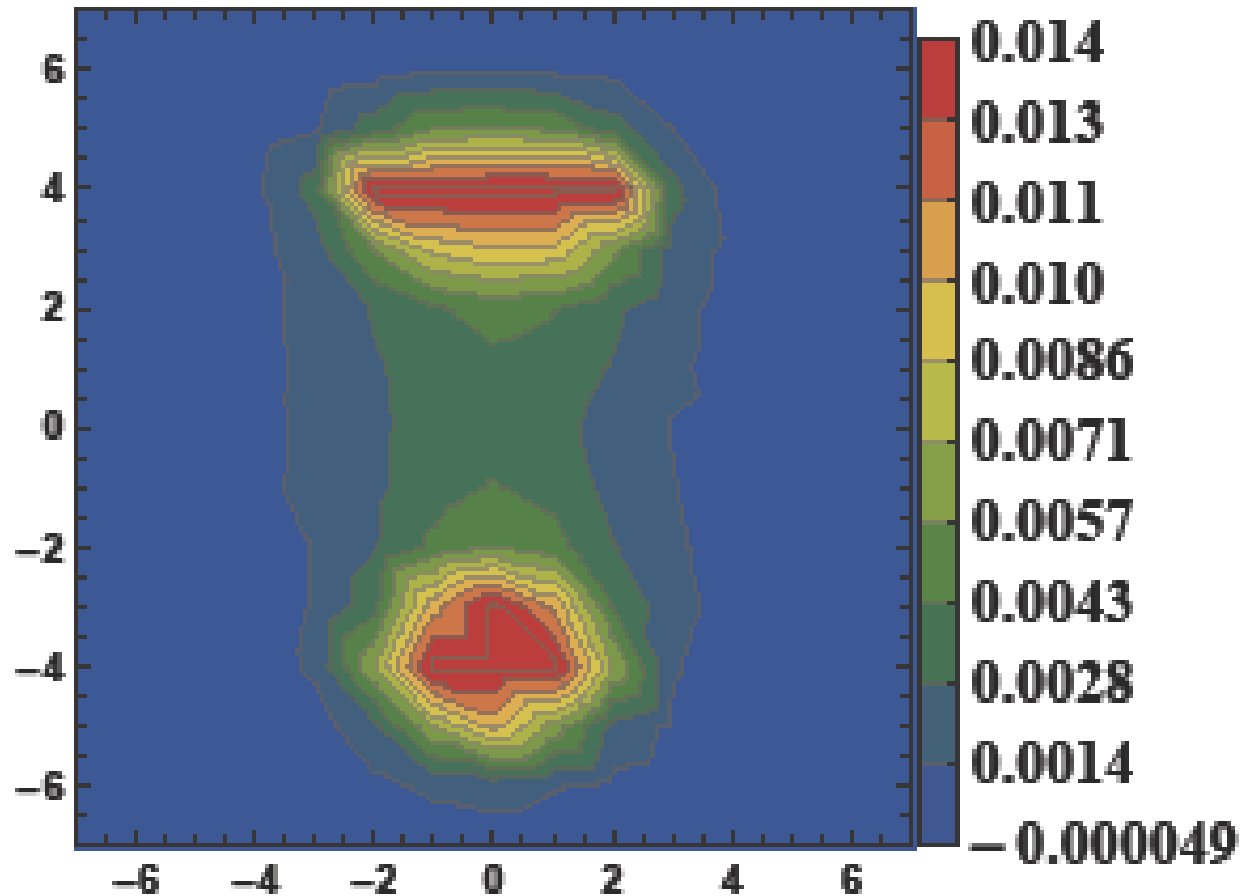
The hybrid QGQ flux tube in lattice QCD

Ex



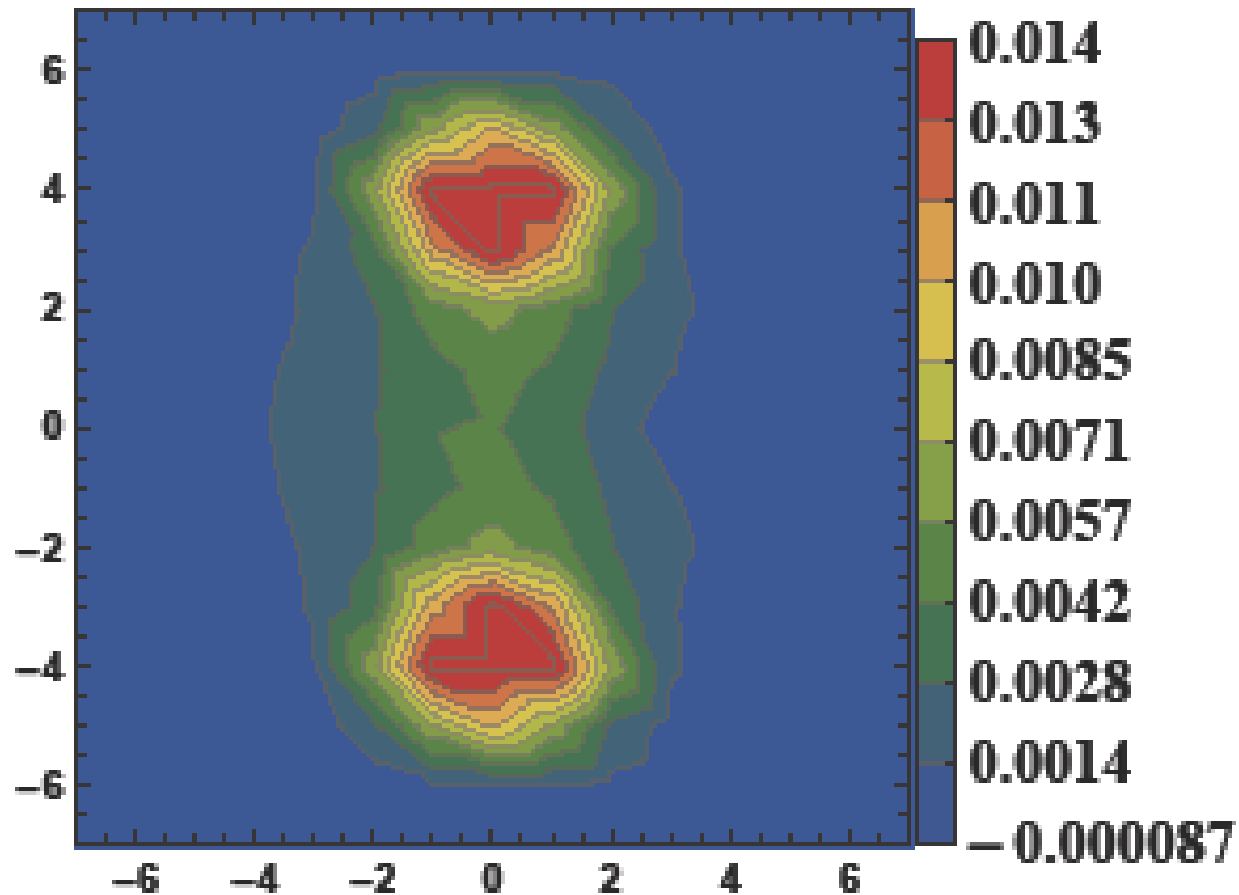
The hybrid QGQ flux tube in lattice QCD

Ex



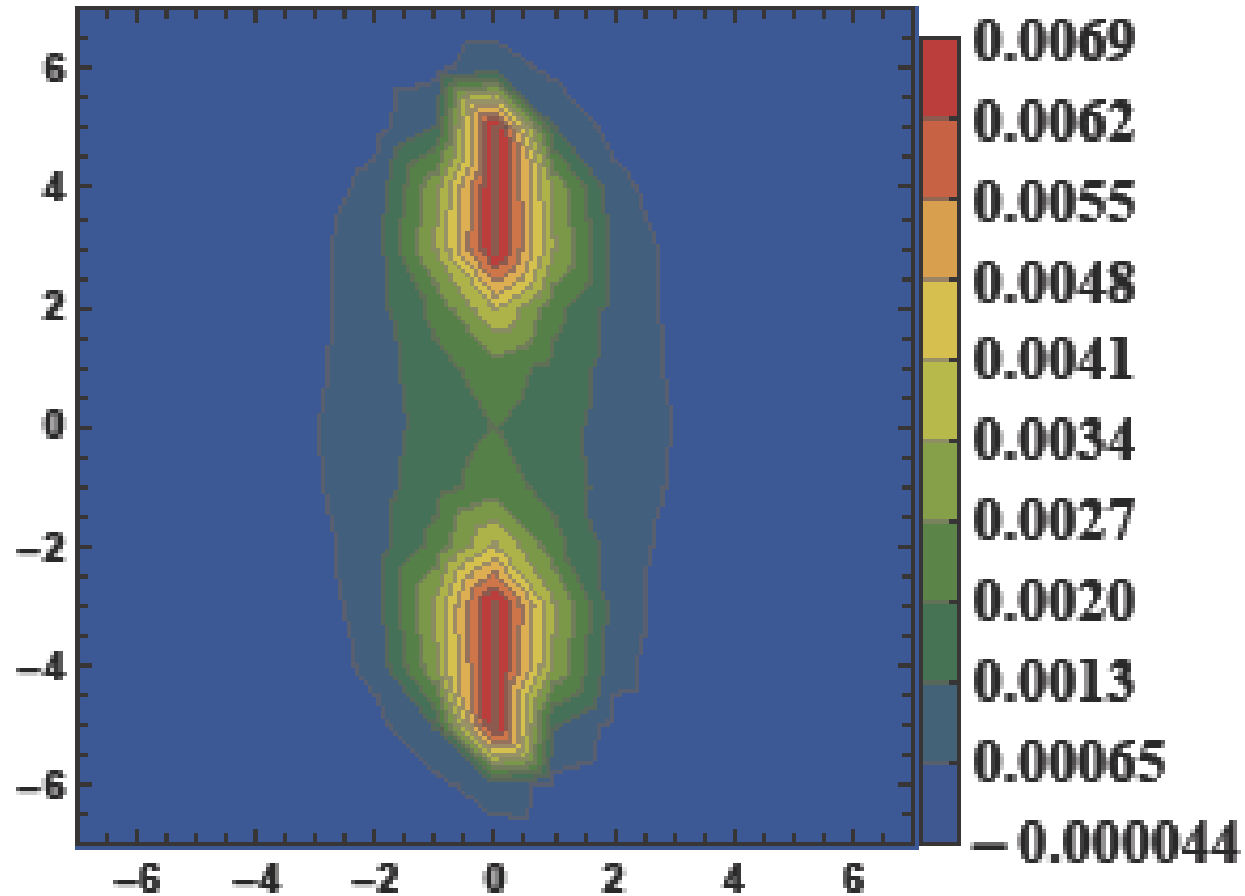
The hybrid QGQ flux tube in lattice QCD

Ex



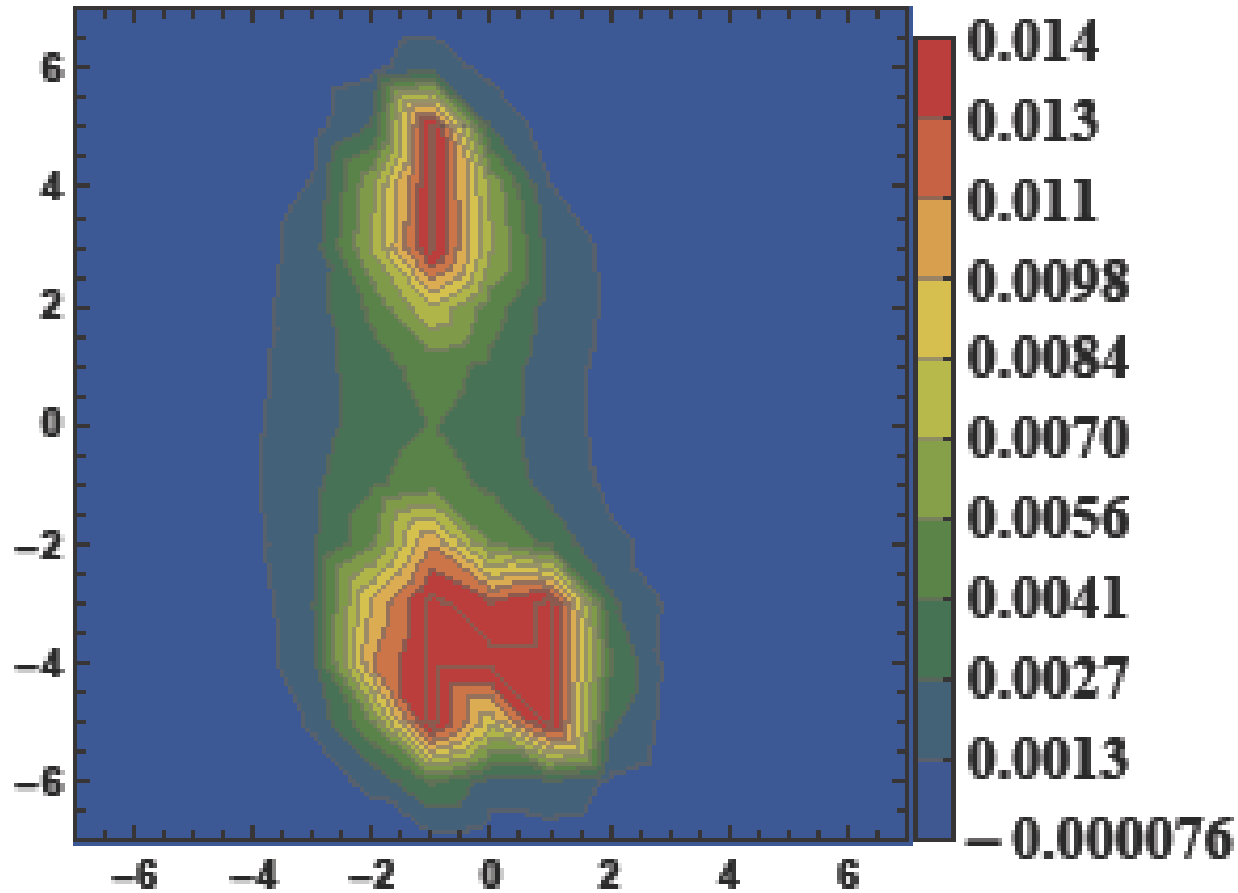
The hybrid QGQ flux tube in lattice QCD

E_y



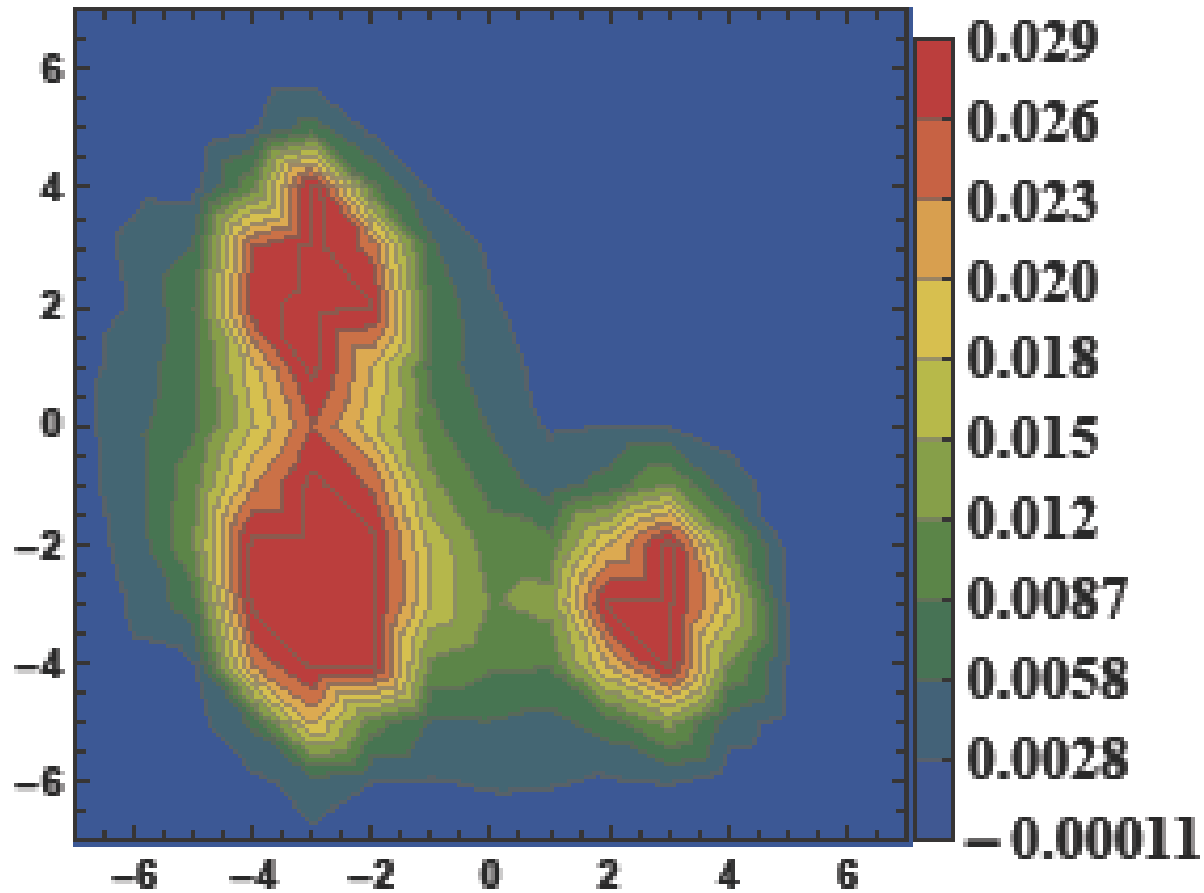
The hybrid QGQ flux tube in lattice QCD

E_y



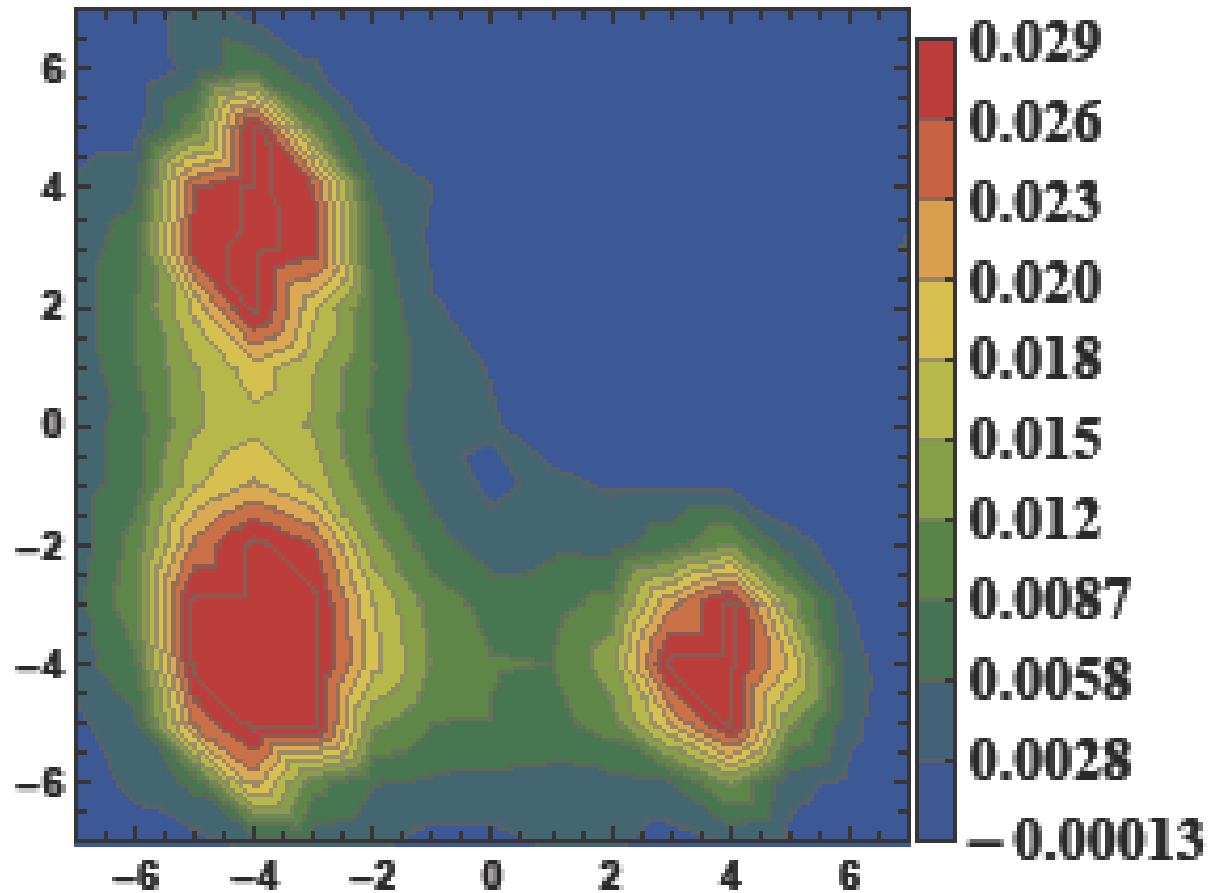
The hybrid QGQ flux tube in lattice QCD

E_y



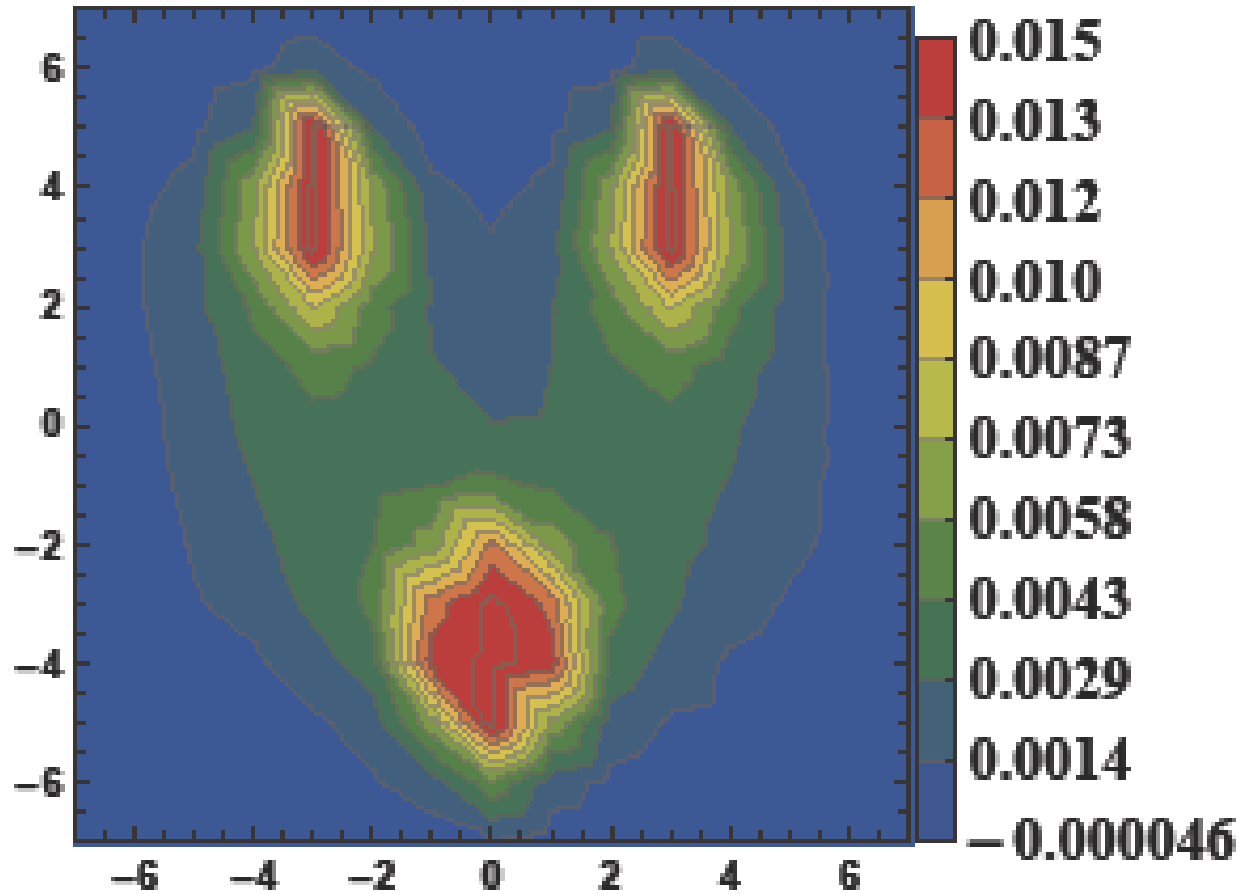
The hybrid QGQ flux tube in lattice QCD

E_y



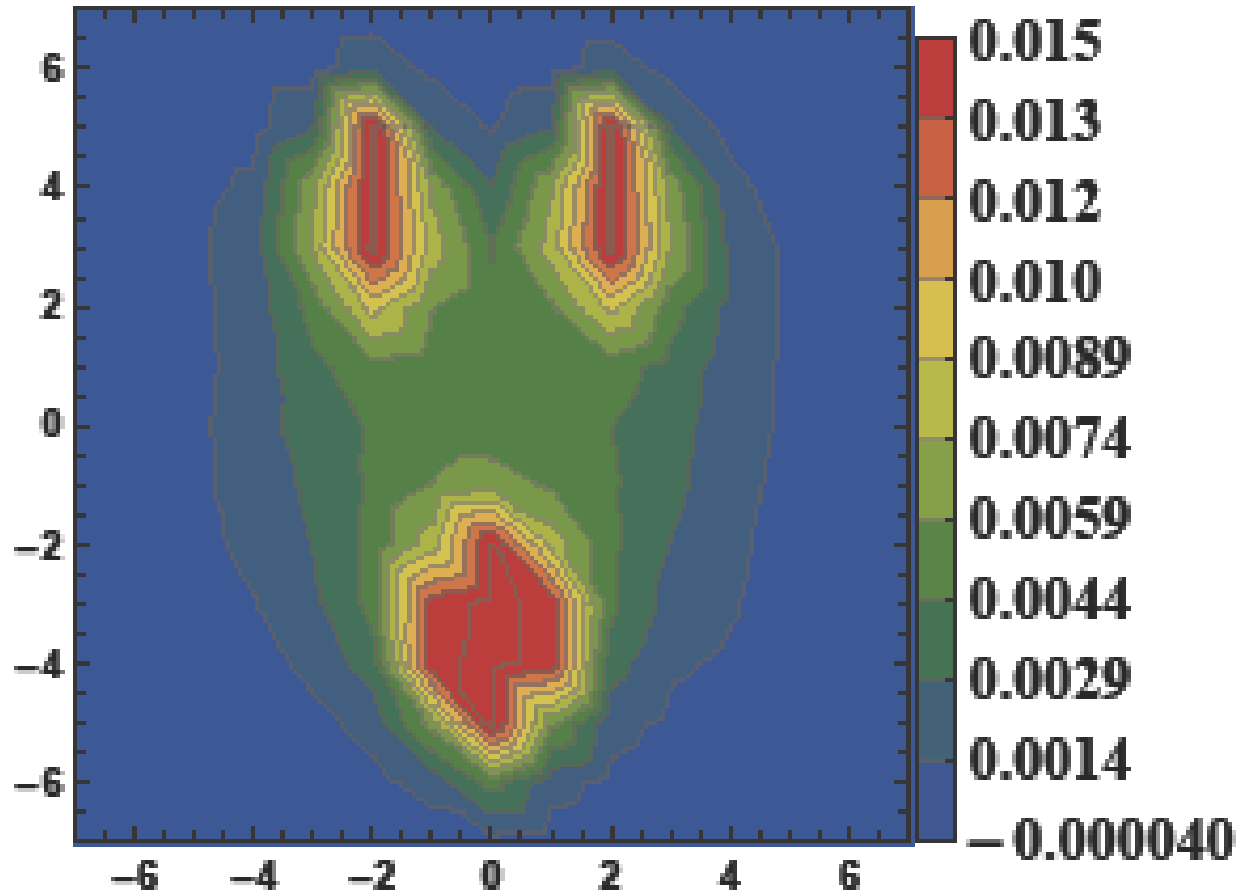
The hybrid $Q\bar{Q}$ flux tube in lattice QCD

E_y



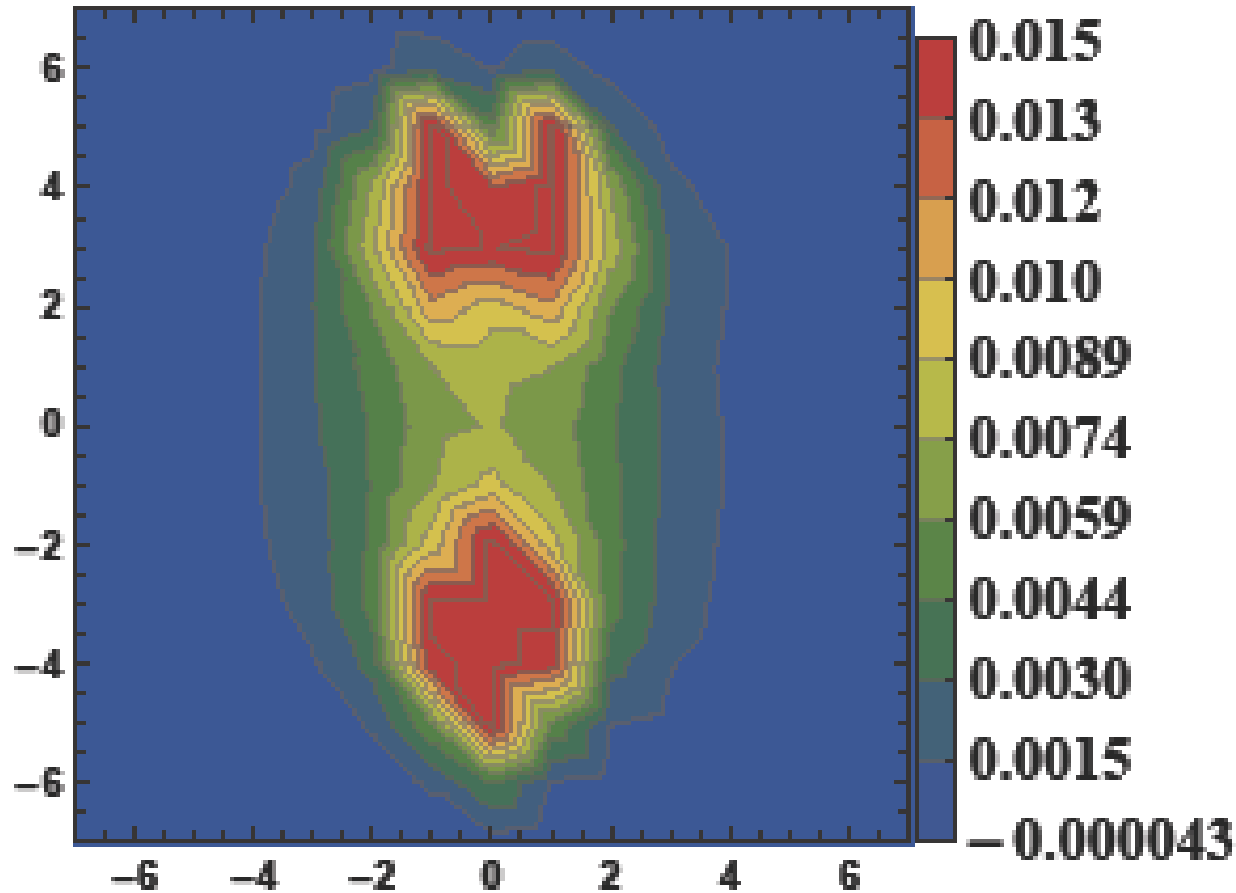
The hybrid QGQ flux tube in lattice QCD

E_y



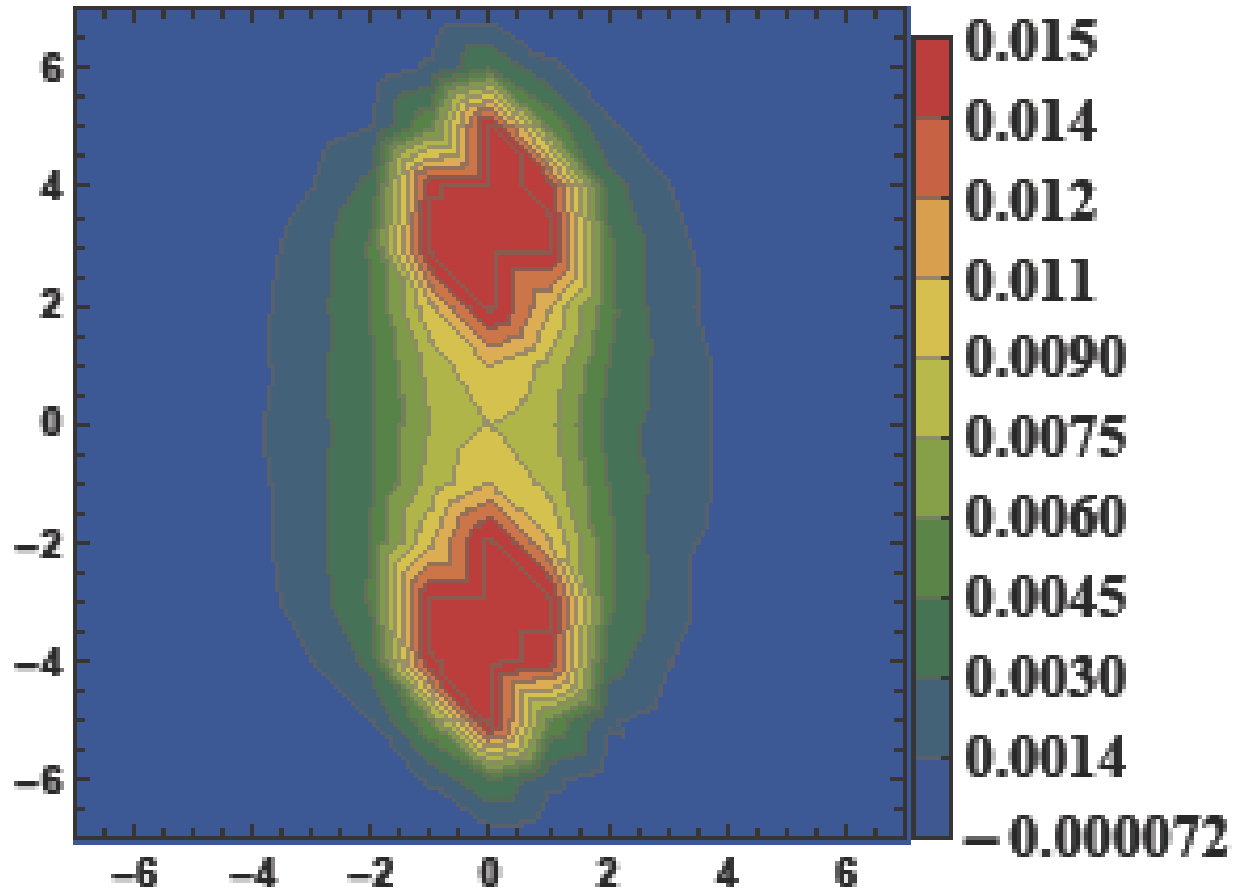
The hybrid QGQ flux tube in lattice QCD

E_y



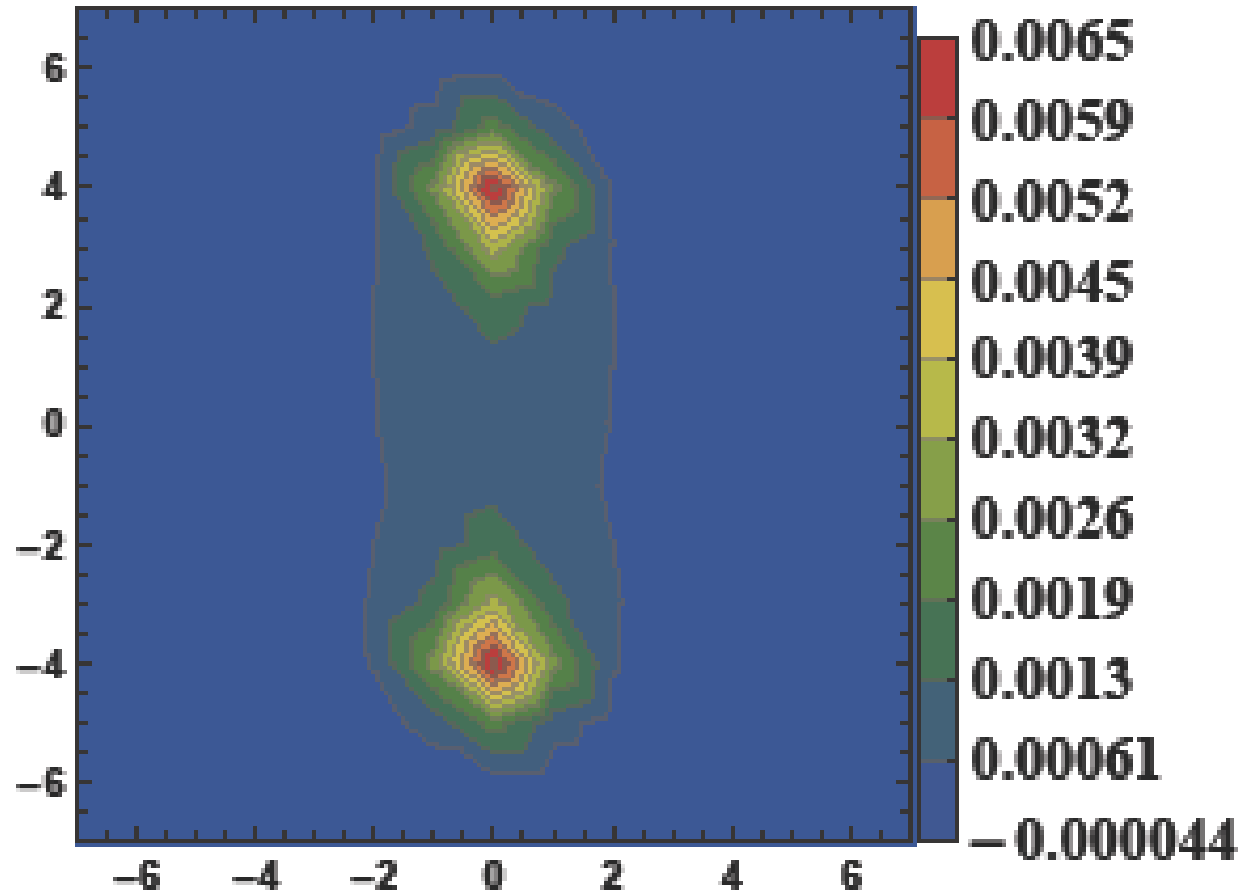
The hybrid QGQ flux tube in lattice QCD

E_y



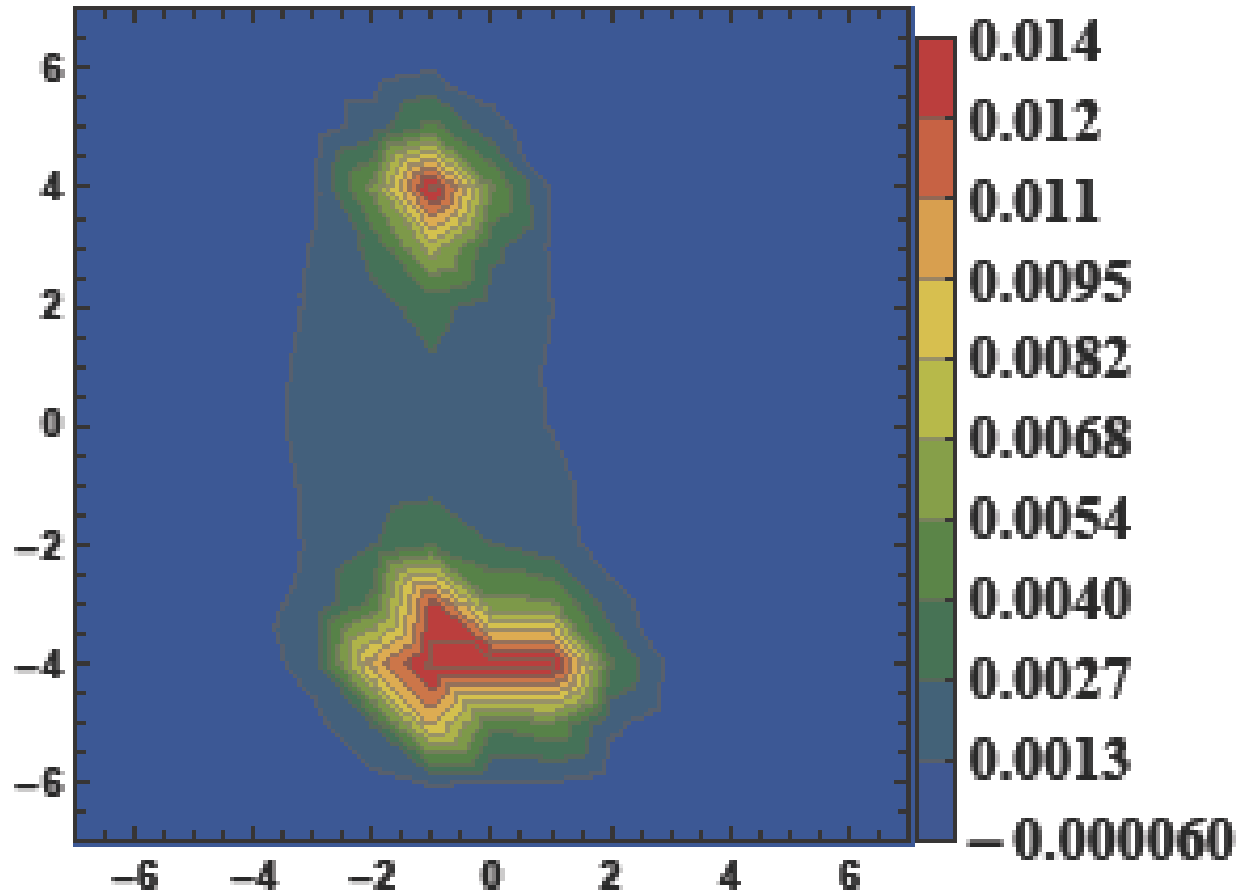
The hybrid QGQ flux tube in lattice QCD

E_z



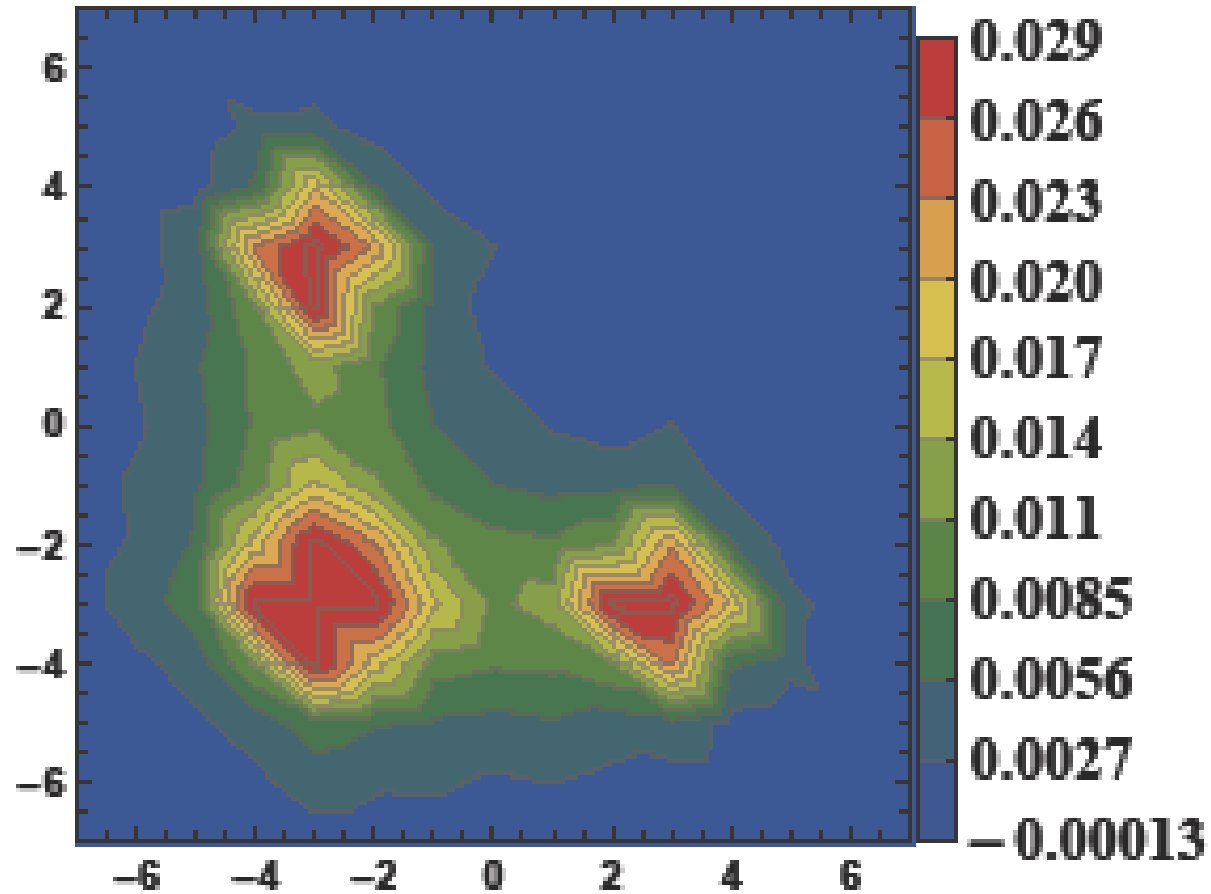
The hybrid QGQ flux tube in lattice QCD

E_z



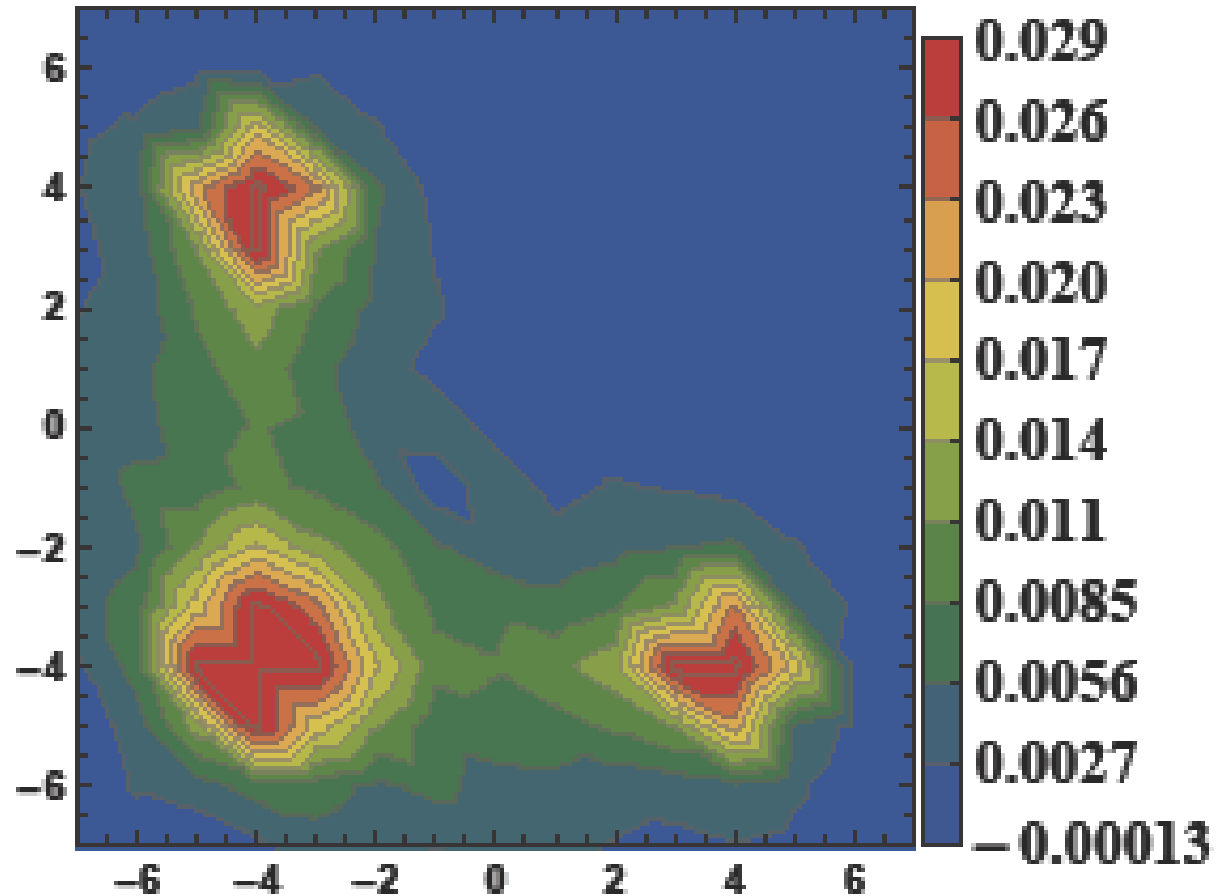
The hybrid QGQ flux tube in lattice QCD

E_z



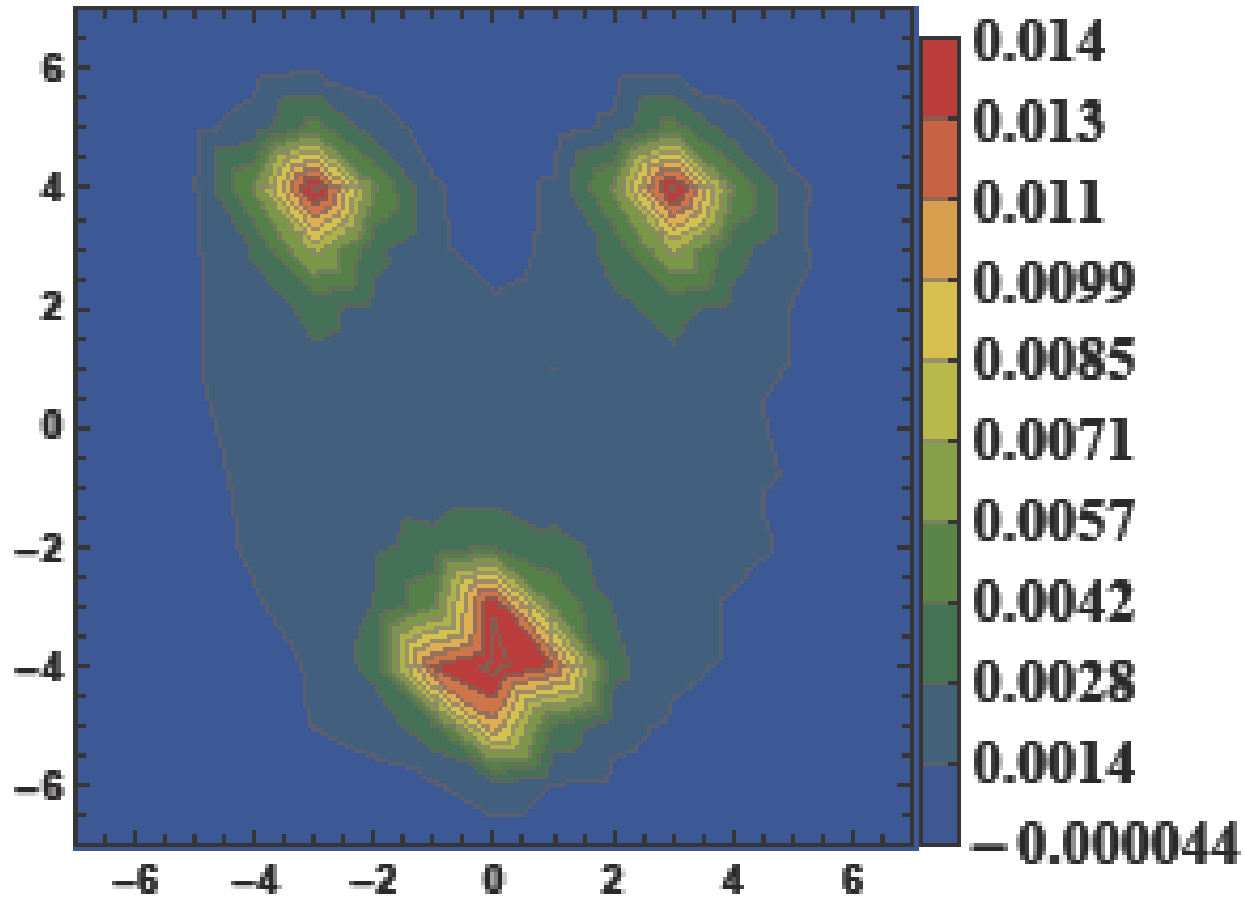
The hybrid QGQ flux tube in lattice QCD

E_z



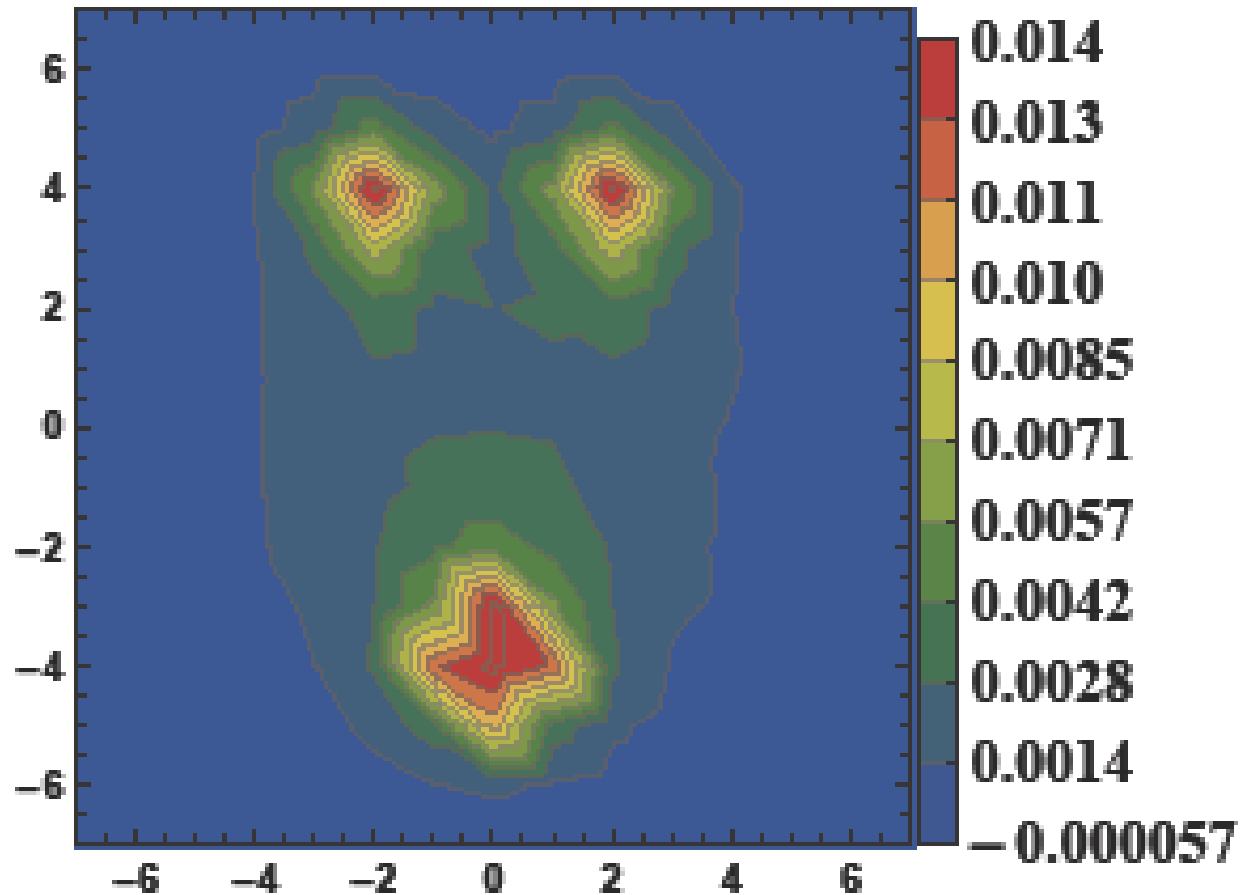
The hybrid QGQ flux tube in lattice QCD

E_z



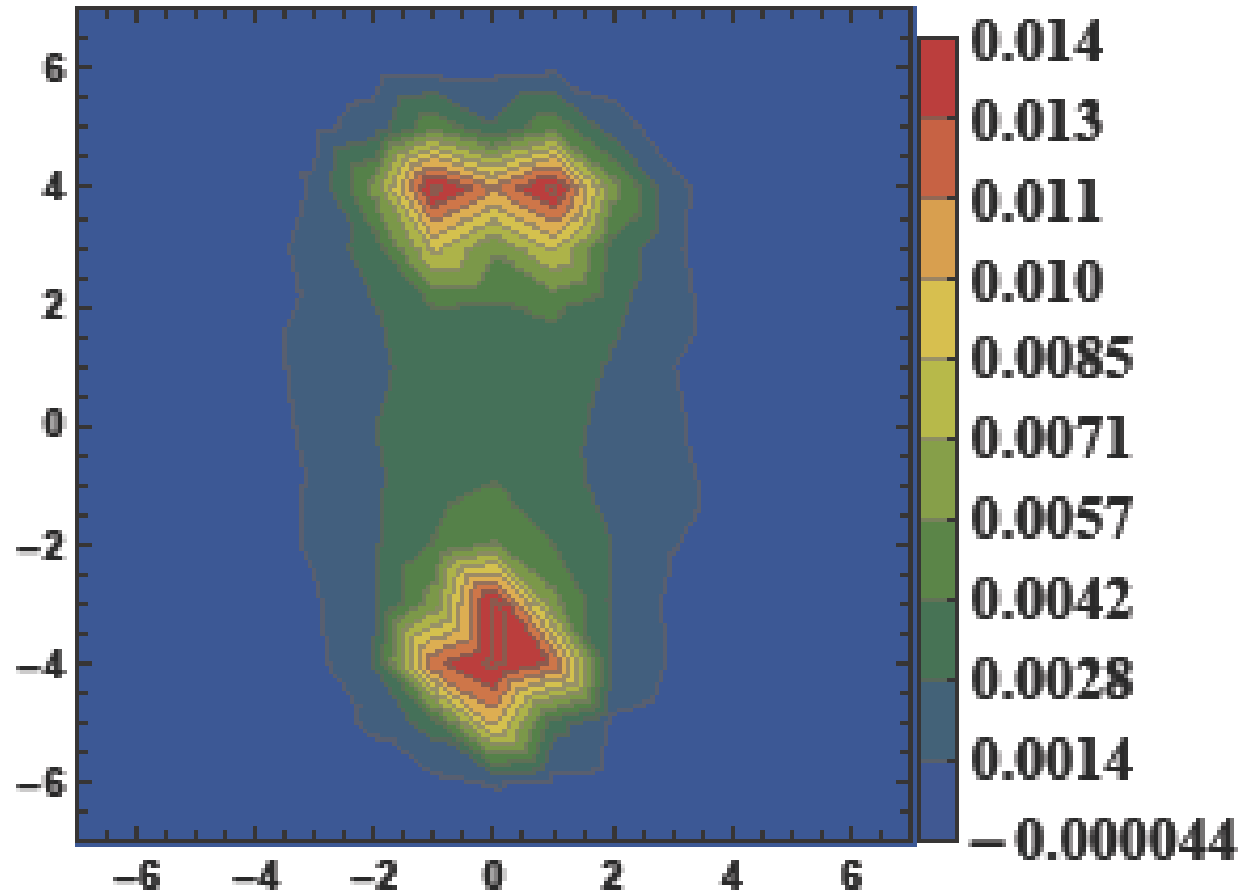
The hybrid QGQ flux tube in lattice QCD

E_z



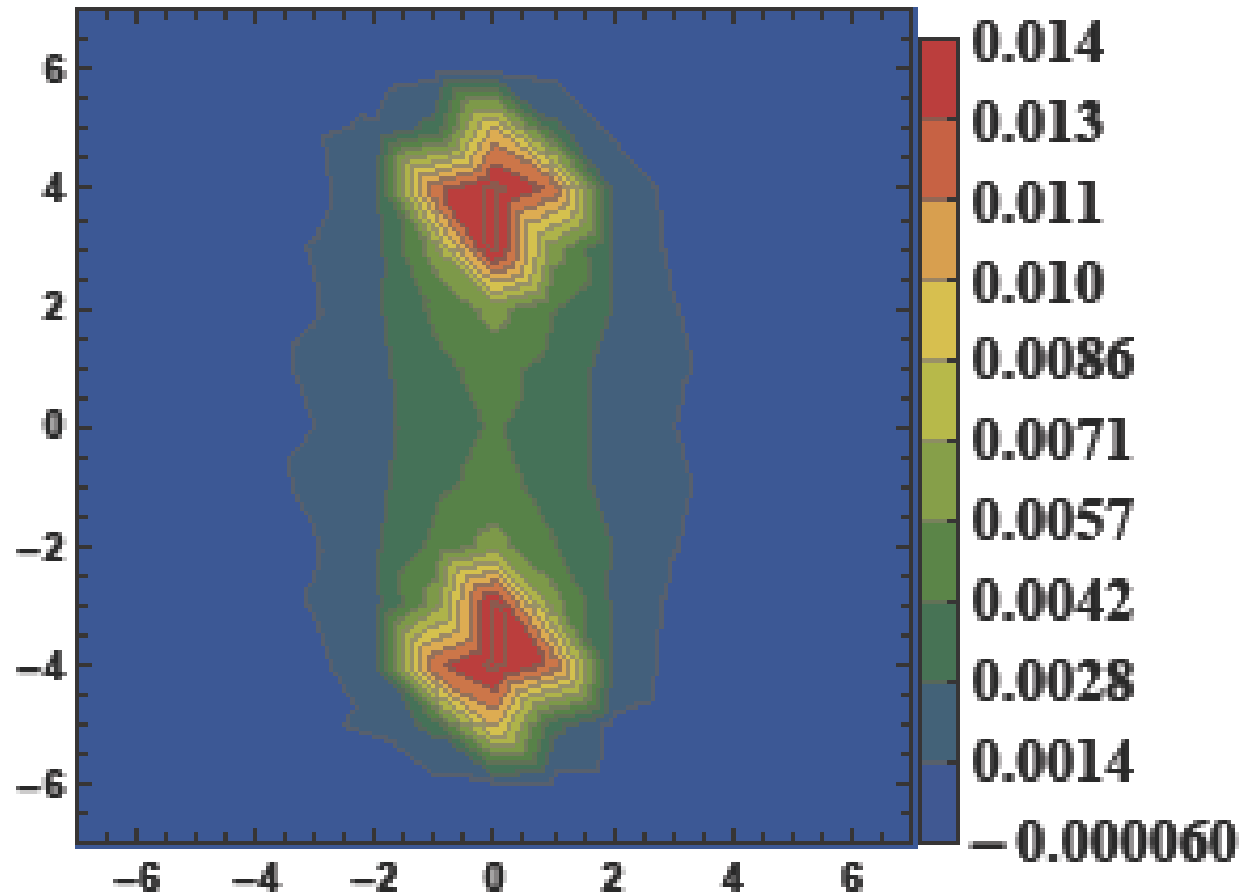
The hybrid QGQ flux tube in lattice QCD

E_z



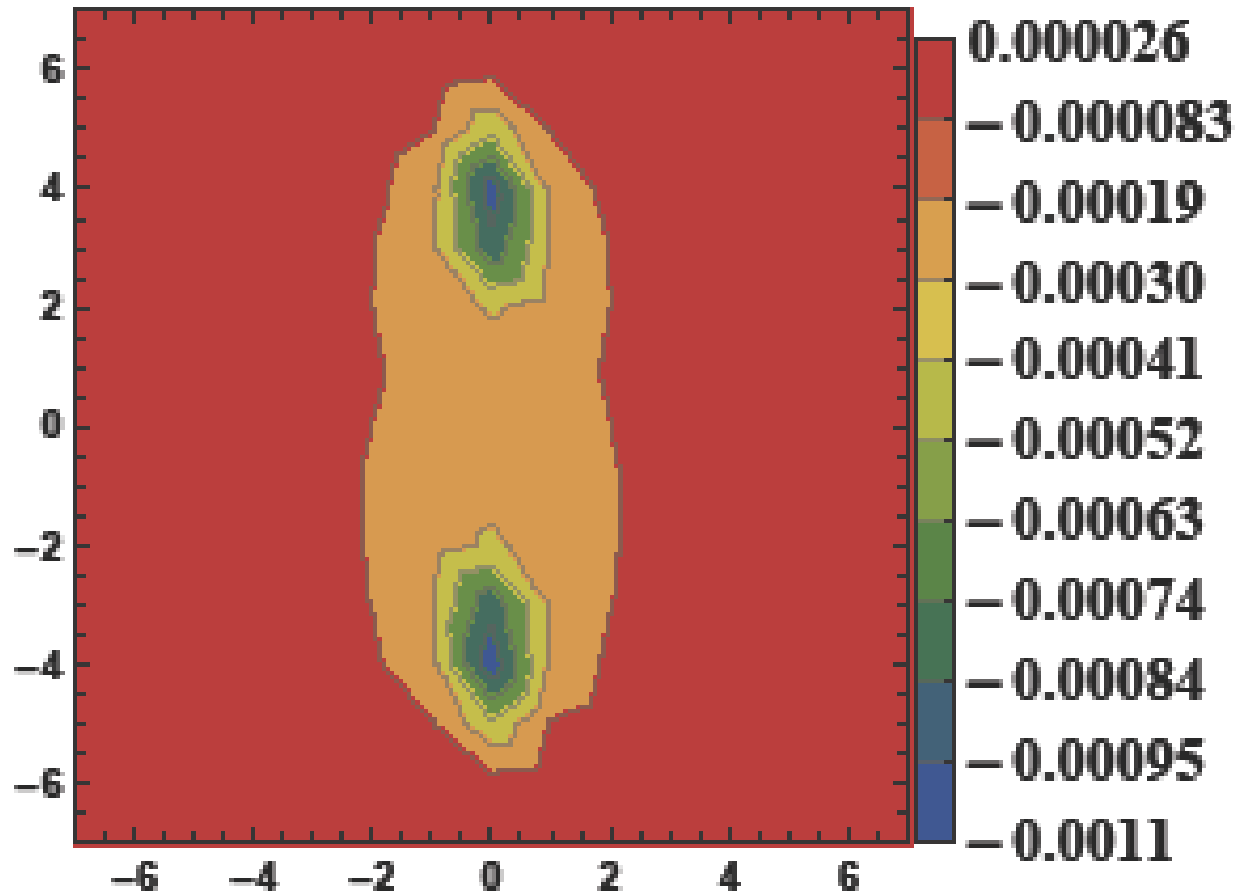
The hybrid QGQ flux tube in lattice QCD

E_z



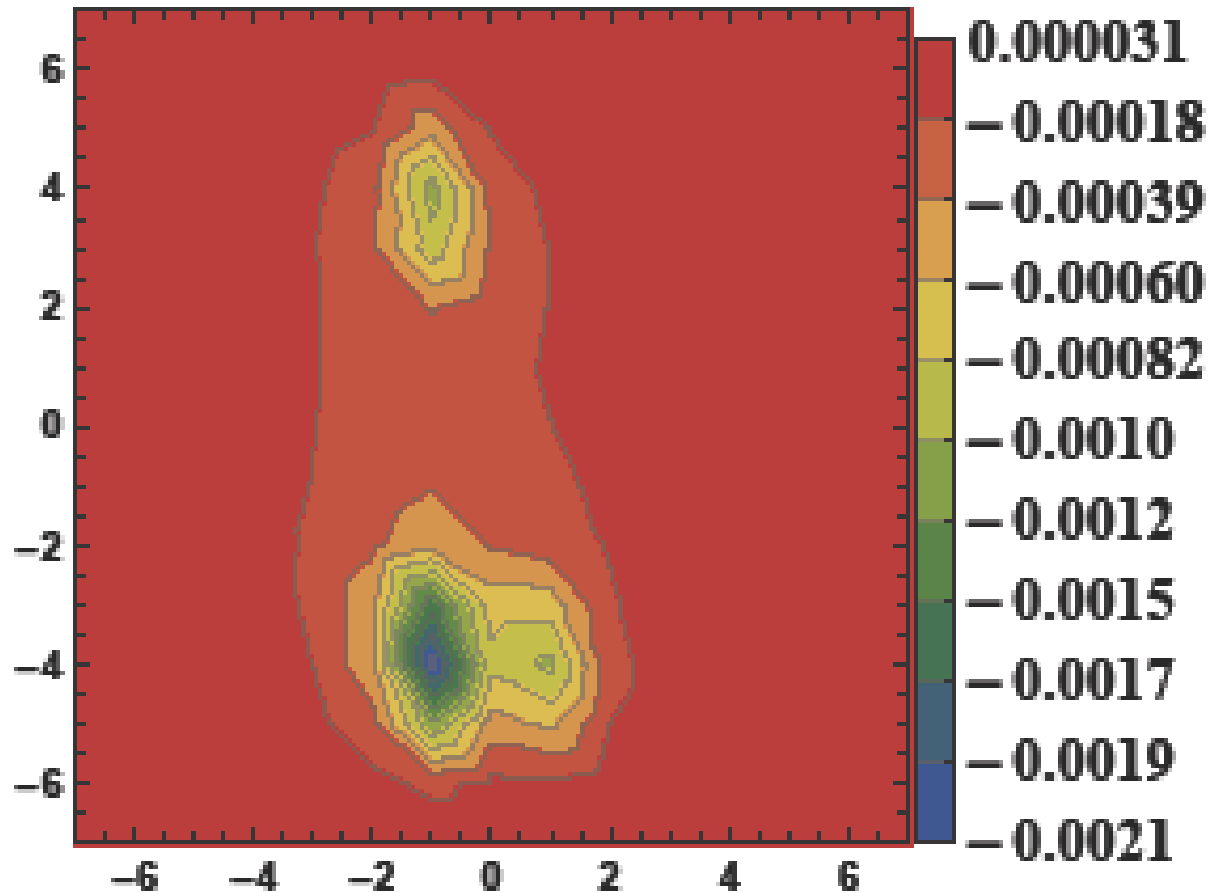
The hybrid QGQ flux tube in lattice QCD

B_x



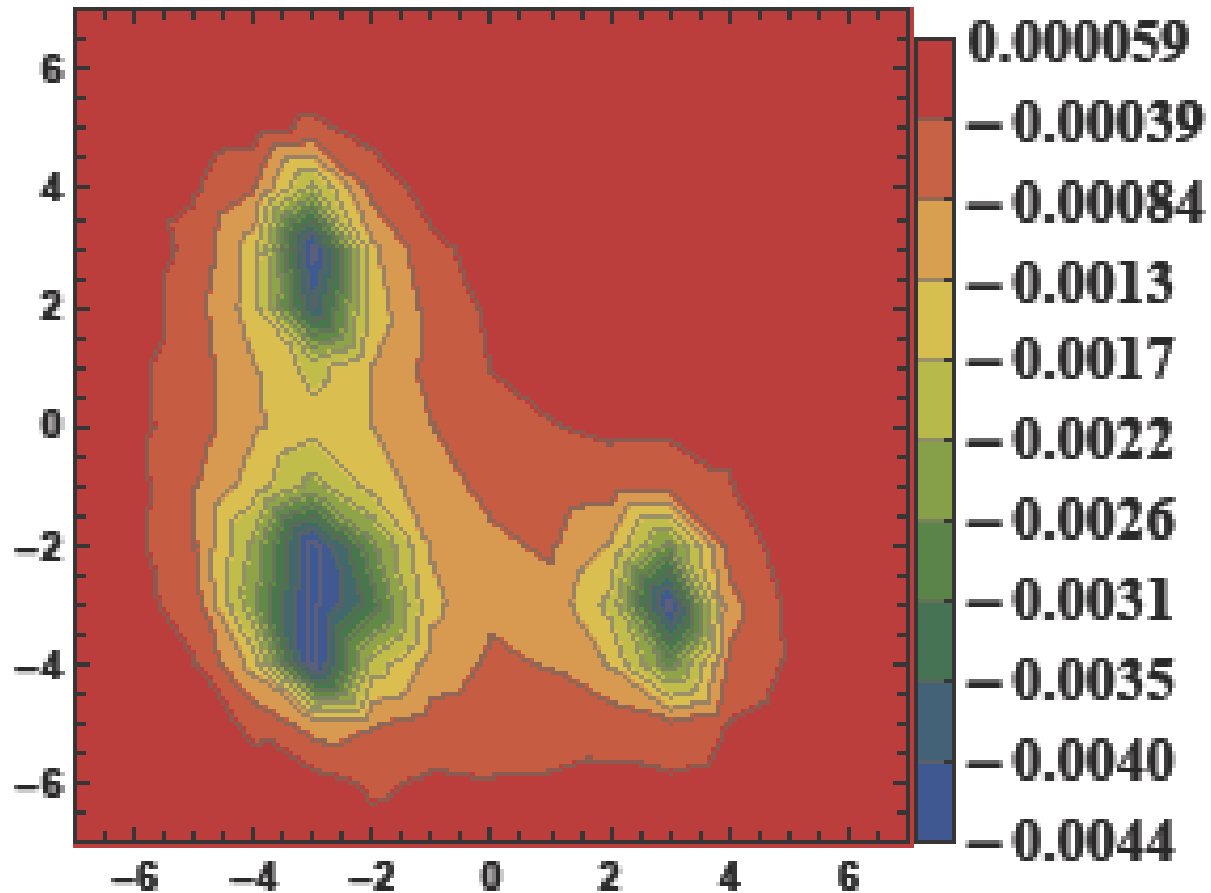
The hybrid QGQ flux tube in lattice QCD

B_x



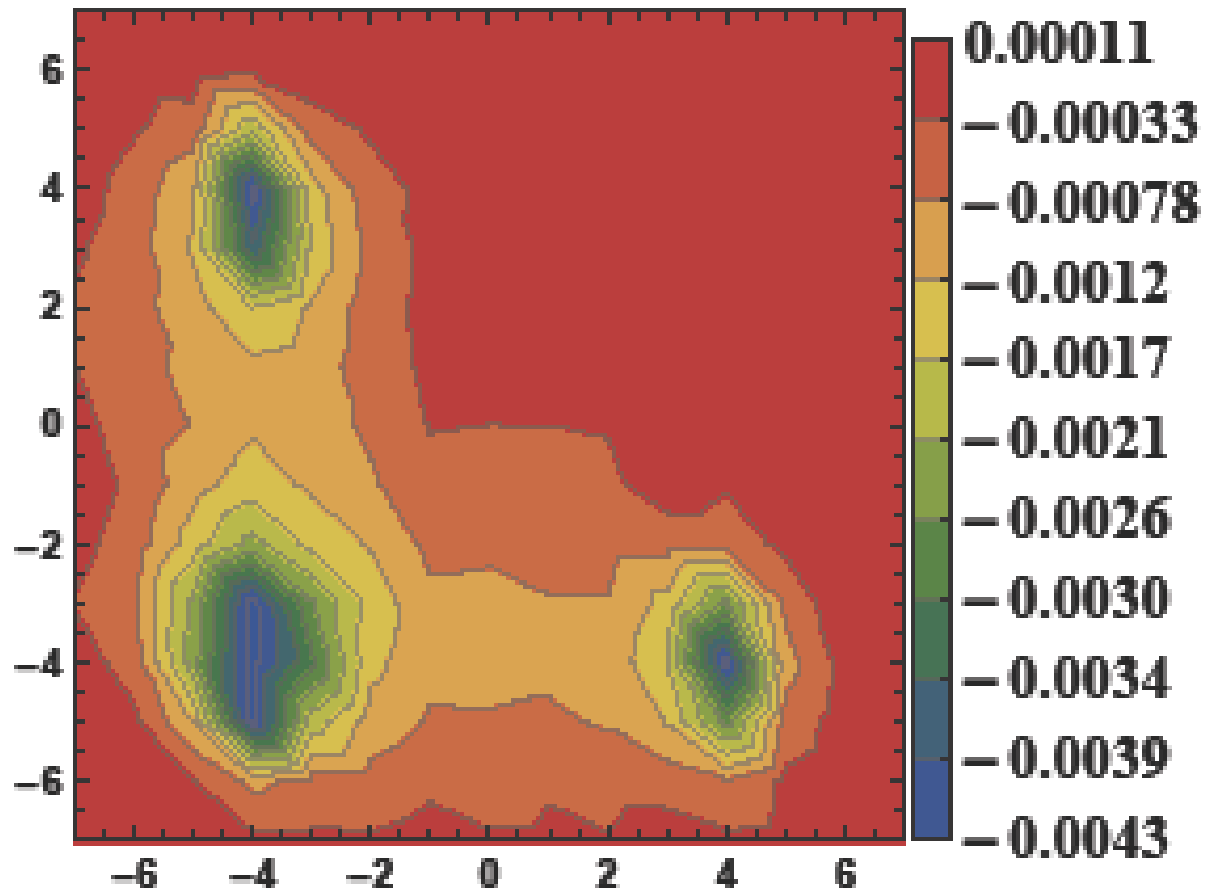
The hybrid QGQ flux tube in lattice QCD

B_x



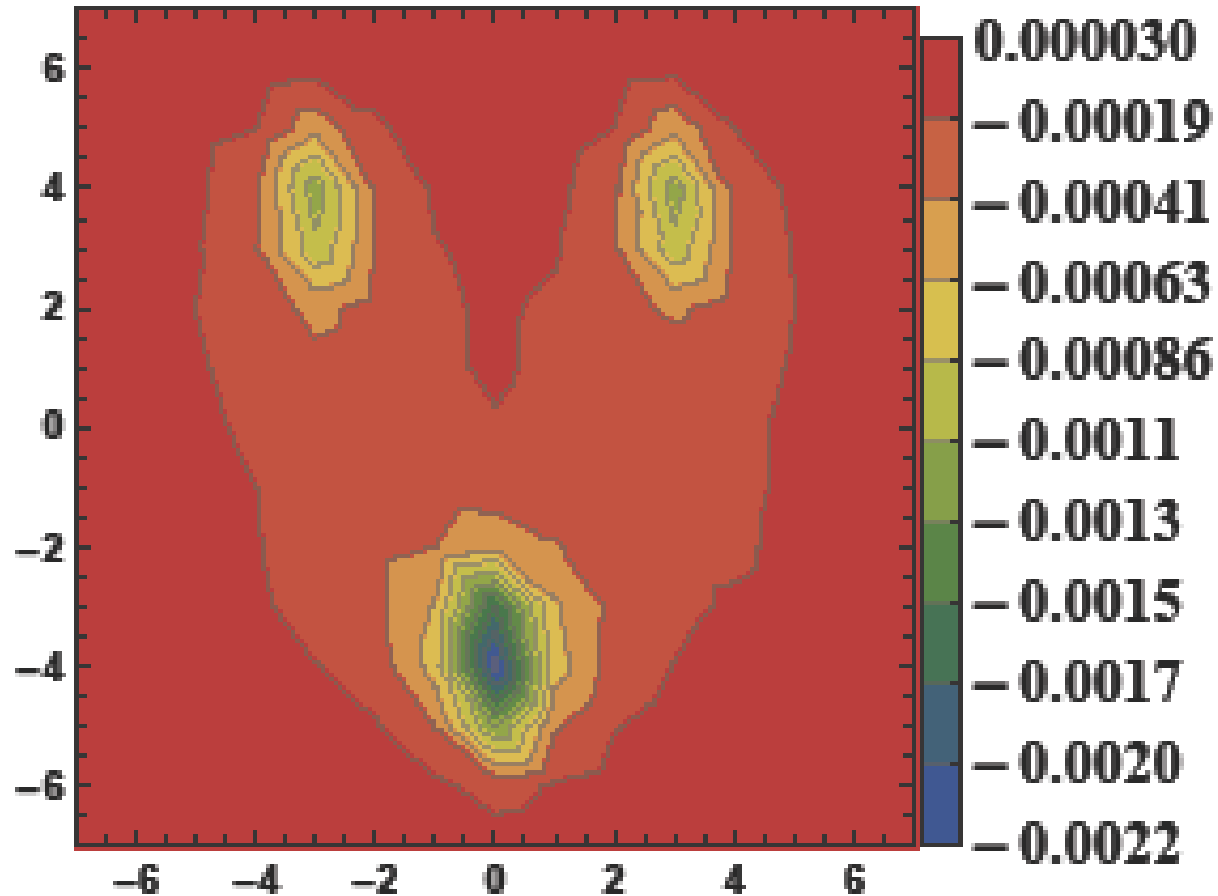
The hybrid QGQ flux tube in lattice QCD

B_x



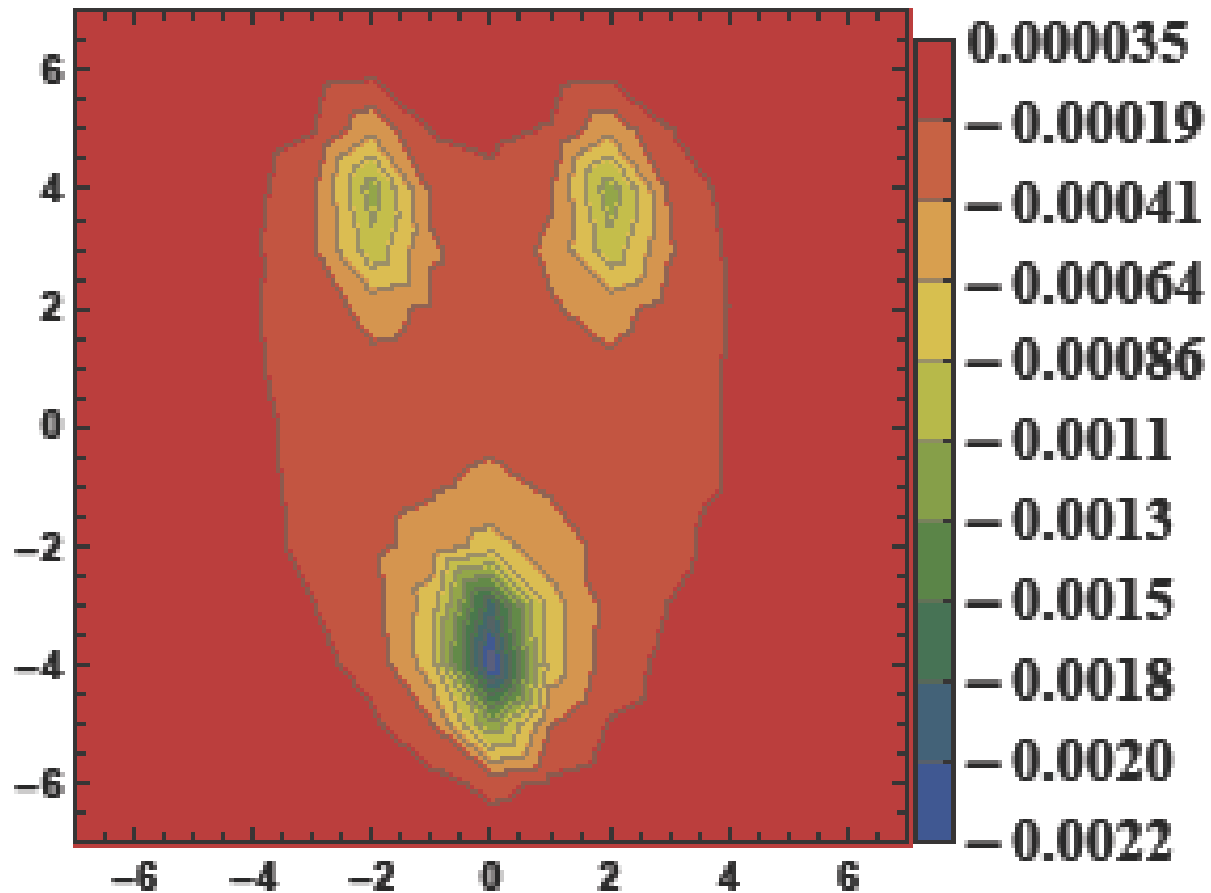
The hybrid QGQ flux tube in lattice QCD

B_x



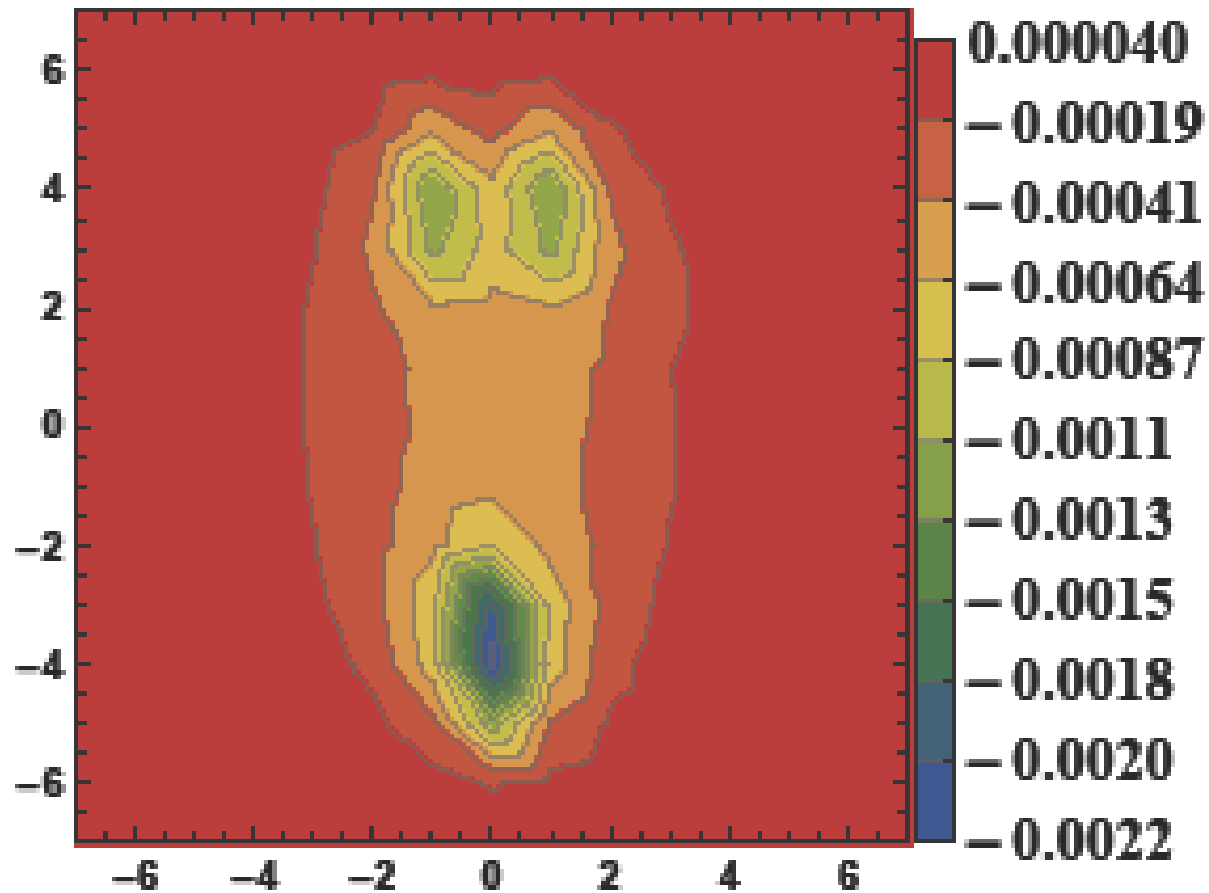
The hybrid QGQ flux tube in lattice QCD

B_x



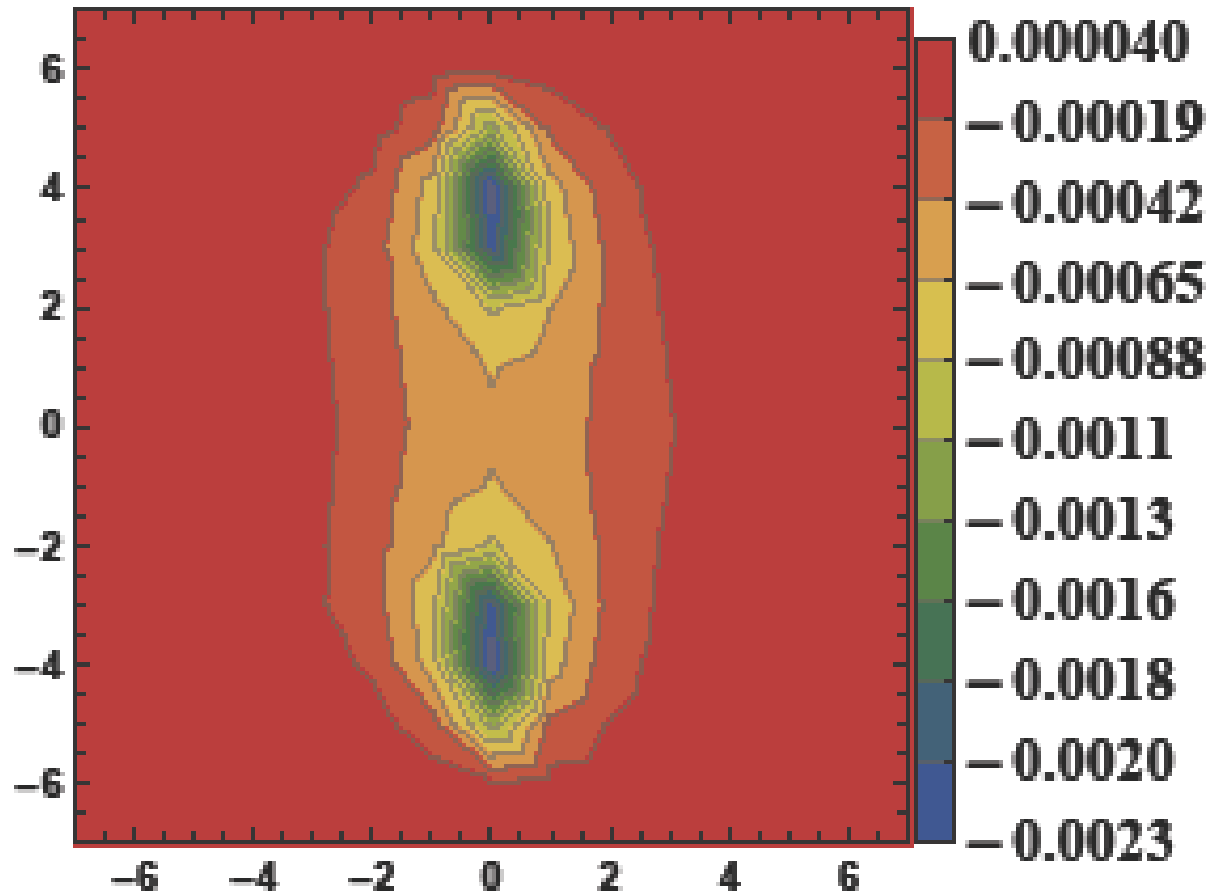
The hybrid QGQ flux tube in lattice QCD

B_x



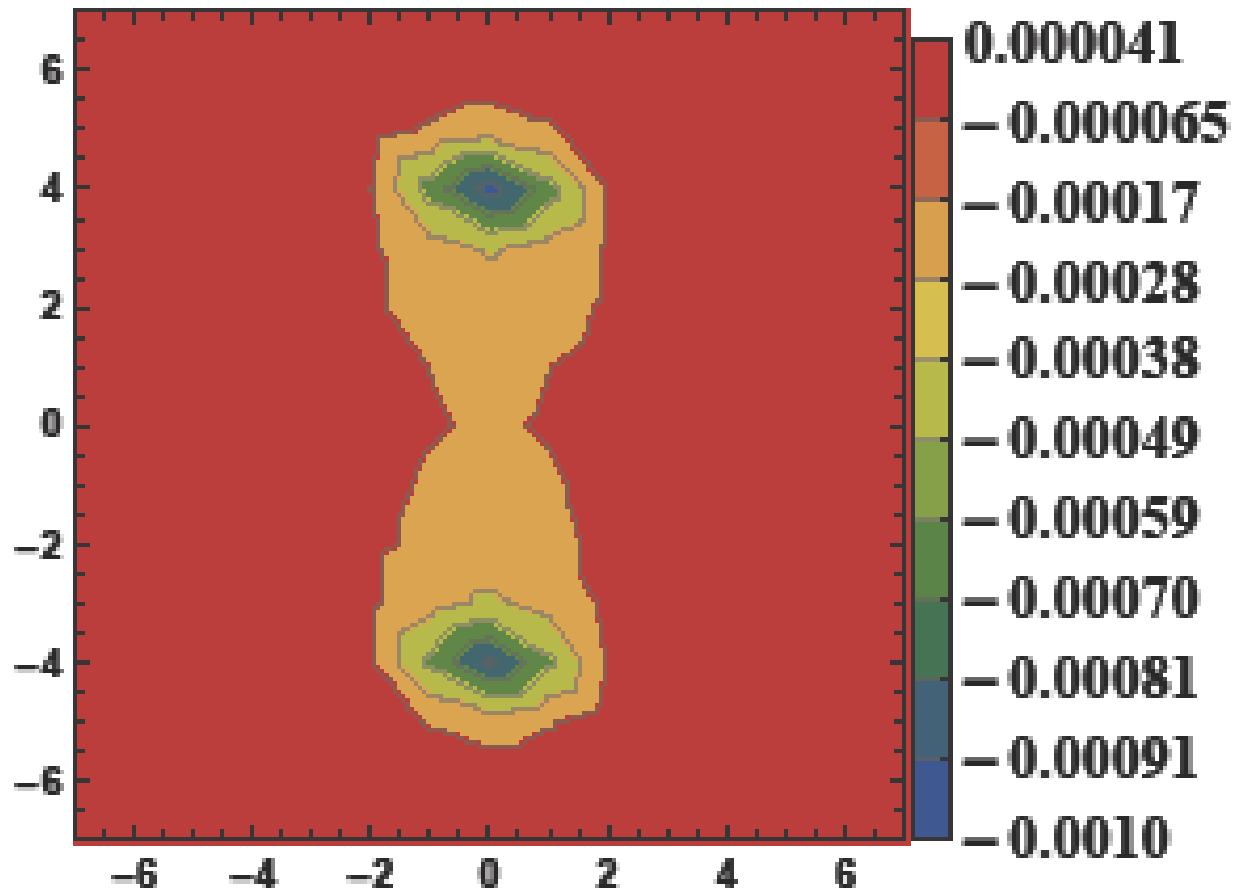
The hybrid QGQ flux tube in lattice QCD

B_x



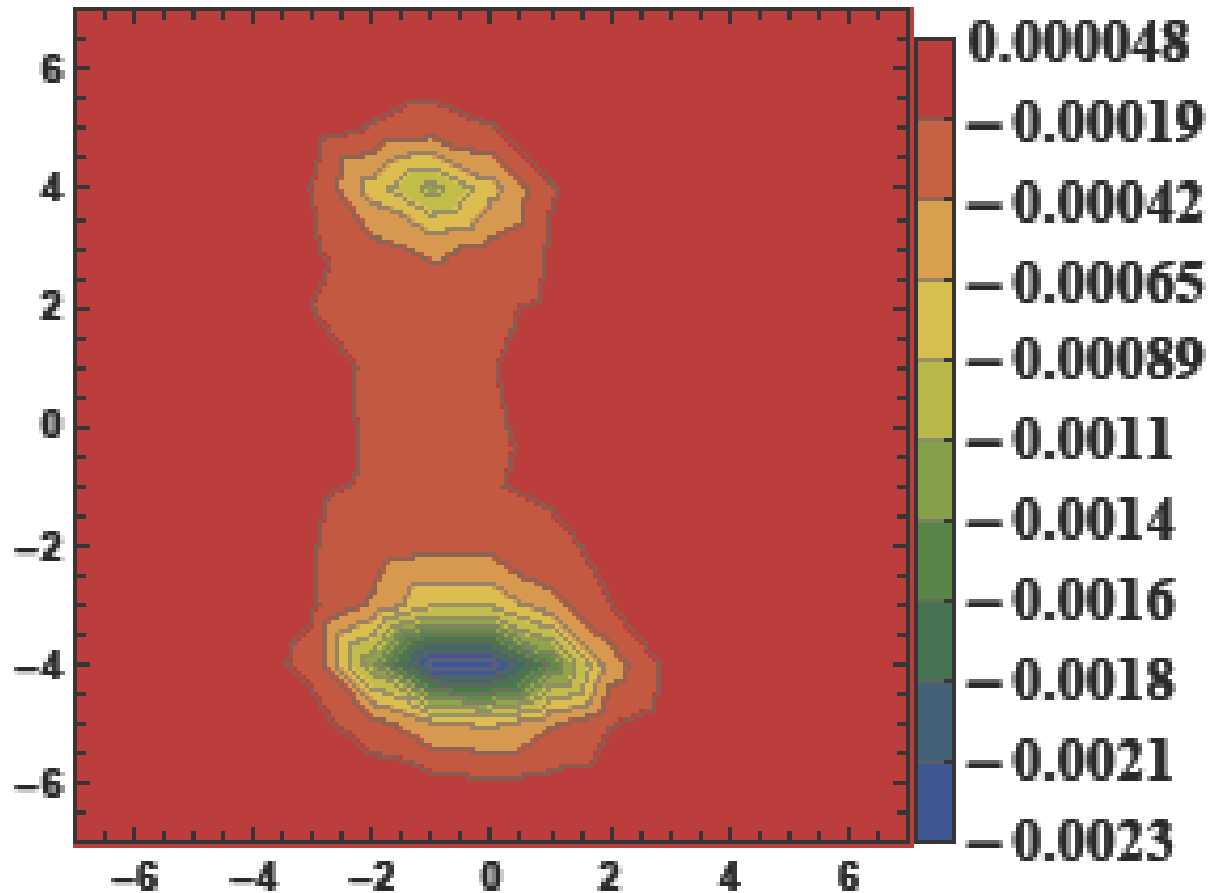
The hybrid QGQ flux tube in lattice QCD

By



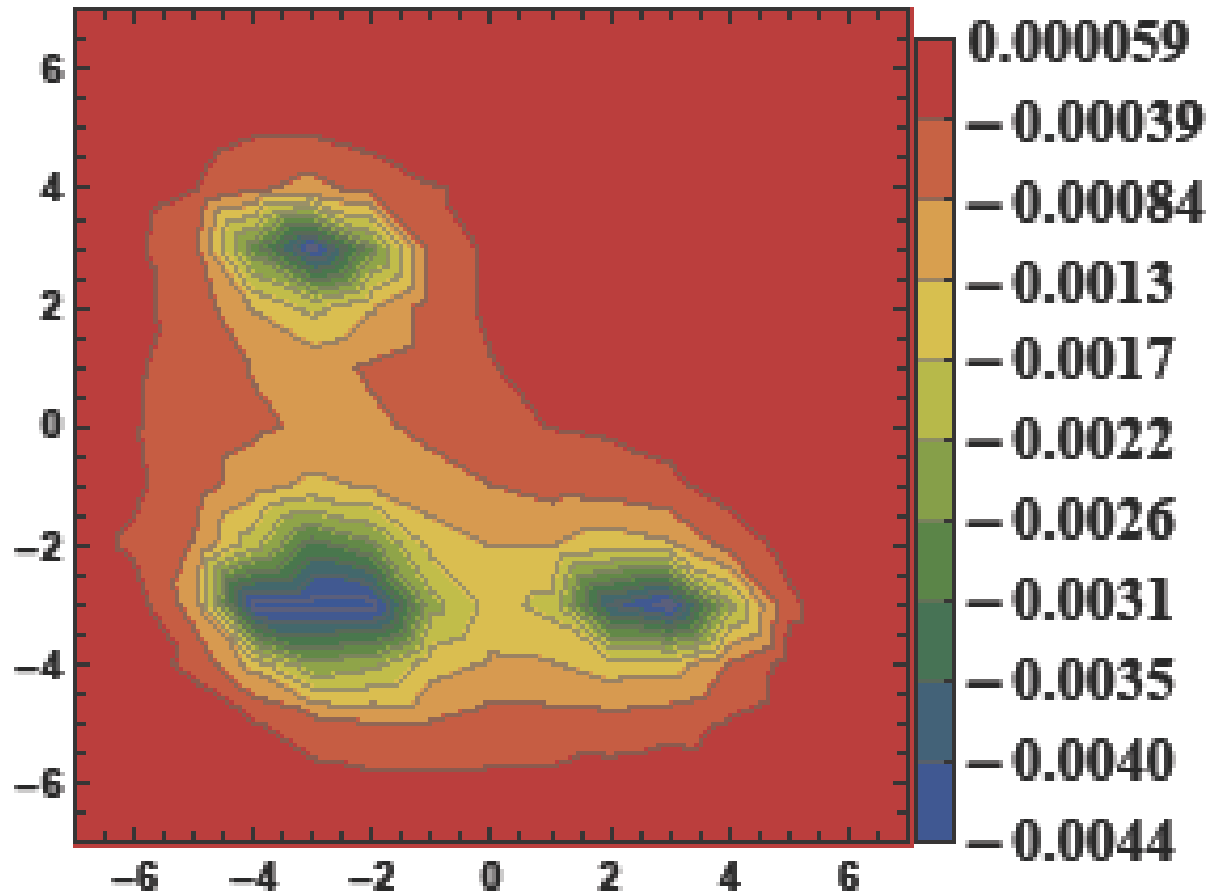
The hybrid QGQ flux tube in lattice QCD

By



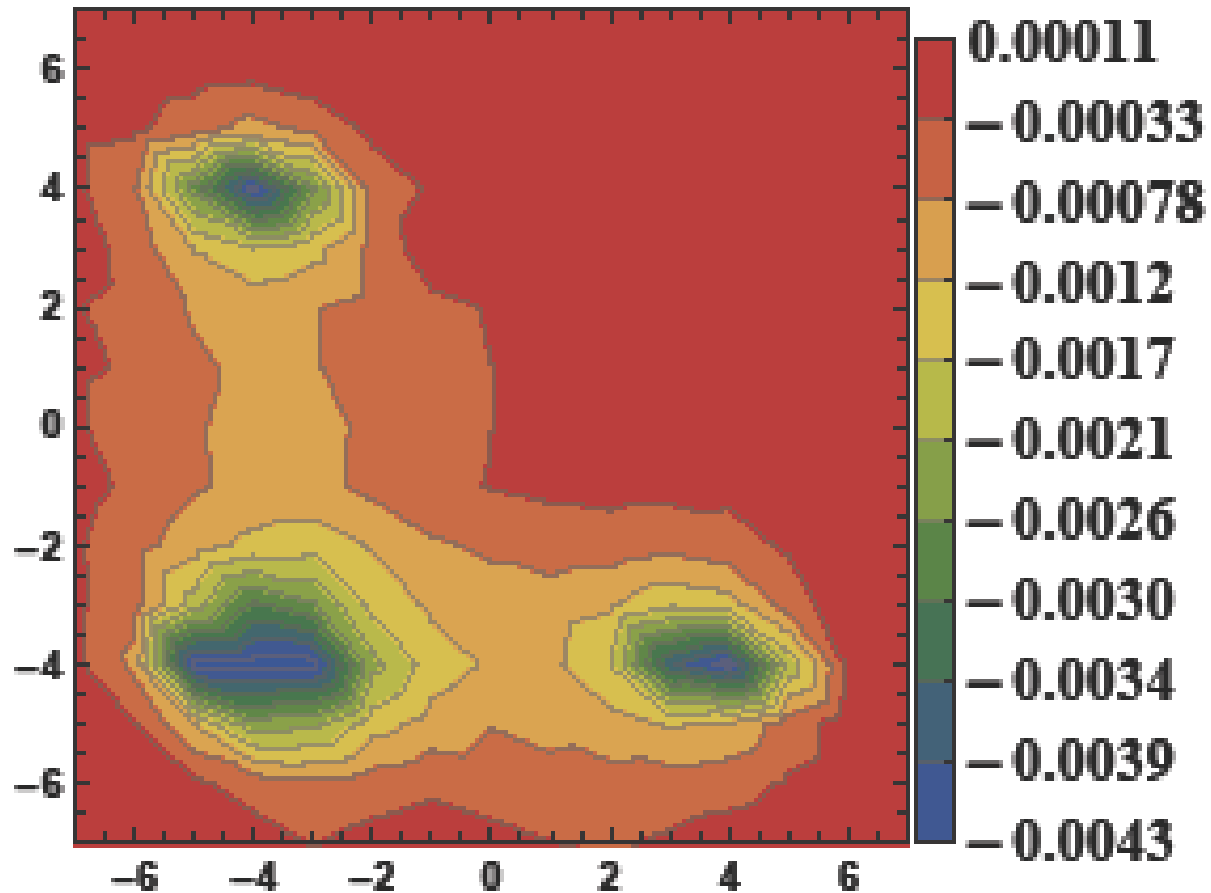
The hybrid QGQ flux tube in lattice QCD

By



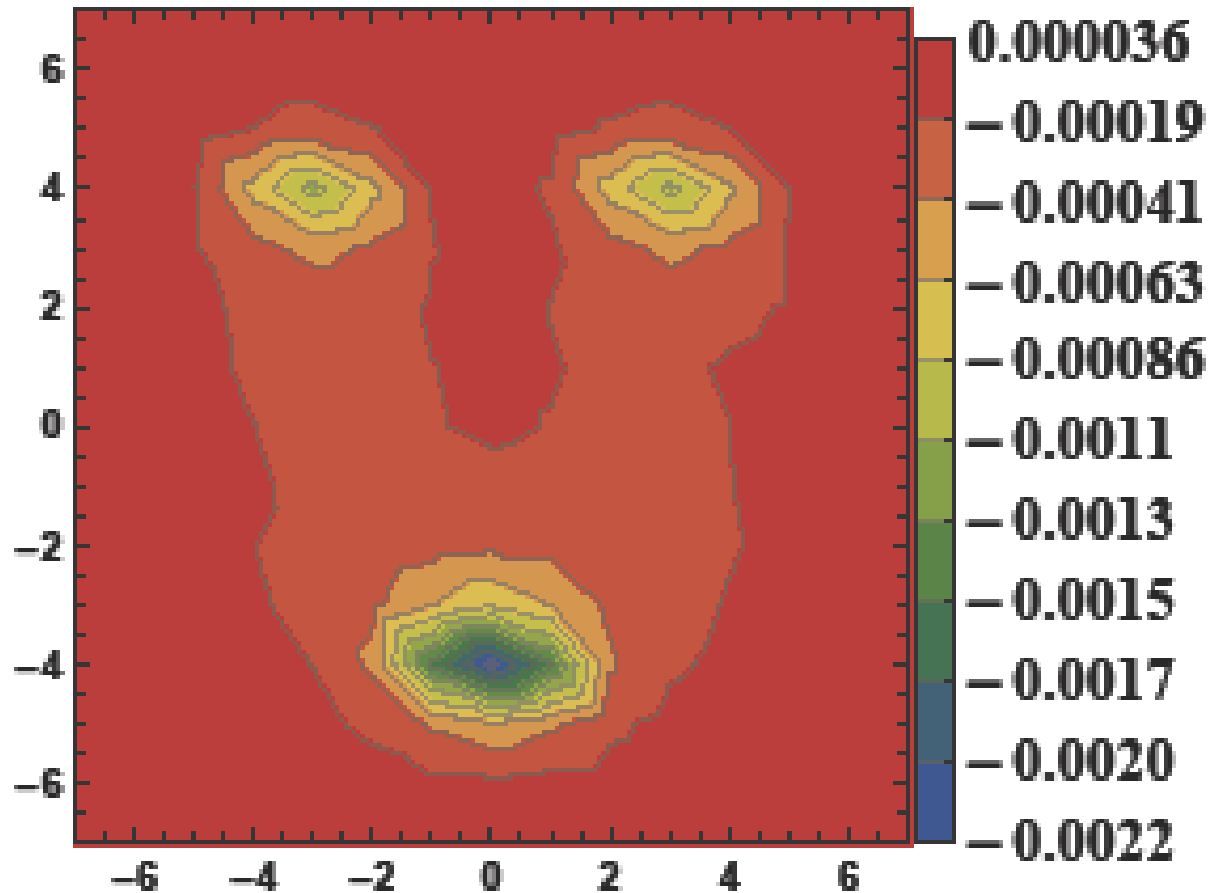
The hybrid QGQ flux tube in lattice QCD

By



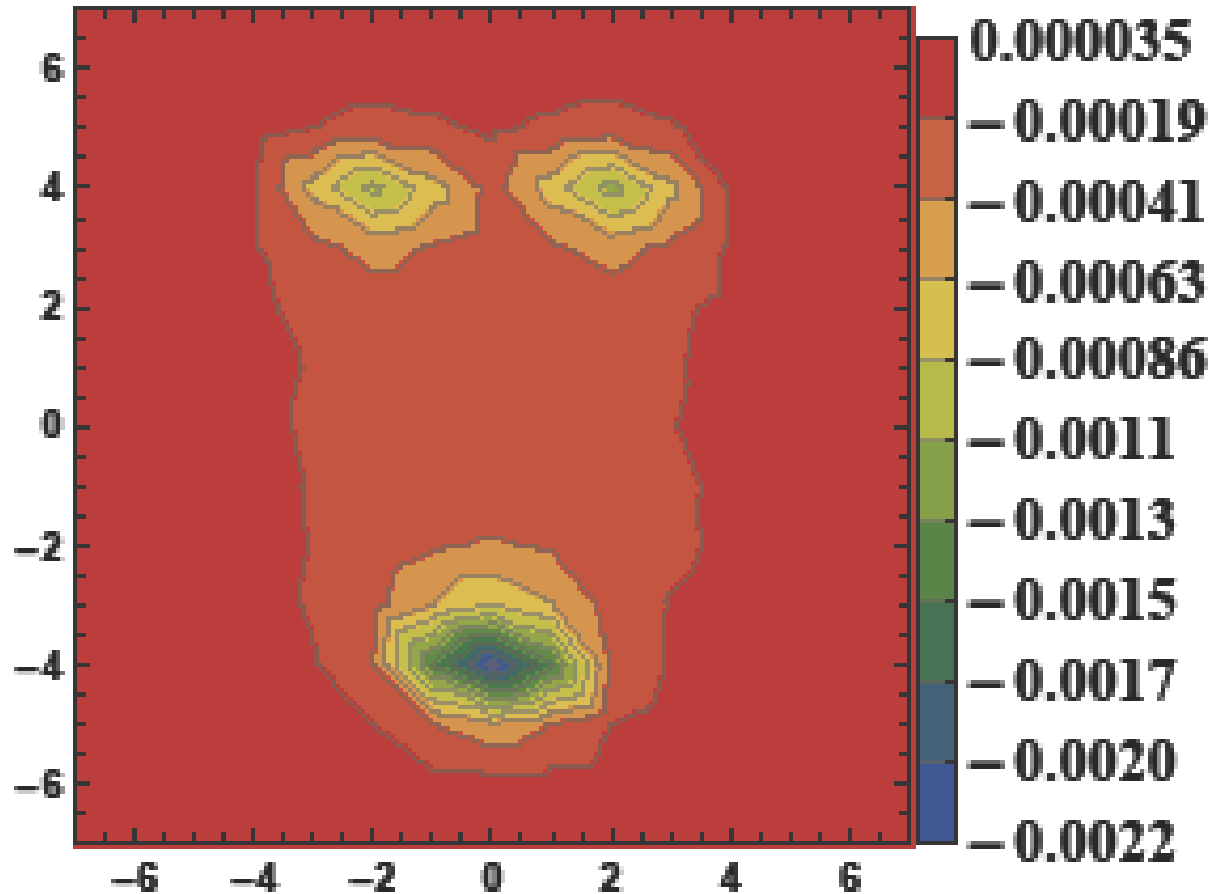
The hybrid QGQ flux tube in lattice QCD

By



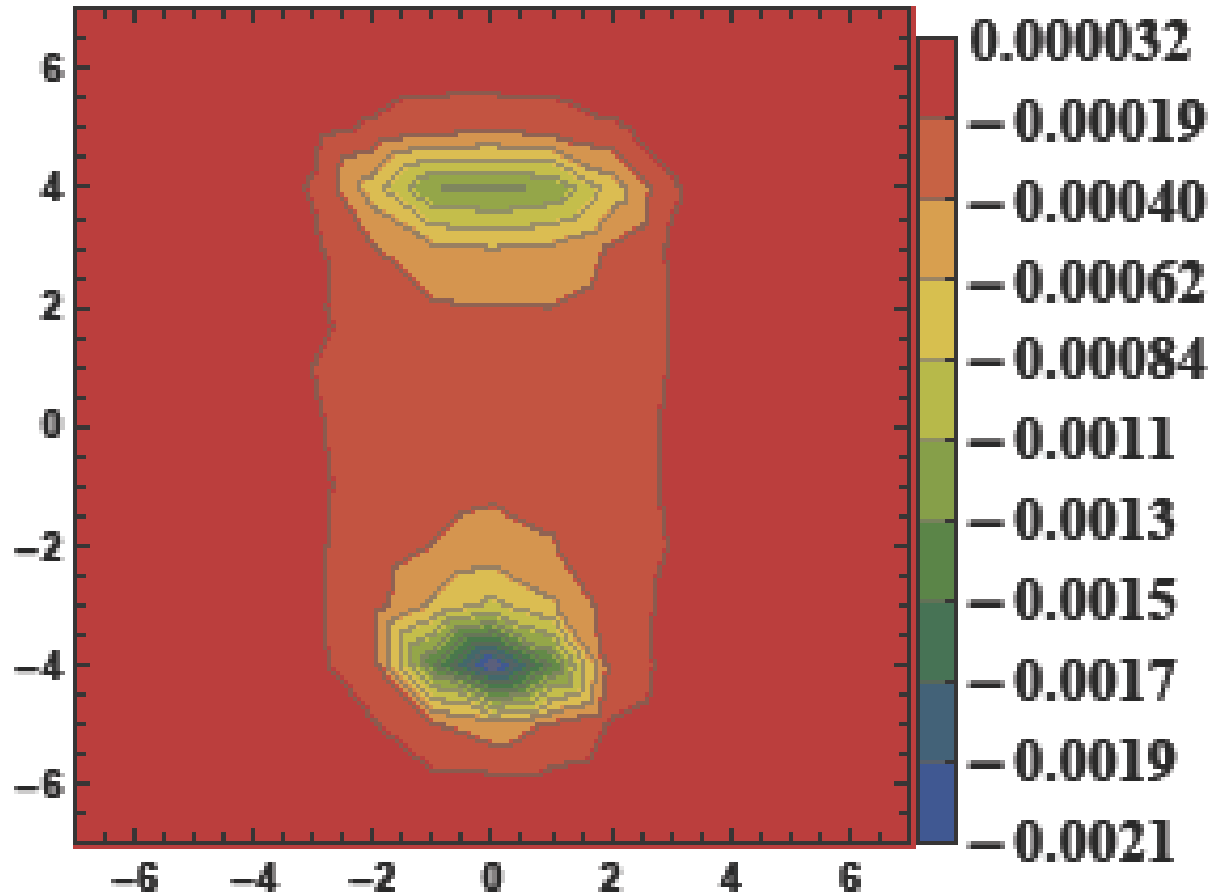
The hybrid QGQ flux tube in lattice QCD

By



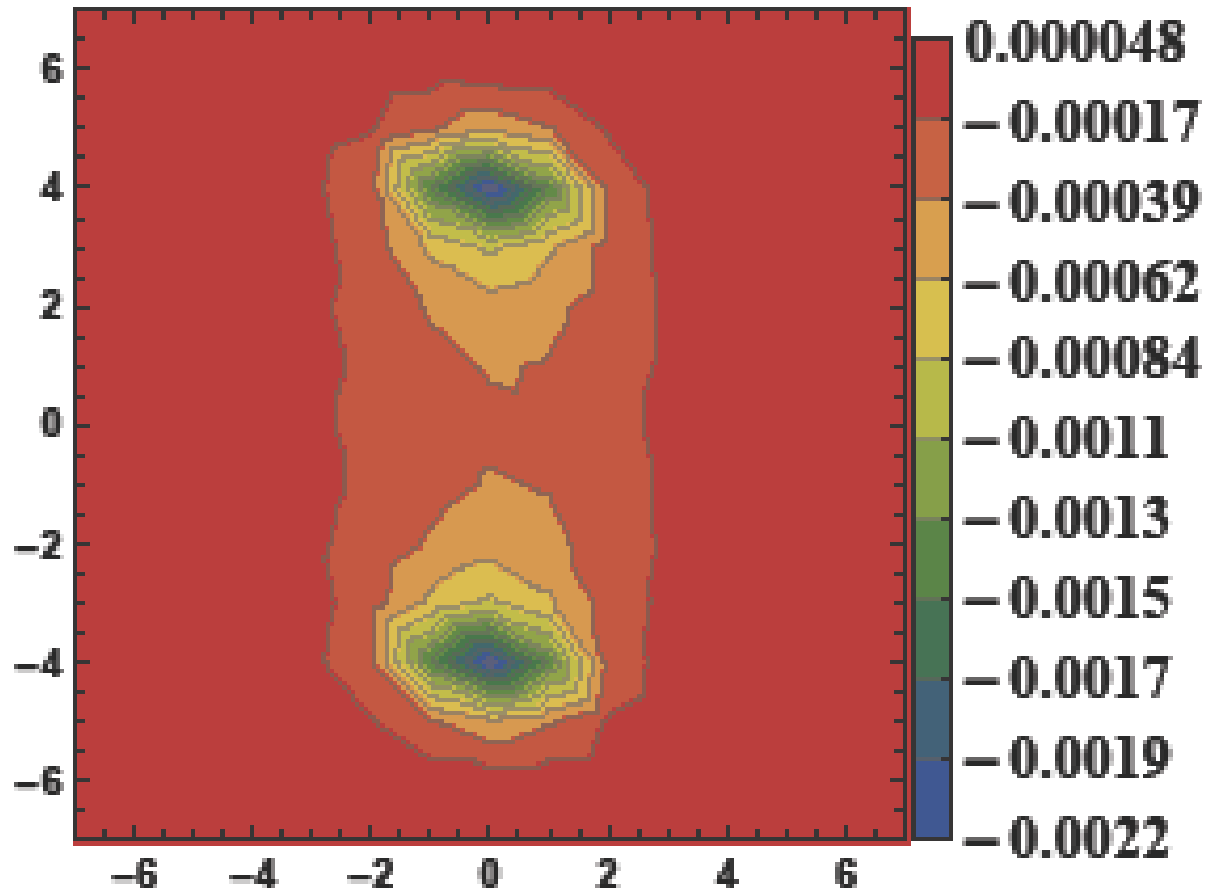
The hybrid QGQ flux tube in lattice QCD

By



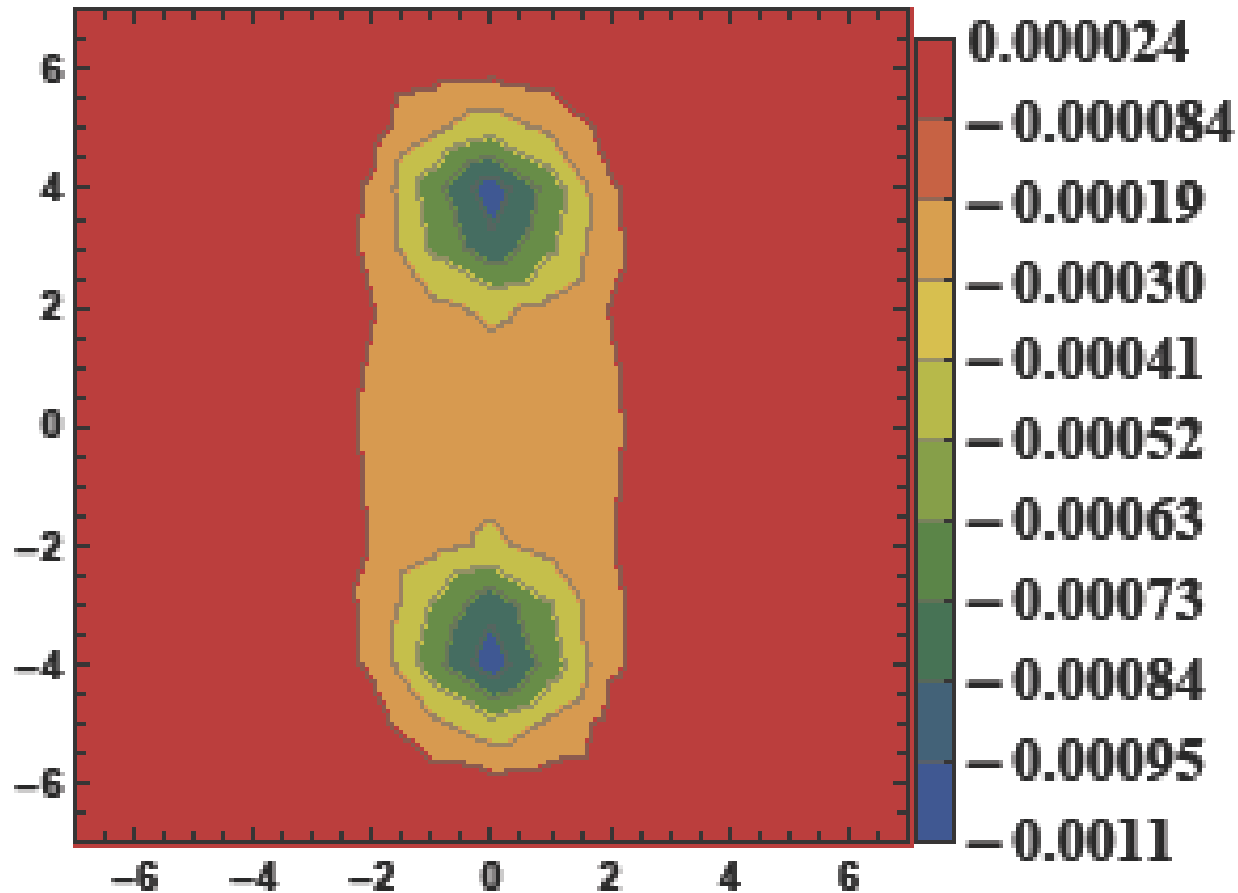
The hybrid QGQ flux tube in lattice QCD

By



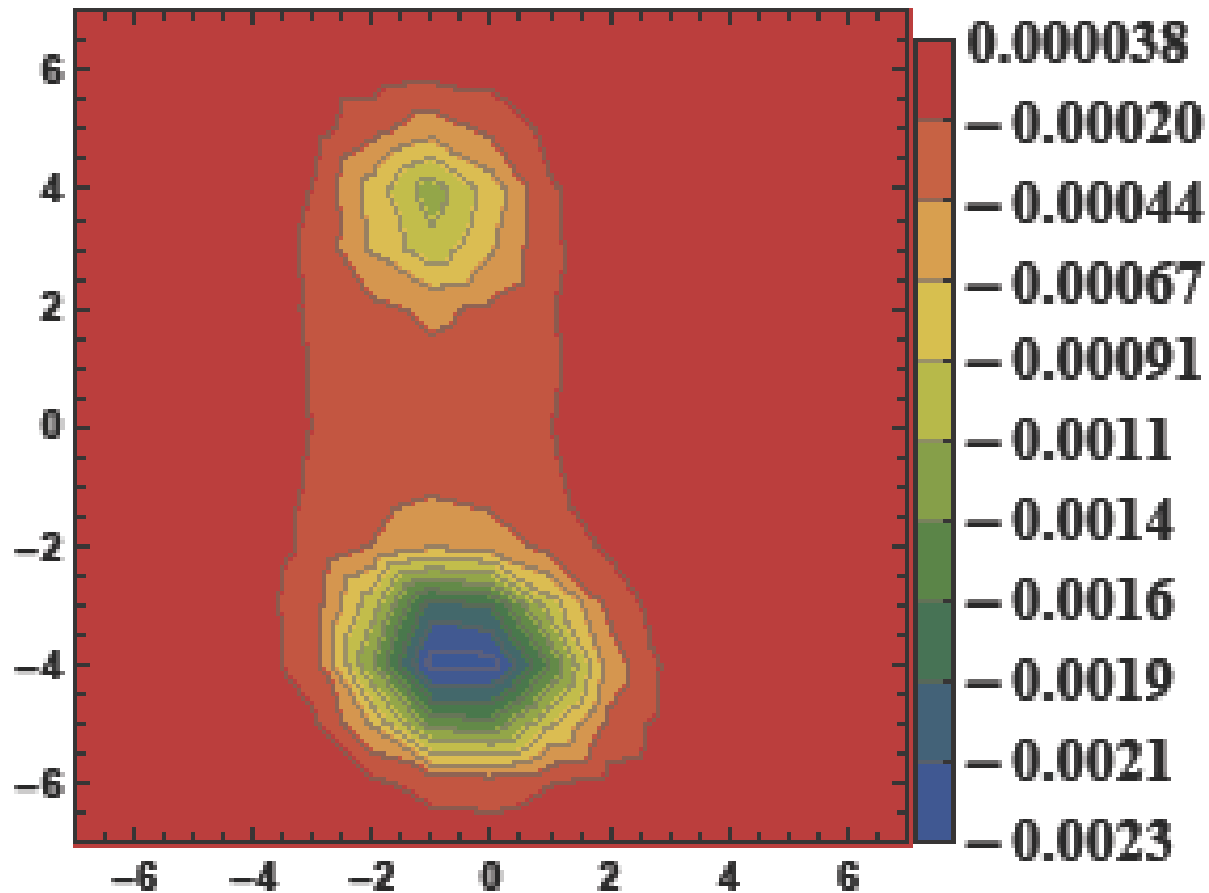
The hybrid QGQ flux tube in lattice QCD

Bz



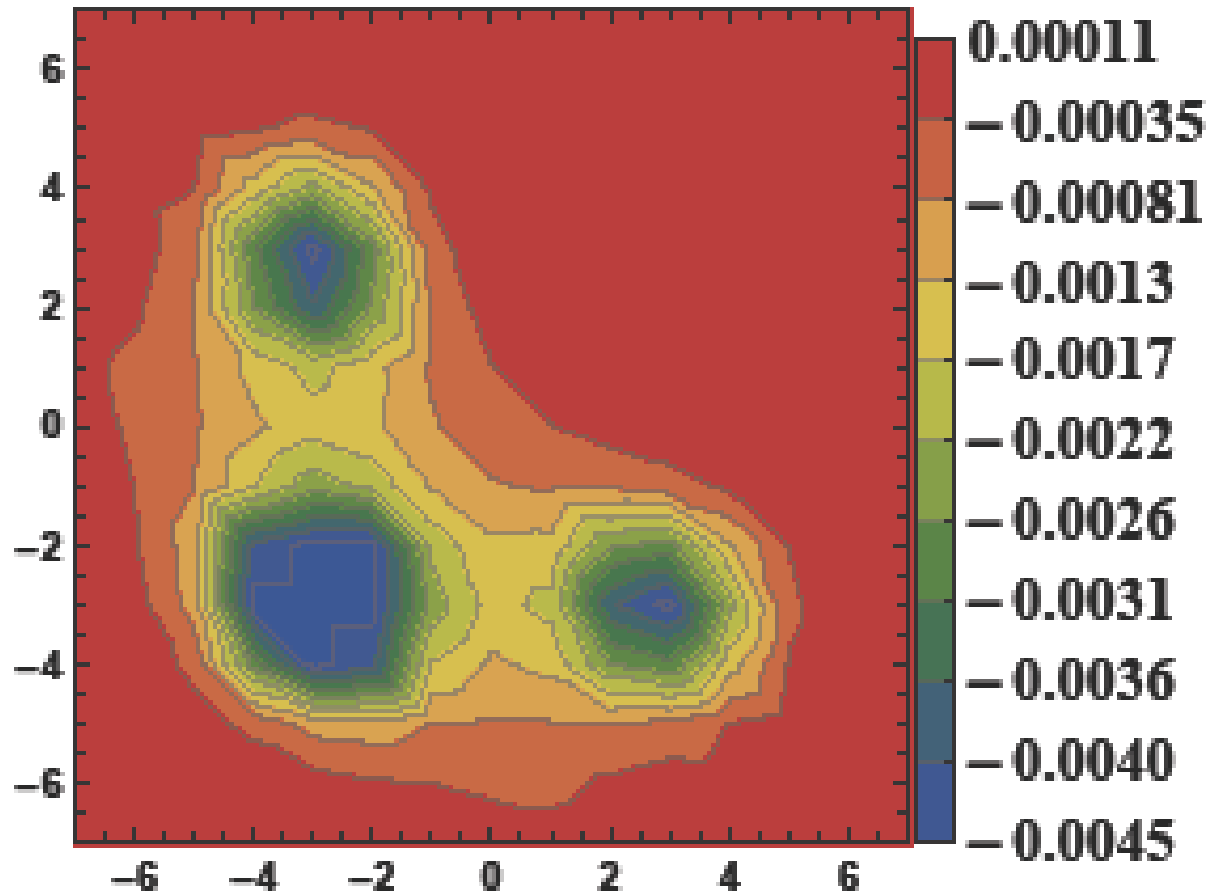
The hybrid QGQ flux tube in lattice QCD

Bz



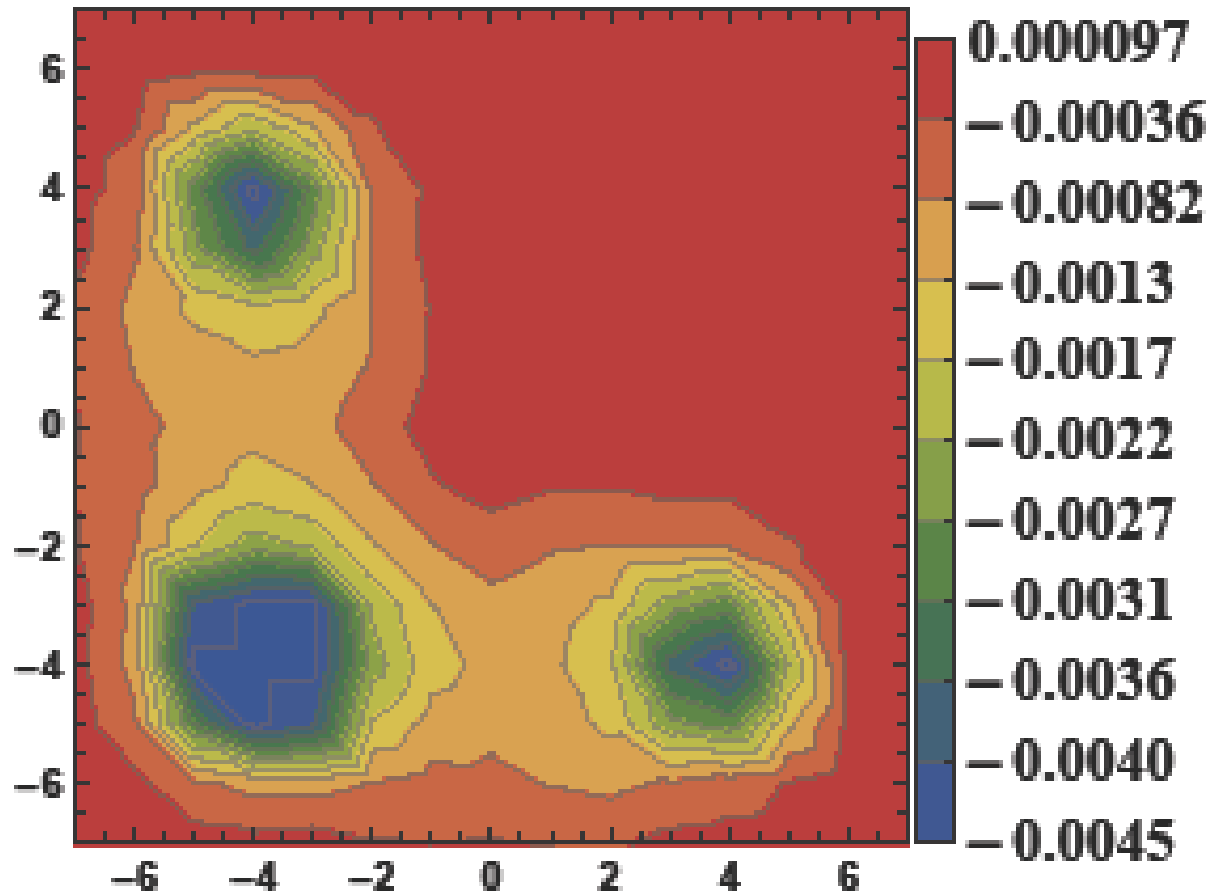
The hybrid QGQ flux tube in lattice QCD

B_z



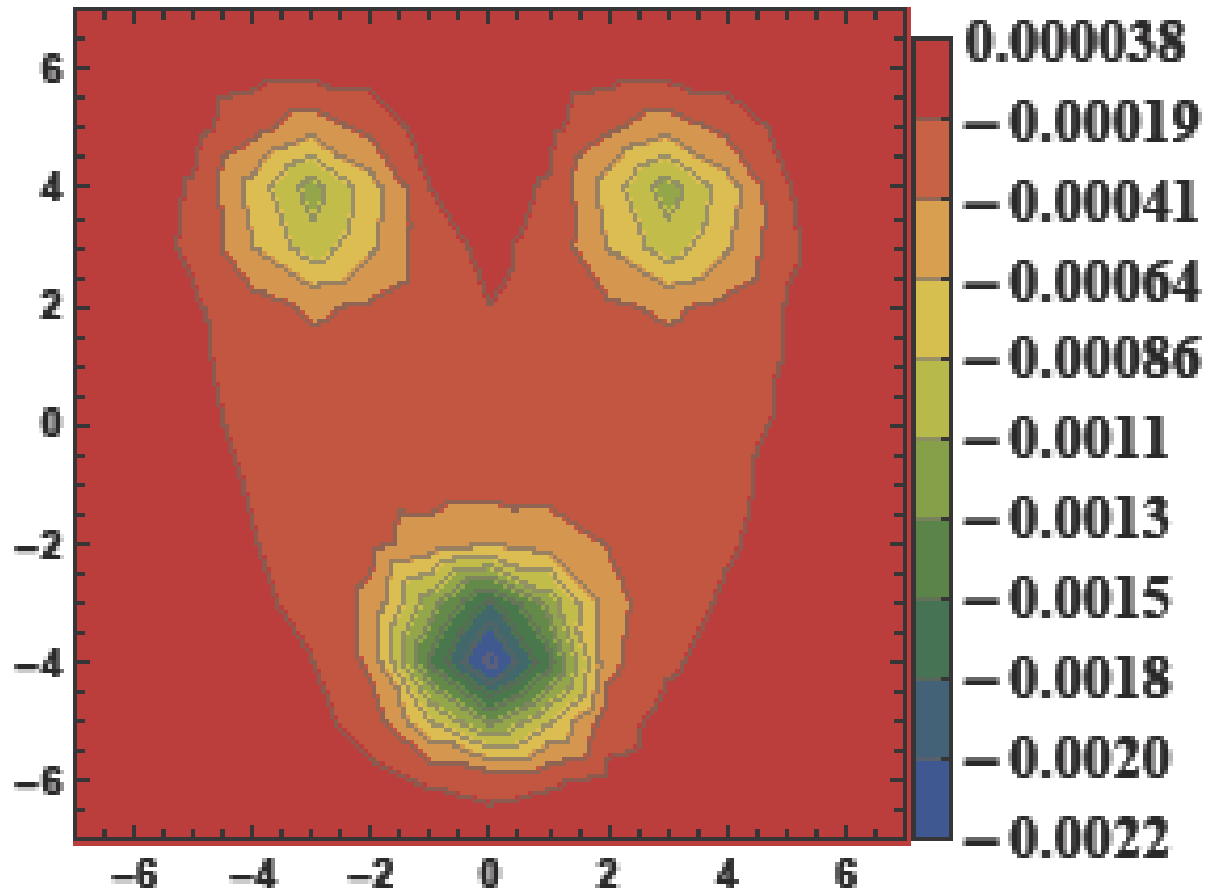
The hybrid QGQ flux tube in lattice QCD

Bz



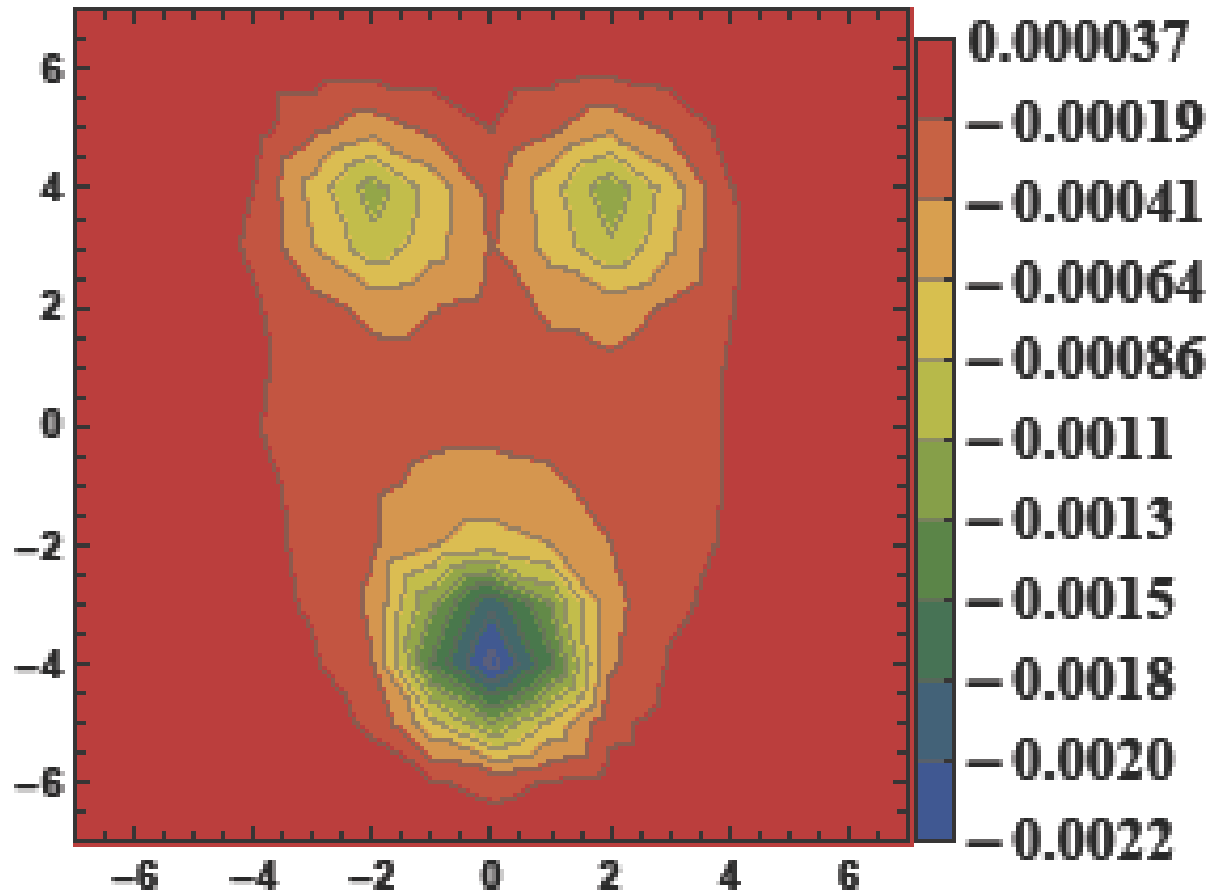
The hybrid QGQ flux tube in lattice QCD

Bz



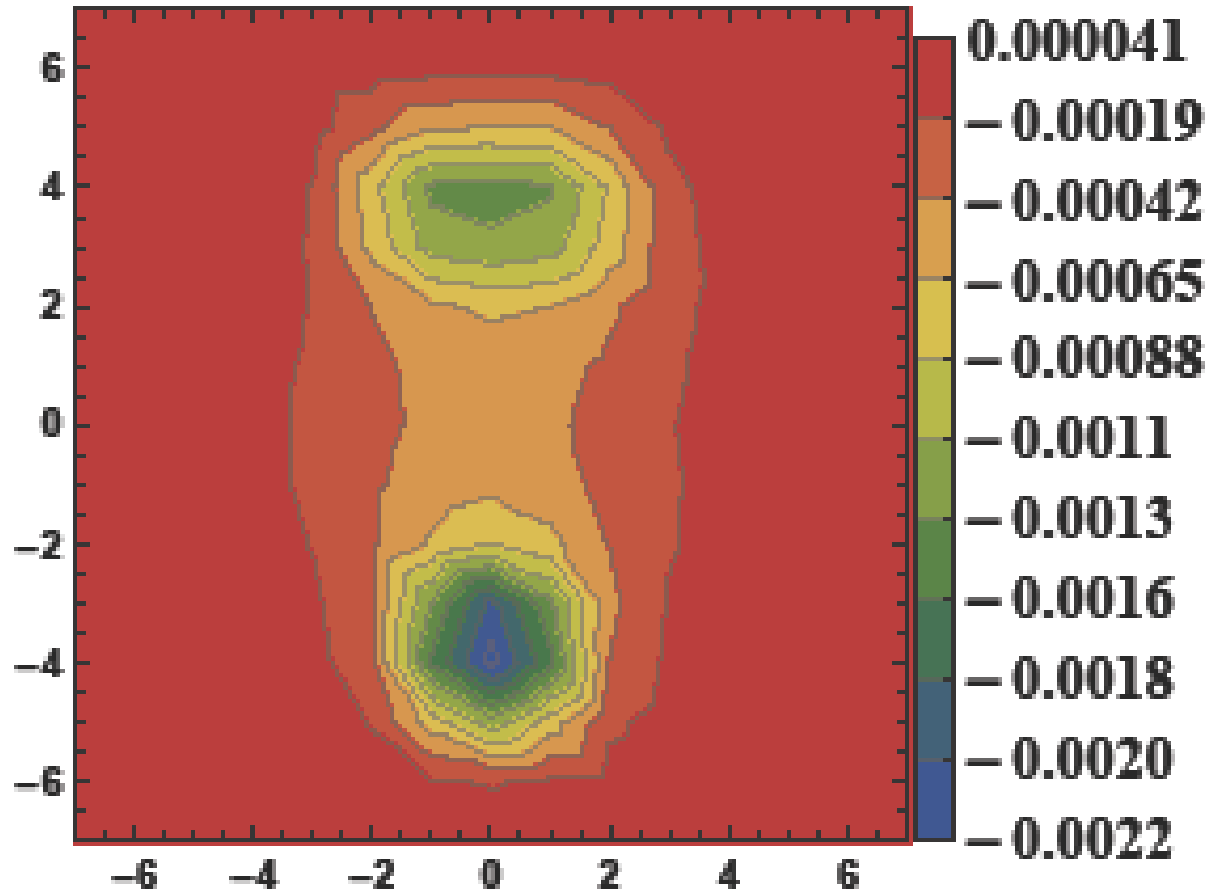
The hybrid QGQ flux tube in lattice QCD

Bz



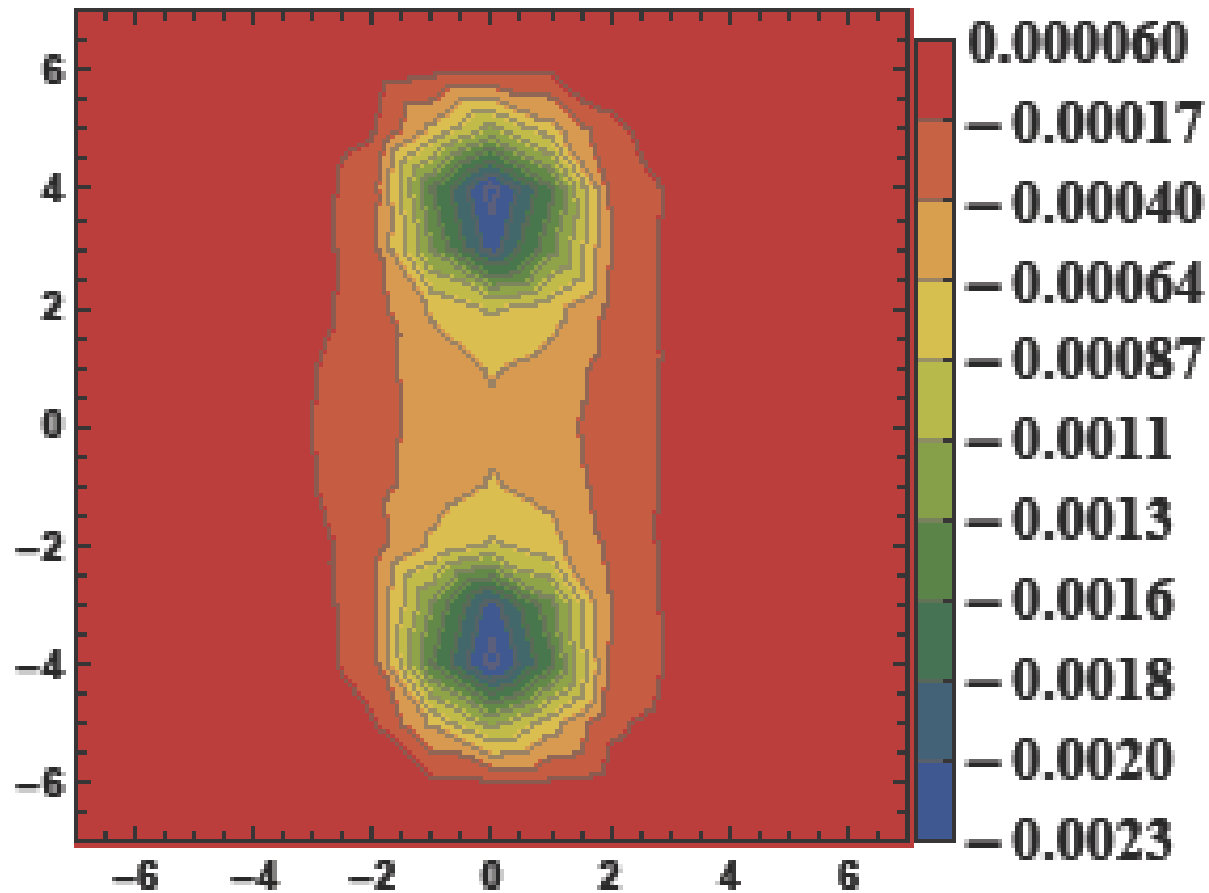
The hybrid QGQ flux tube in lattice QCD

B_z



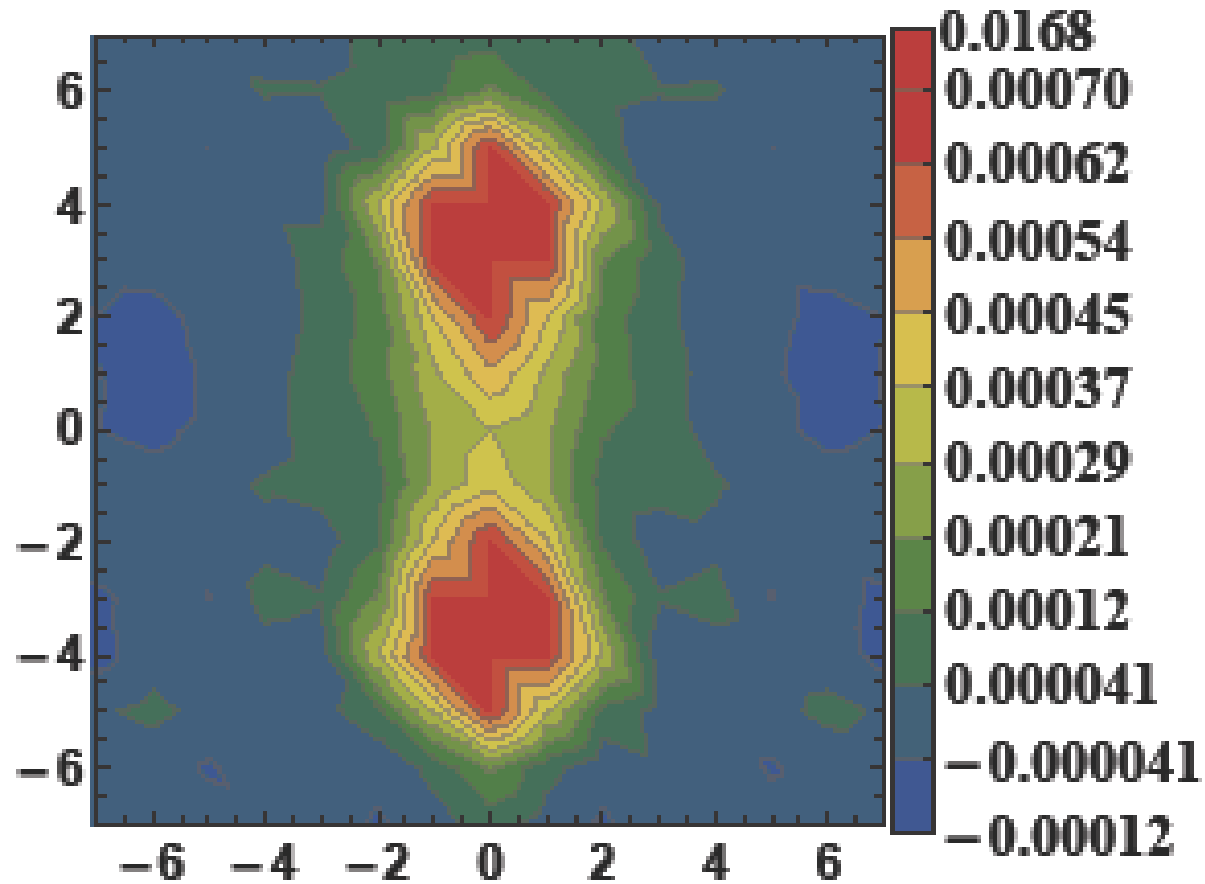
The hybrid QGQ flux tube in lattice QCD

Bz



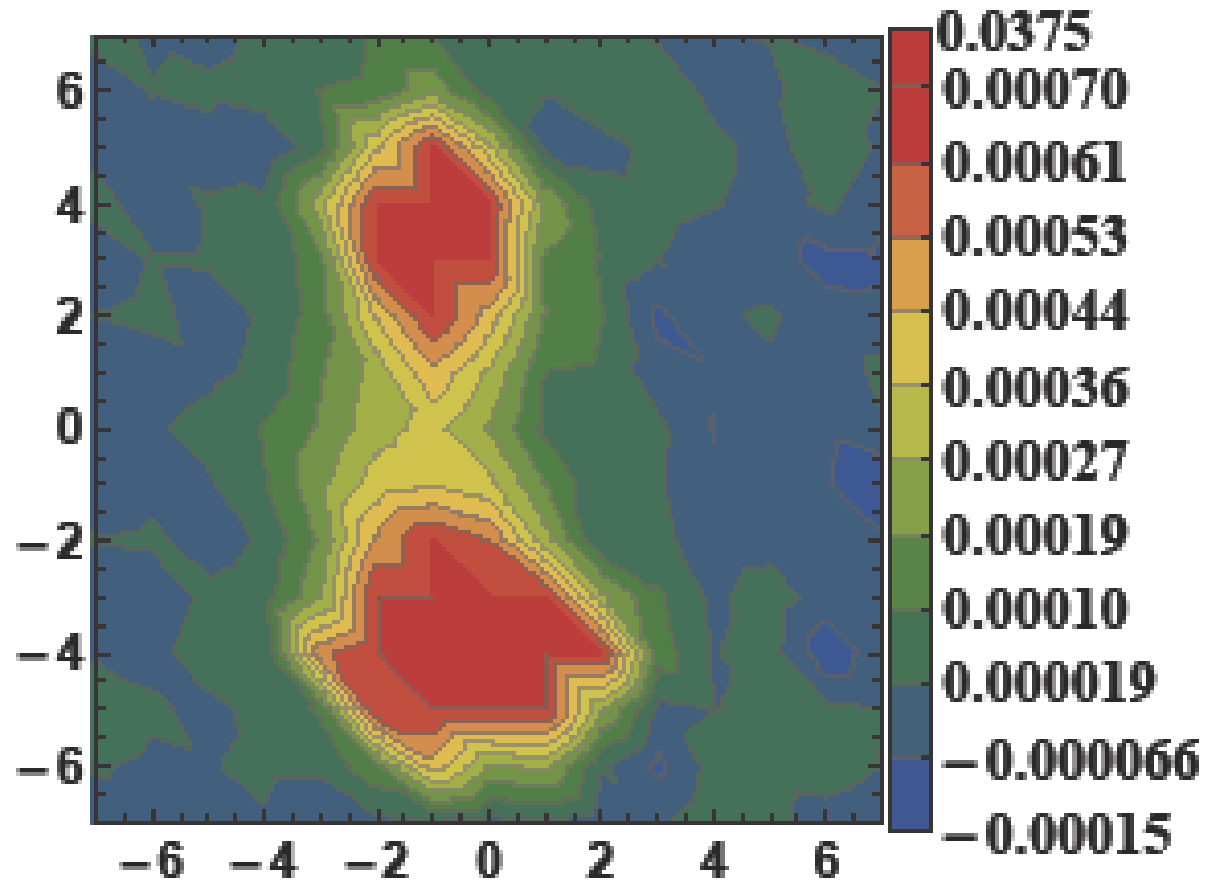
The hybrid QGQ flux tube in lattice QCD

U



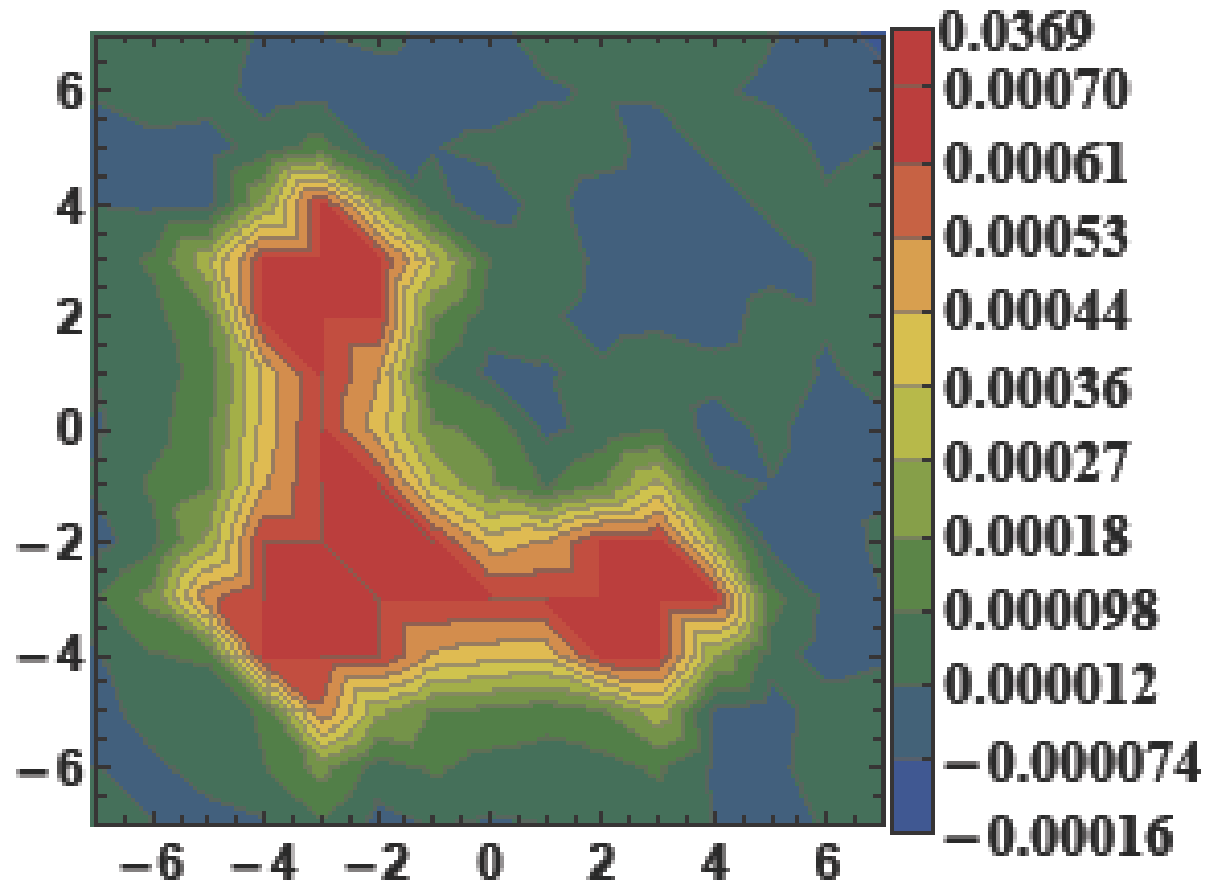
The hybrid $QG\bar{Q}$ flux tube in lattice QCD

U



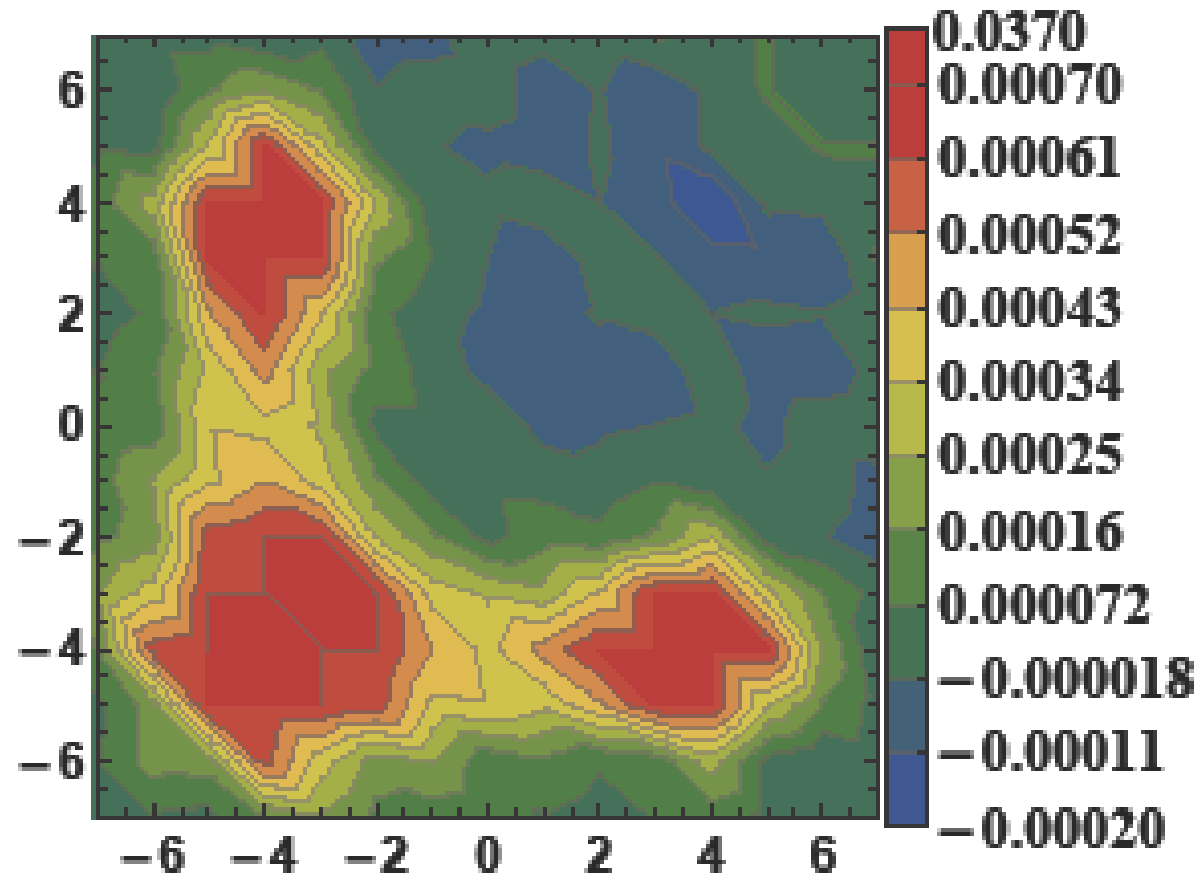
The hybrid $QG\bar{Q}$ flux tube in lattice QCD

U



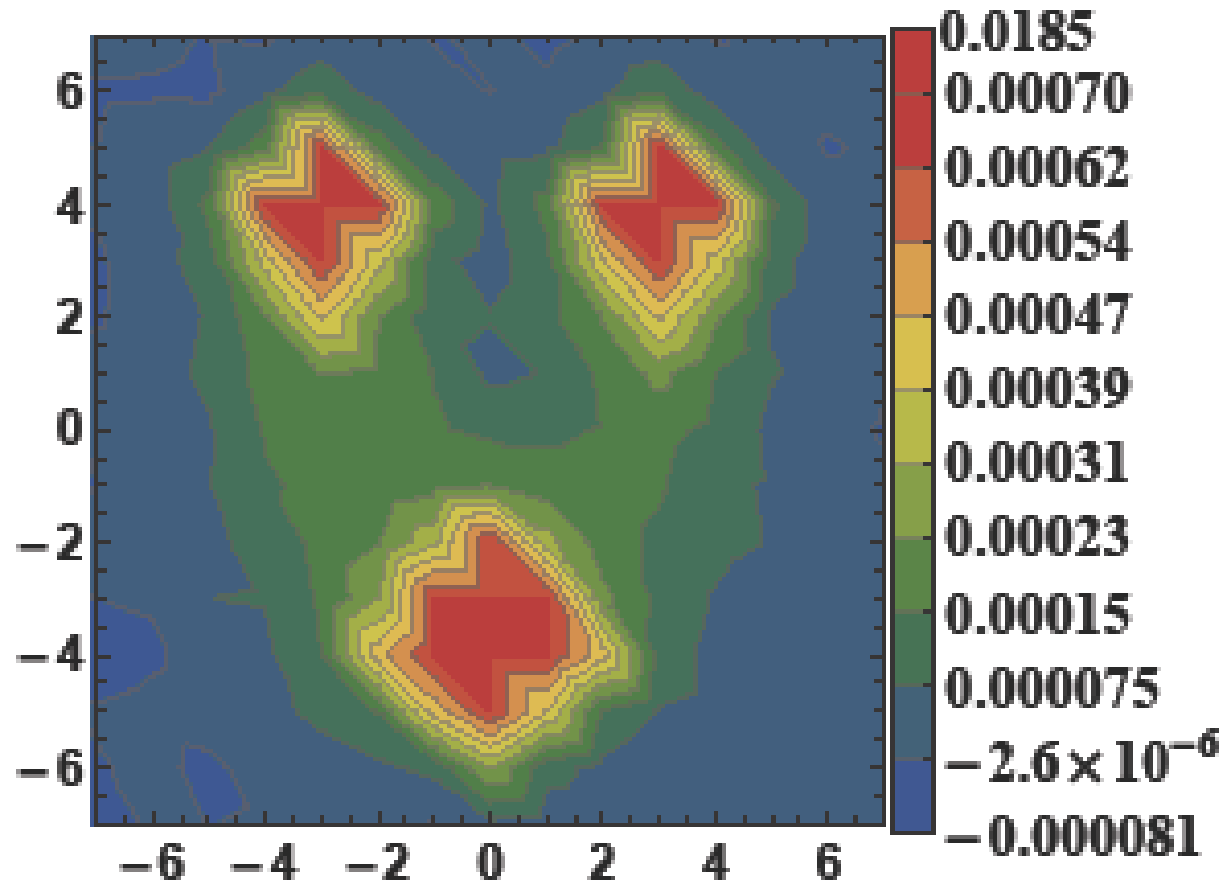
The hybrid QGQ flux tube in lattice QCD

U



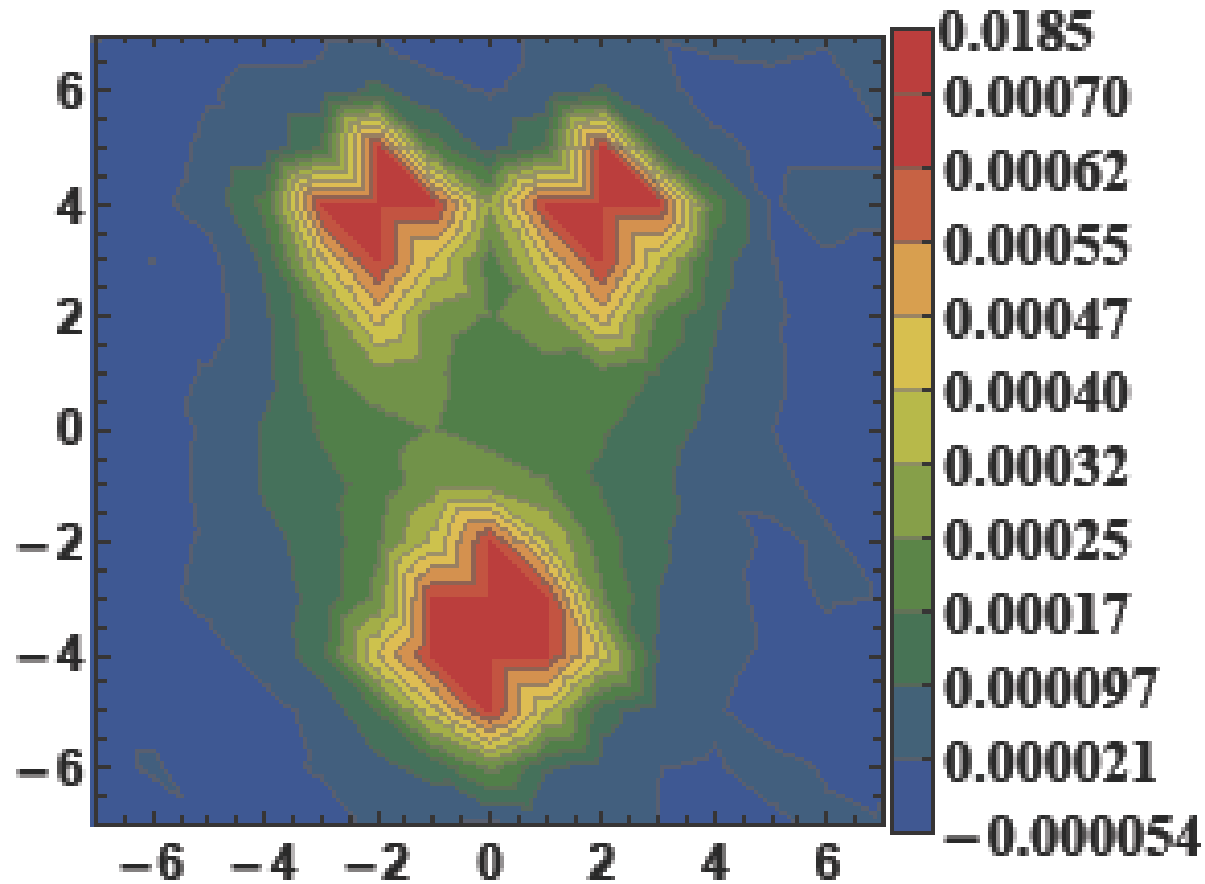
The hybrid QGQ flux tube in lattice QCD

U



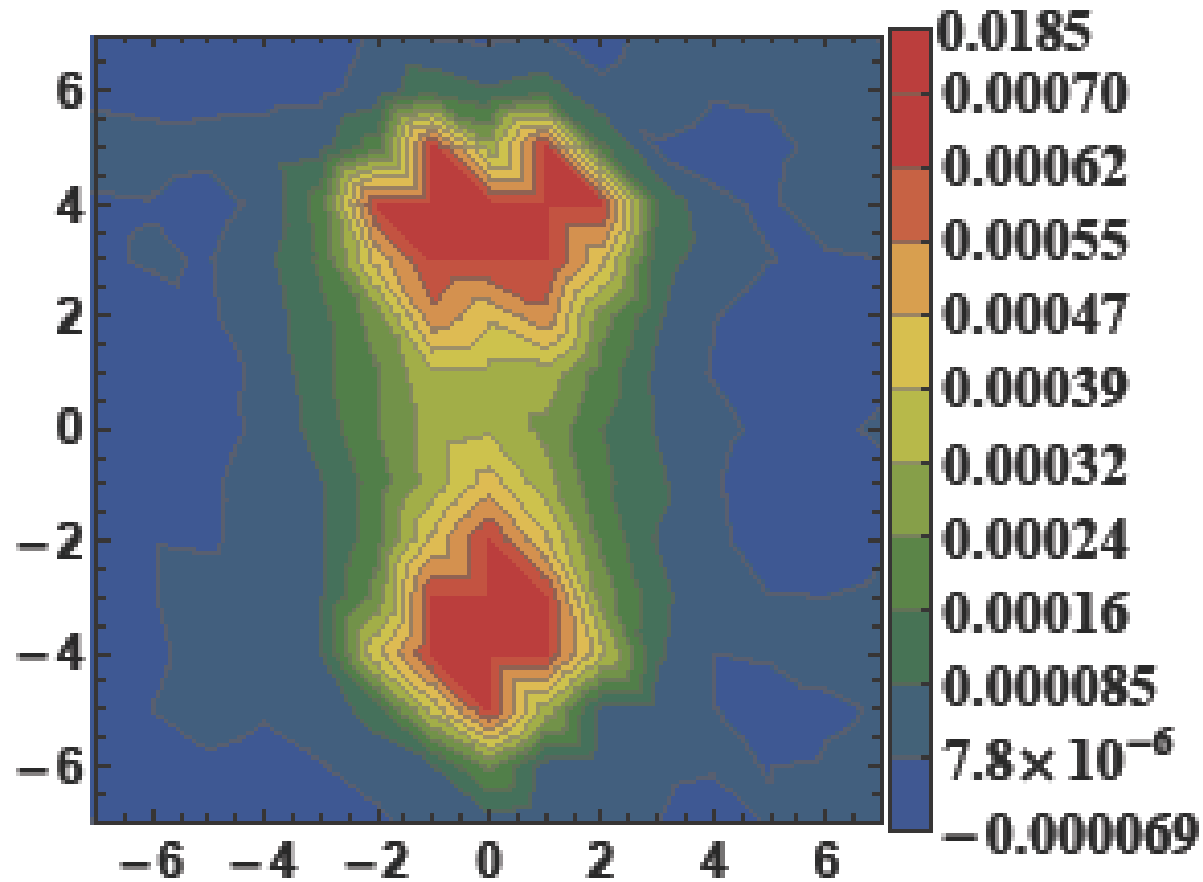
The hybrid QGQ flux tube in lattice QCD

U



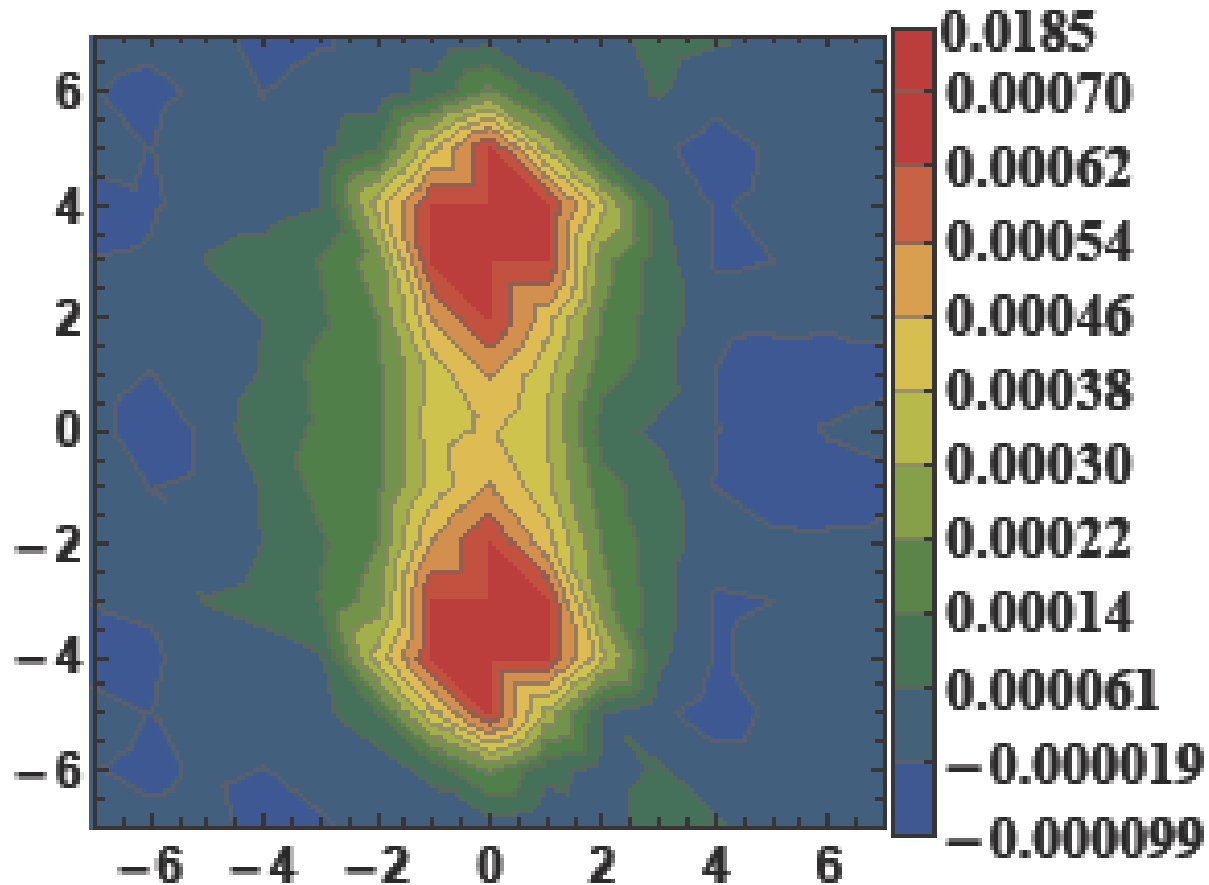
The hybrid QGQ flux tube in lattice QCD

U



The hybrid $QG\bar{Q}$ flux tube in lattice QCD

U

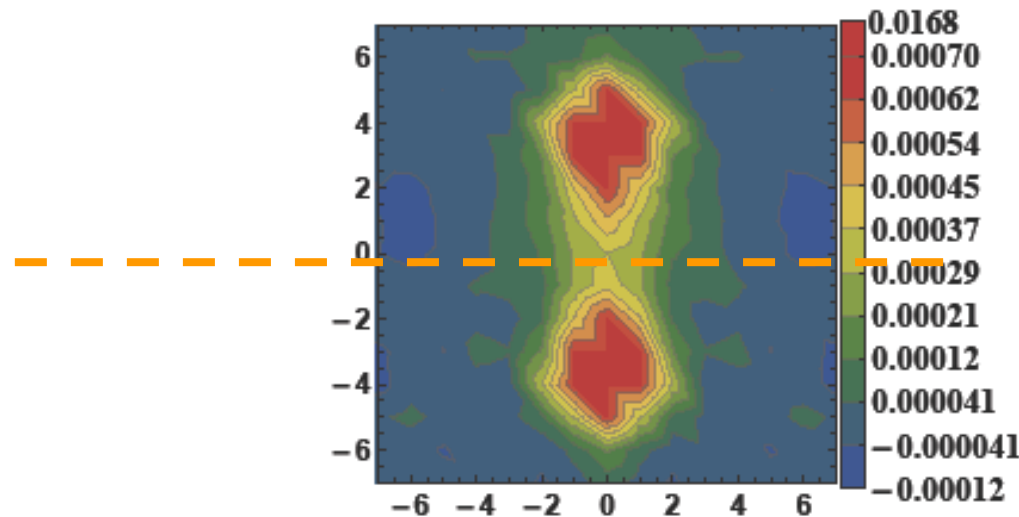


The hybrid QGQ flux tube in lattice QCD

Moreover we can fit the decay, or penetration length, of the chromofields in the vacuum.

For instance with a fit of the field energy in the quark-antiquark system,

with a cut
at the mid
distance
quark-antiquark

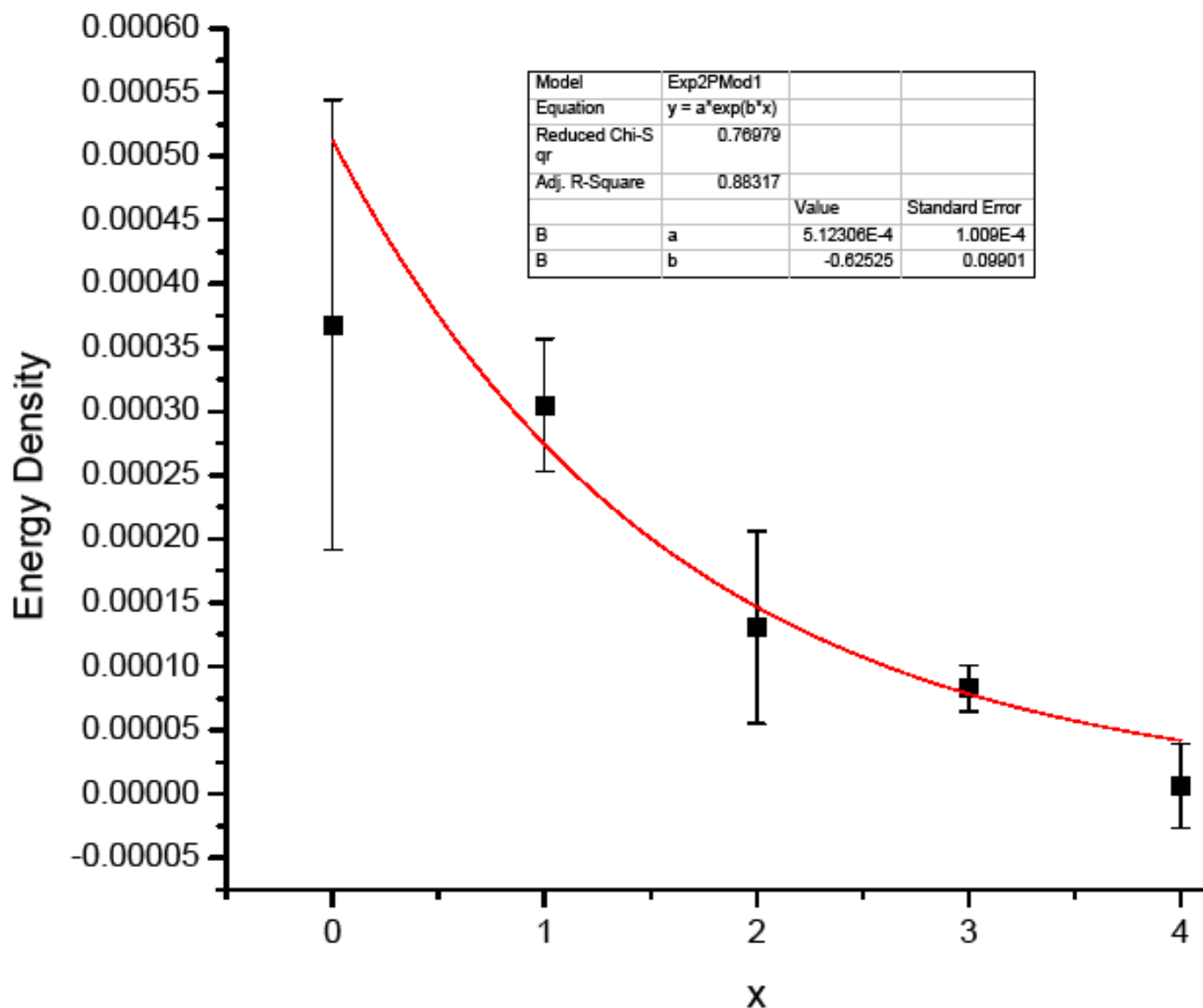


we find a scale similar of $\sim 1.7 \text{ GeV}$ similar to the confinement scale of Hideo Suganuma or the $\text{mass}_{\text{monopole}} \sim 2 \text{ mass}_{\text{gluon}}$ of Mike Cornwall and to the monopole size used by Claudia Ratti.

The hybrid $Q\bar{Q}$ flux tube in lattice QCD

we get for
 $u = A \text{Exp}[-m r]$
A penetration
length of
 $m \sim 0.63 \text{ a}^{-1}$

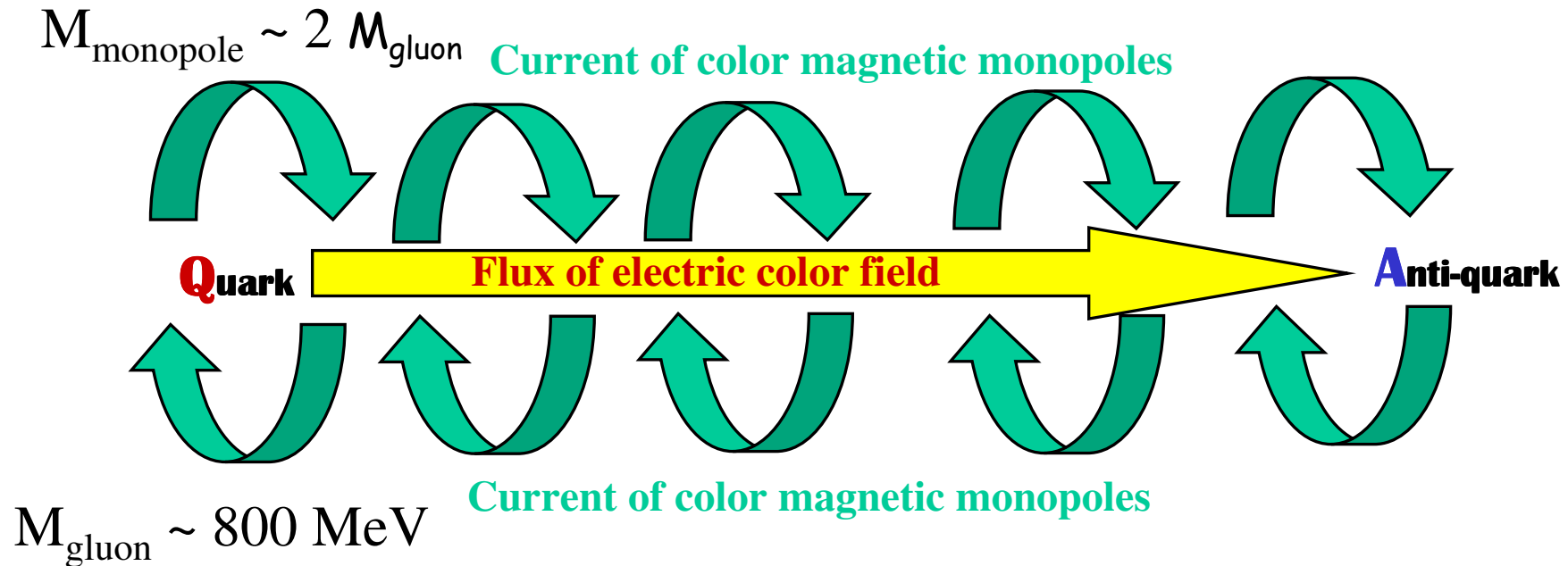
where
 $\sigma = 0.19 \text{ GeV}^2$
 $\text{a}^{-1} = 2.710 \text{ GeV}$
comparing with the
London photon mass
in superconductors,
this provides a scale
for a mass of
 $m \sim 1.7 \text{ GeV}$



Scalar confinement in Schwinger Dyson equations

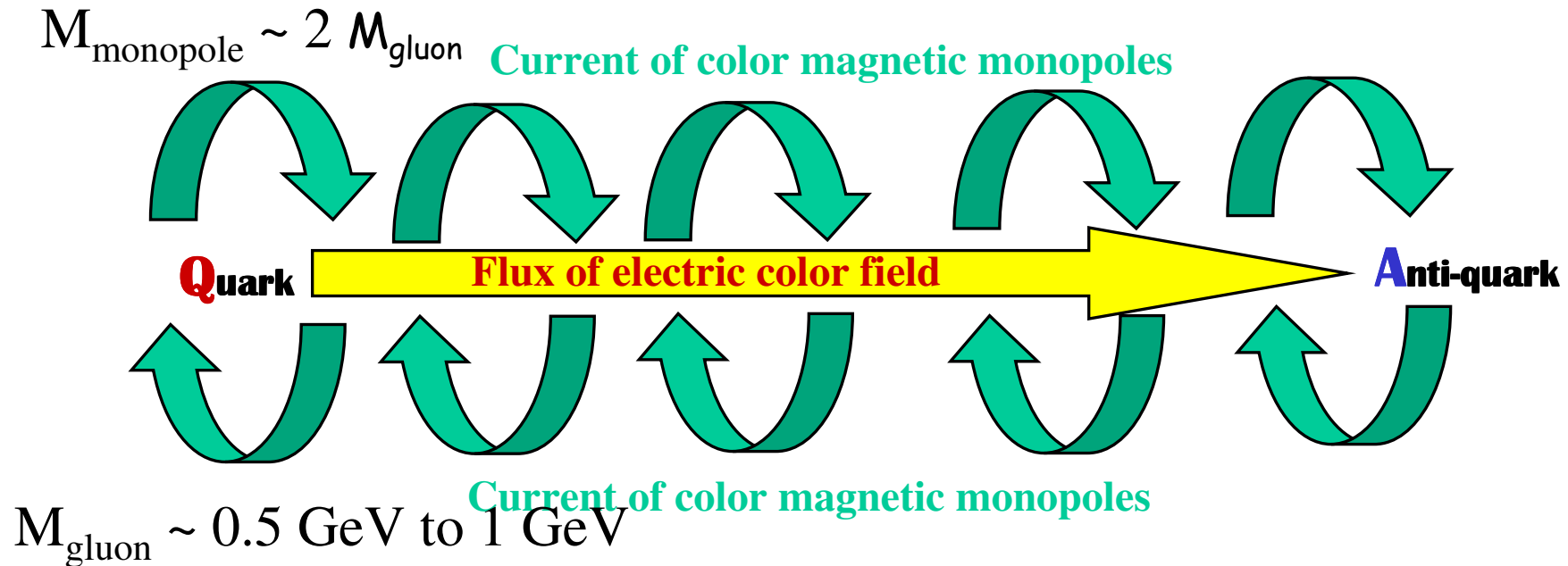
Scalar confinement in Schwinger Dyson Equations

The confinement picture in Lattice QCD exhibits a **flux tube, or string**, with tension $\sigma \sim 1 \text{ GeV} / \text{Fm}$.



Scalar confinement in Schwinger Dyson Equations

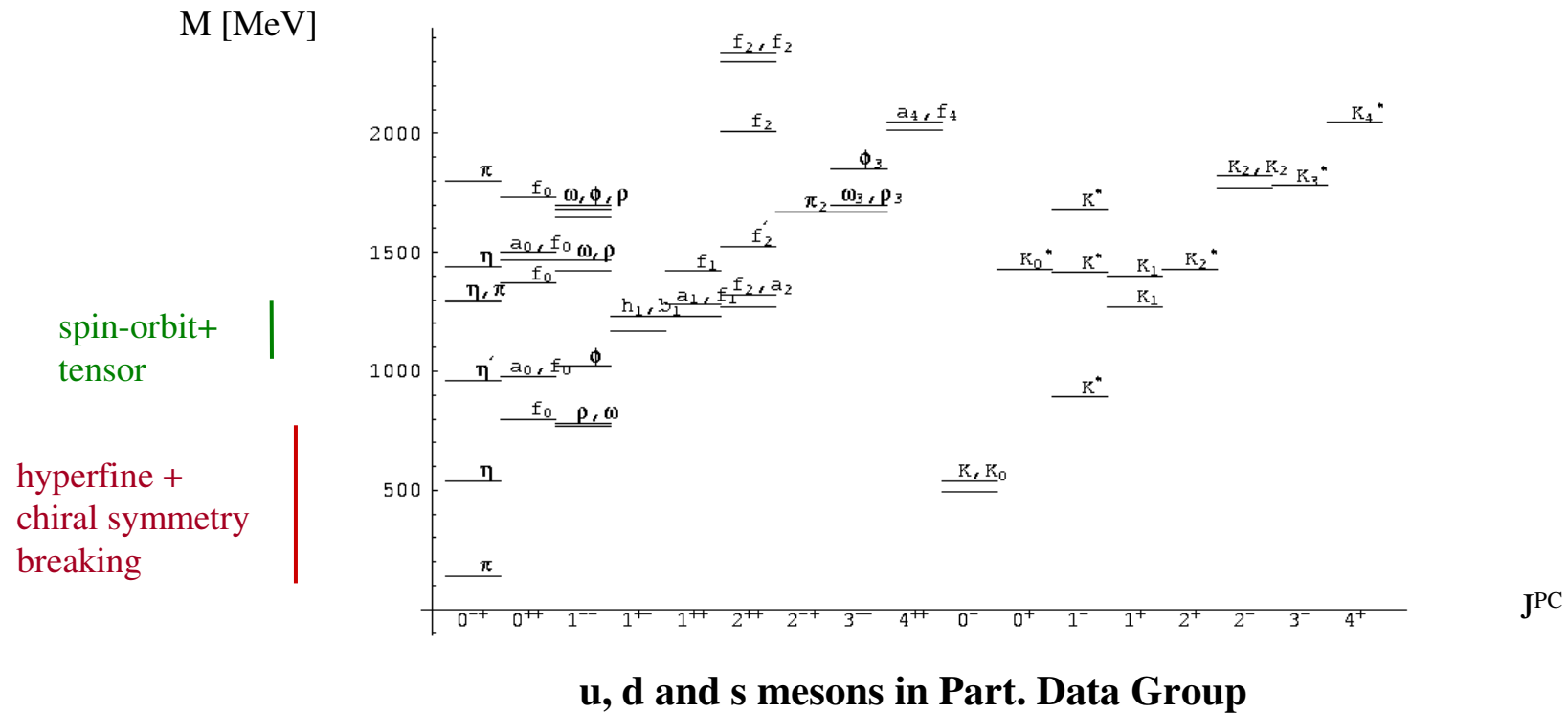
The confinement picture in Lattice QCD exhibits a **flux tube, or string**, with tension $\sigma \sim 1 \text{ GeV} / \text{Fm}$.



Although different perspectives of confinement exist, **the string dynamics** suggests that the groundstate of a thin string should be a **scalar** object, only higher energy excitations would gain angular momentum.

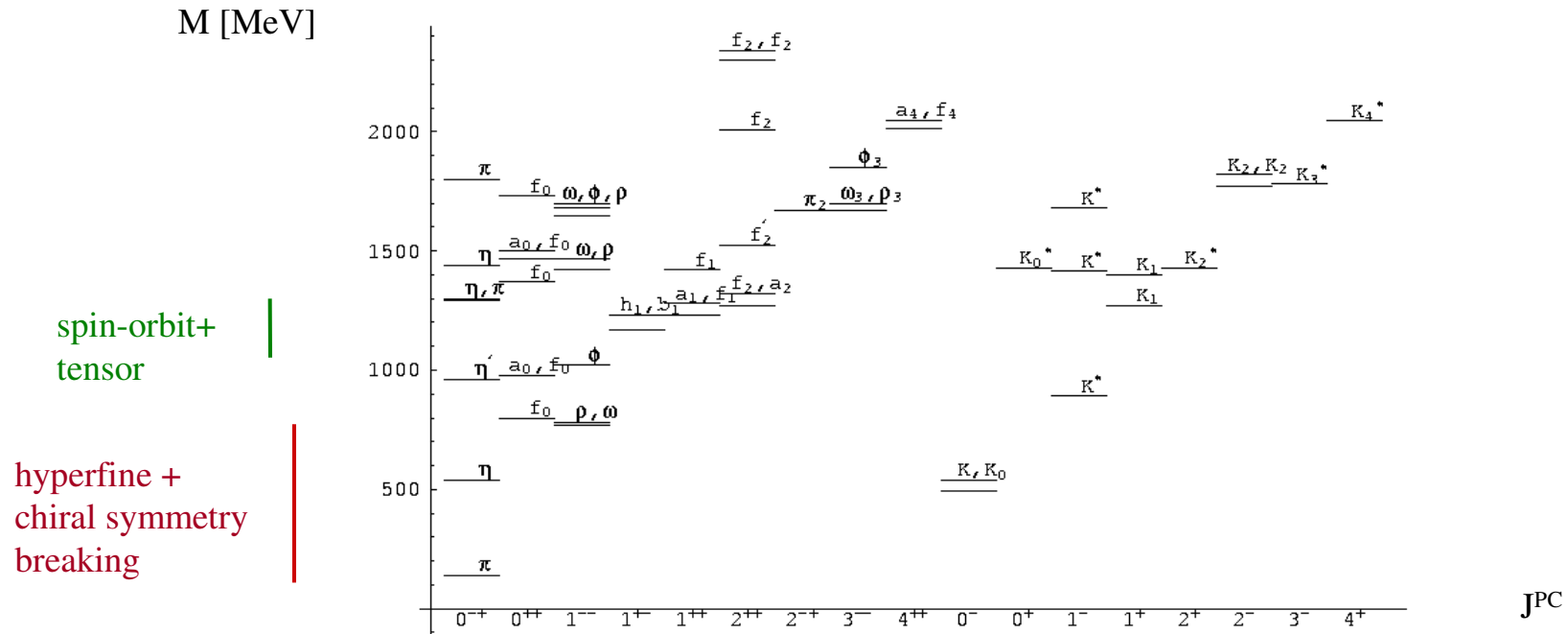
Scalar confinement in Schwinger Dyson Equations

Indeed the confining potential for constituent quarks is probably **scalar**!



Scalar confinement in Schwinger Dyson Equations

Indeed the confining potential for constituent quarks is probably **scalar!**



u, d and s mesons in Part. Data Group

The suppression of the Spin-Orbit potential happens in all families of hadrons. *This is an evidence of non-perturbative QCD.* A short-range vector potential plus a long-range scalar potential cancel the **S.L**.

A. Henriques, B. Kellett, R. Moorhouse, Phys.Lett.B **64**, 85 (1976)

Scalar confinement in Schwinger Dyson Equations

And the NNNNLO study of the static quark potential suggest that many gluon exchange is needed for the linear confinement

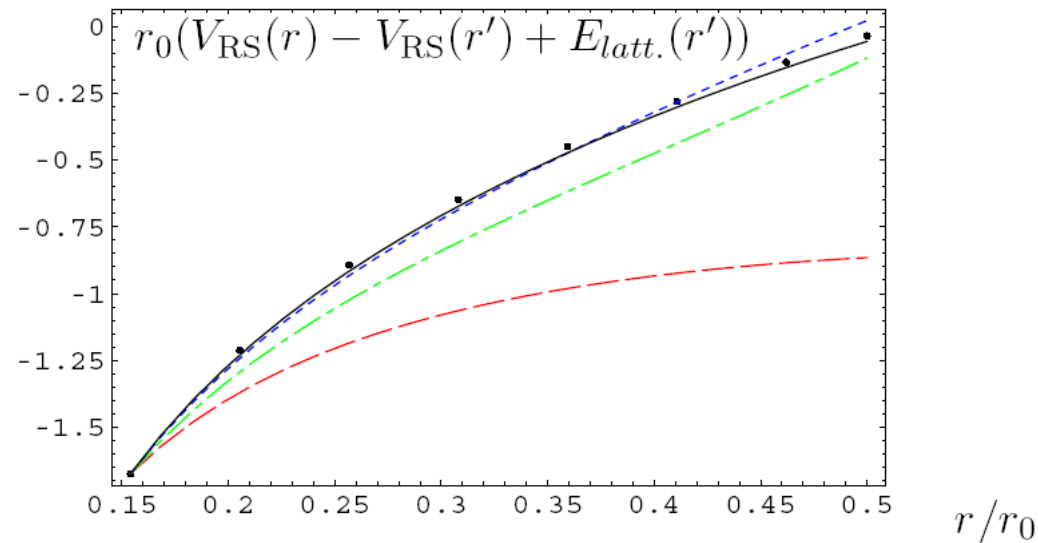
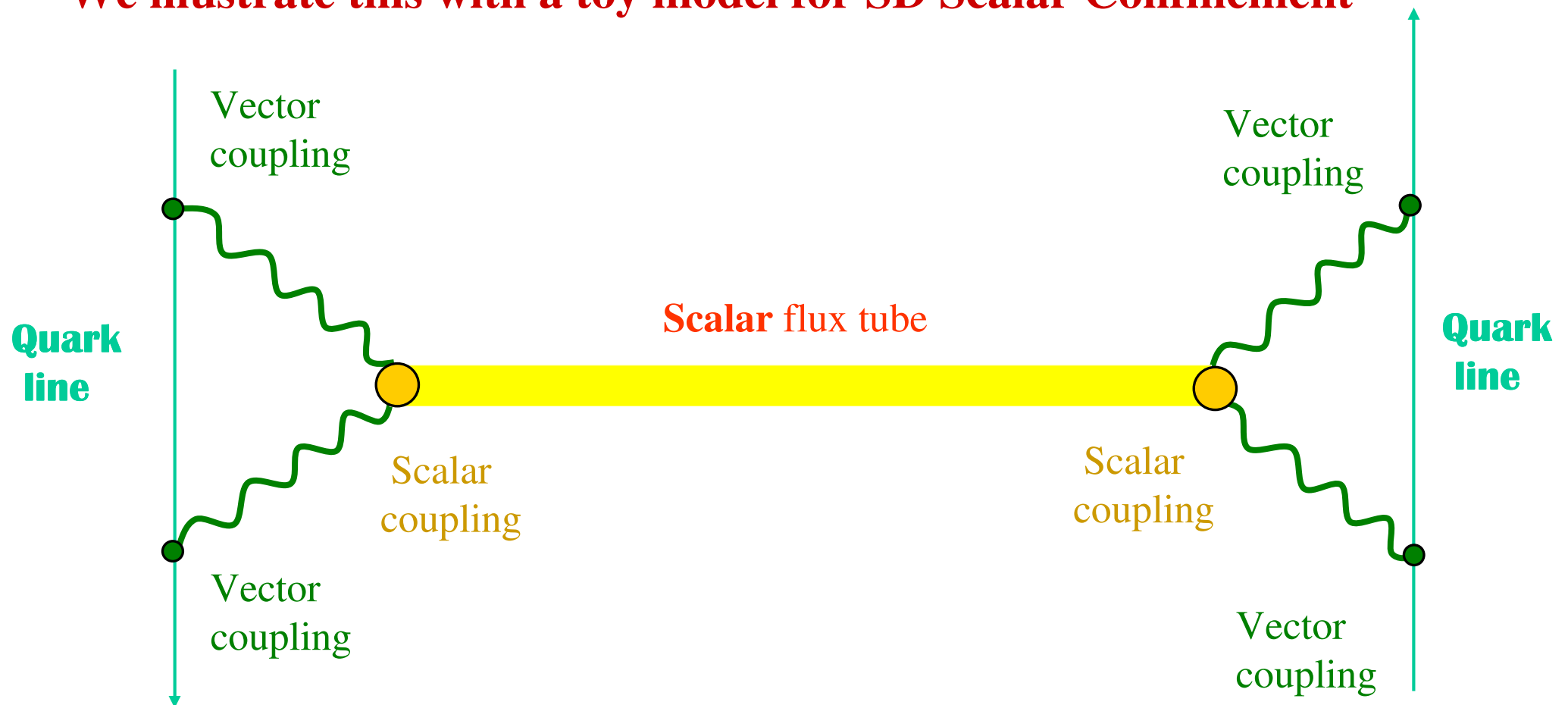


FIG. 14 Plot of $r_0(V_{RS}(r) - V_{RS}(r') + E_{latt.}(r'))$ versus r at tree (dashed line), one-loop (dash-dotted line), two-loop (dotted line) and three-loop level (estimate) plus the RG expression for the US logarithms (solid line) compared with the lattice simulations $E_{latt.}(r)$ (Necco and Sommer, 2002). For the scale of $\alpha_s(\nu)$, we set $\nu = 1/r$. Further, $\nu_f = \nu_{us} = 2.5 r_0^{-1}$, $\Lambda_{\overline{MS}} = 0.602 r_0^{-1}$ (Capitani et al., 1999), and $r' = 0.15399 r_0$. From (Pineda, 2003b).

Scalar confinement in Schwinger Dyson Equations


We illustrate this with a toy model for SD Scalar Confinement



We would like to couple a quark line in a Feynman diagram with a scalar string, using the vector coupling of QCD. This can be performed with a double vertex, similar to the vertices that couple a quark to a gluon ladder in pomeron models.

Scalar confinement in Schwinger Dyson Equations

We remark that in the limit of a vanishing quark mass the double vertex remains a vector coupling, however


$$\gamma^\mu (\not{p} + m) \gamma_\mu = -2 \not{p} + 4m$$
A Feynman diagram representing a double vertex. It consists of a horizontal green line with two black dots at its ends. From each dot, a green arrow points to the left, indicating the direction of the fermion flow.

The scalar coupling is generated by the mass

and we expect that the dynamical generation of a quark mass will also generate a scalar coupling.

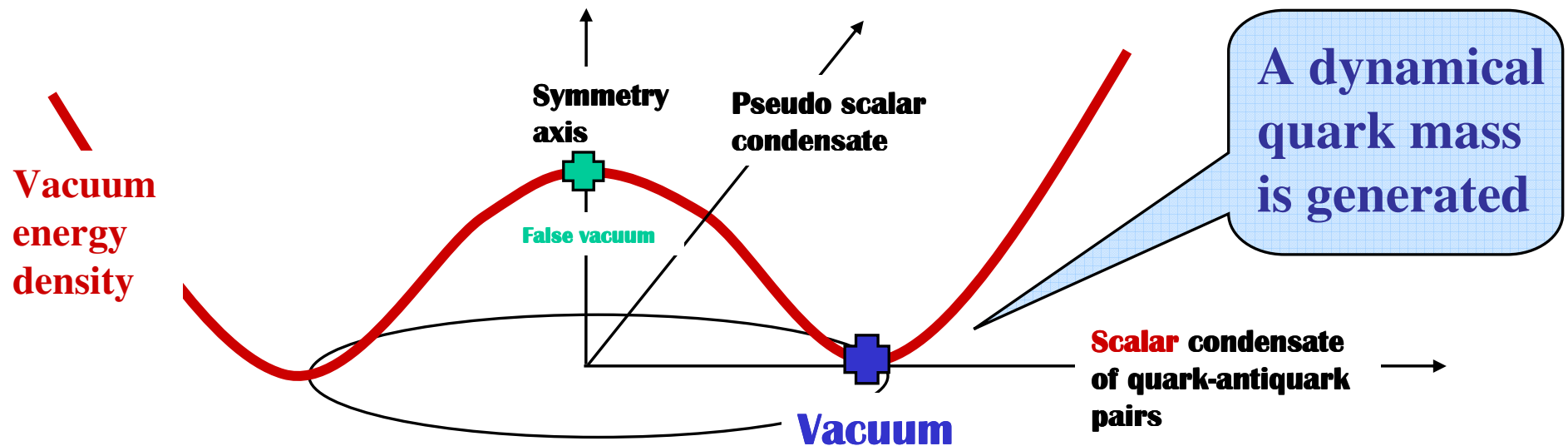
Scalar confinement in Schwinger Dyson Equations

We remark that in the limit of a vanishing quark mass the double vertex remains a vector coupling, however

$$\gamma^\mu (\not{p}+m) \gamma_\mu = -2 \not{p}+4m$$


The scalar coupling is generated by the mass

and we expect that the dynamical generation of a quark mass will also generate a scalar coupling.



Scalar confinement in Schwinger Dyson Equations

More precisely, we use the vertex, that simulates the coupling of a quark line with a scalar string mediated by two vector couplings,

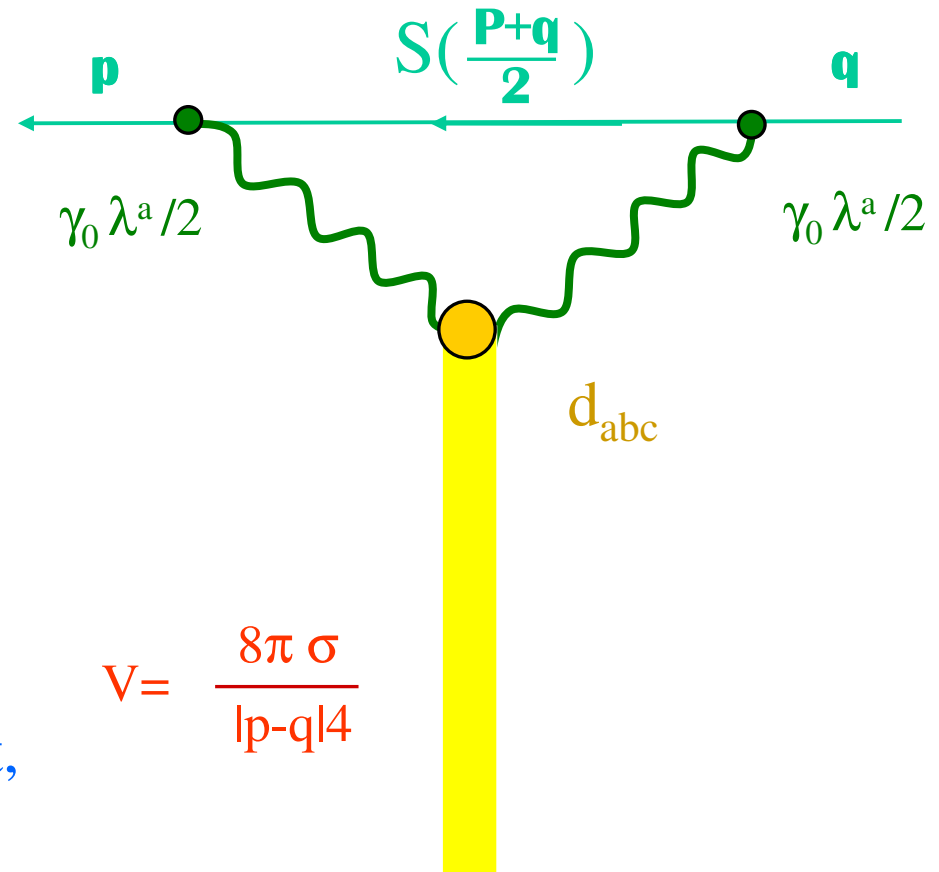
$$\gamma_0 \lambda^a / 2$$

in the colour coupling we choose the symmetric structure function

$$d_{abc}$$

and we reproduce a linear confinement,

$$V = \frac{8\pi \sigma}{|p-q|4}$$



Scalar confinement in Schwinger Dyson Equations

The χ symmetry problem

Vector, chiral
invariant

Scalar, chiral
breaking

The QCD Lagrangian,

$$L_{\text{QCD}} = -\frac{1}{4} F_{\mu\nu}^{(a)} F^{(a)\mu\nu} + i \sum_q \bar{\psi}_q^i \gamma^\mu (D_\mu)_{ij} \psi_q^j - \sum_q m_q \bar{\psi}_q^i \psi_{qi} ,$$
$$F_{\mu\nu}^{(a)} = \partial_\mu A_\nu^a - \partial_\nu A_\mu^a - g_s f_{abc} A_\mu^b A_\nu^c ,$$
$$(D_\mu)_{ij} = \delta_{ij} \partial_\mu + ig_s \sum_a \frac{\lambda_{i,j}^a}{2} A_\mu^a ,$$

is **chiral invariant** in the limit of vanishing quark masses.

$$m_u, m_d \ll m_s < \Lambda_{\text{QCD}} < M_N/3$$

Scalar confinement in Schwinger Dyson Equations

The χ symmetry problem

Vector, chiral
invariant

Scalar, chiral
breaking

The QCD Lagrangian,

$$L_{\text{QCD}} = -\frac{1}{4} F_{\mu\nu}^{(a)} F^{(a)\mu\nu} + i \sum_q \bar{\psi}_q^i \gamma^\mu (D_\mu)_{ij} \psi_q^j - \sum_q m_q \bar{\psi}_q^i \psi_{qi} ,$$
$$F_{\mu\nu}^{(a)} = \partial_\mu A_\nu^a - \partial_\nu A_\mu^a - g_s f_{abc} A_\mu^b A_\nu^c ,$$
$$(D_\mu)_{ij} = \delta_{ij} \partial_\mu + ig_s \sum_a \frac{\lambda_{i,j}^a}{2} A_\mu^a ,$$

is **chiral invariant** in the limit of vanishing quark masses. This is crucial because spontaneous chiral symmetry breaking is accepted to occur in low energy hadronic physics, for the light flavors u, d and s, where,

$$m_u, m_d \ll m_s < \Lambda_{\text{QCD}} < M_N/3$$

This results for instance in the several successful theorems of PCAC.

Scalar confinement in Schwinger Dyson Equations

This is solved with the Mass gap equation

We solve the mass gap equation using the Schwinger-Dyson formalism,

$$S^{-1} = S_0^{-1} - \Sigma, \quad S = i / (\not{p} - m_p)$$

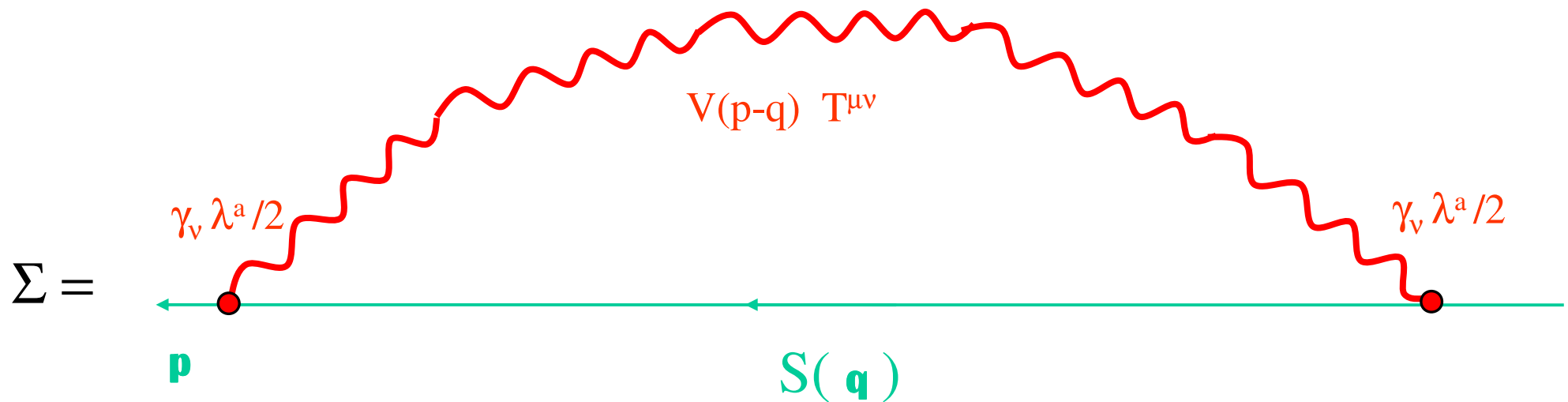
Scalar confinement in Schwinger Dyson Equations

This is solved with the Mass gap equation

We now solve the mass gap equation using the Schwinger-Dyson formalism,

$$S^{-1} = S_0^{-1} - \Sigma, \quad S = i / (\not{p} - m_p)$$

usually the self energy is computed with a 1 loop diagram, using an effective one gluon exchange model (first cumulant),



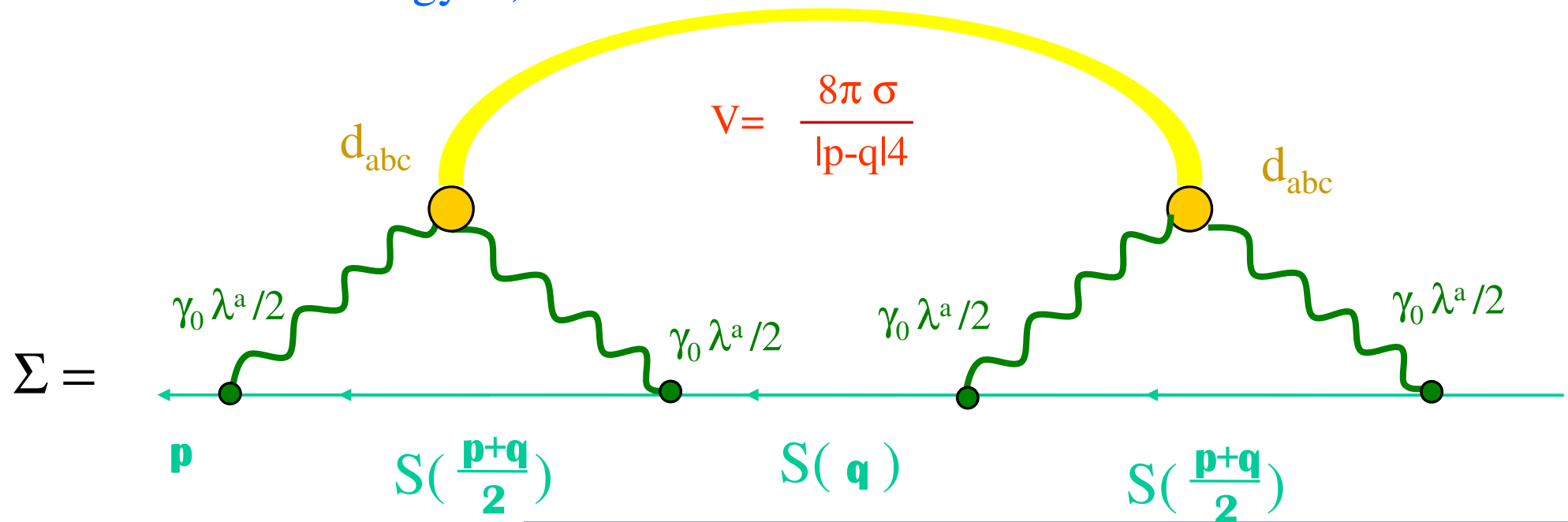
Scalar confinement in Schwinger Dyson Equations

This is solved with the Mass gap equation

We now solve the mass gap equation using the Schwinger-Dyson formalism,

$$S^{-1} = S_0^{-1} - \Sigma, \quad S = i / (\not{p} - m_p)$$

but here the self energy is,



The mass gap equation is a difficult non-linear integral equation,

$$2 \mathbf{q} m_q = \frac{4}{3} \int \frac{d^3 q}{(2\pi)^3} D_k^2 D_q D_p V(|\mathbf{p} - \mathbf{q}|) \left[(k^2 - m_k^2) m_q \mathbf{p} + 2k m_k m_q m_p \hat{\mathbf{k}} \cdot \hat{\mathbf{p}} - \right. \\ \left. (k^2 + m_k^2) q m_p \hat{\mathbf{q}} \cdot \hat{\mathbf{p}} - 2k m_k q p \hat{\mathbf{k}} \cdot \hat{\mathbf{q}} + 2k^2 q m_p \hat{\mathbf{k}} \cdot \hat{\mathbf{q}} \hat{\mathbf{k}} \cdot \hat{\mathbf{p}} \right]$$

$$D_k = \frac{1}{\sqrt{k^2 + m_k^2}}, \quad \mathbf{k} = \frac{\mathbf{p} + \mathbf{q}}{2}$$

that does not converge with the usual methods.

The mass gap equation is a difficult non-linear integral equation,

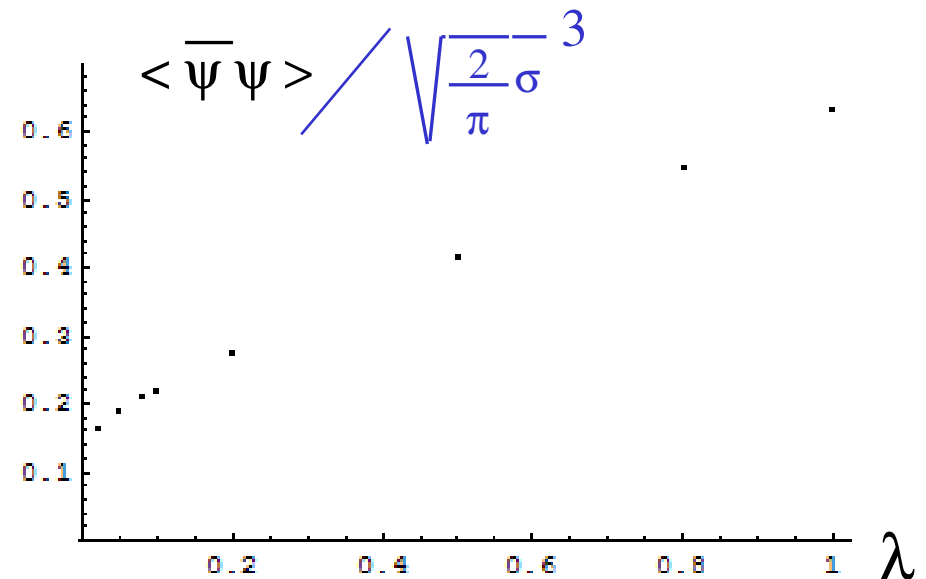
$$2 \mathbf{q} m_q = \frac{4}{3} \int \frac{d^3 q}{(2\pi)^3} D_k^2 D_q D_p V(|\mathbf{p} - \mathbf{q}|) \left[(k^2 - m_k^2) m_q \mathbf{p} + 2k m_k m_q m_p \hat{\mathbf{k}} \cdot \hat{\mathbf{p}} - \right. \\ \left. (k^2 + m_k^2) q m_p \hat{\mathbf{q}} \cdot \hat{\mathbf{p}} - 2k m_k q p \hat{\mathbf{k}} \cdot \hat{\mathbf{q}} + 2k^2 q m_p \hat{\mathbf{k}} \cdot \hat{\mathbf{q}} \hat{\mathbf{k}} \cdot \hat{\mathbf{p}} \right]$$

$$D_k = \frac{1}{\sqrt{k^2 + m_k^2}}, \quad \mathbf{k} = \frac{\mathbf{p} + \mathbf{q}}{2}$$

that does not converge with the usual methods. We develop a method to solve it with a differential equation, using a convergence parameter $\lambda \rightarrow 0$.

We test the convergence of the method computing the quark condensate,

$$\langle \bar{\psi} \psi \rangle \longrightarrow -0.17 \sqrt{\frac{2}{\pi}} \sigma^3$$



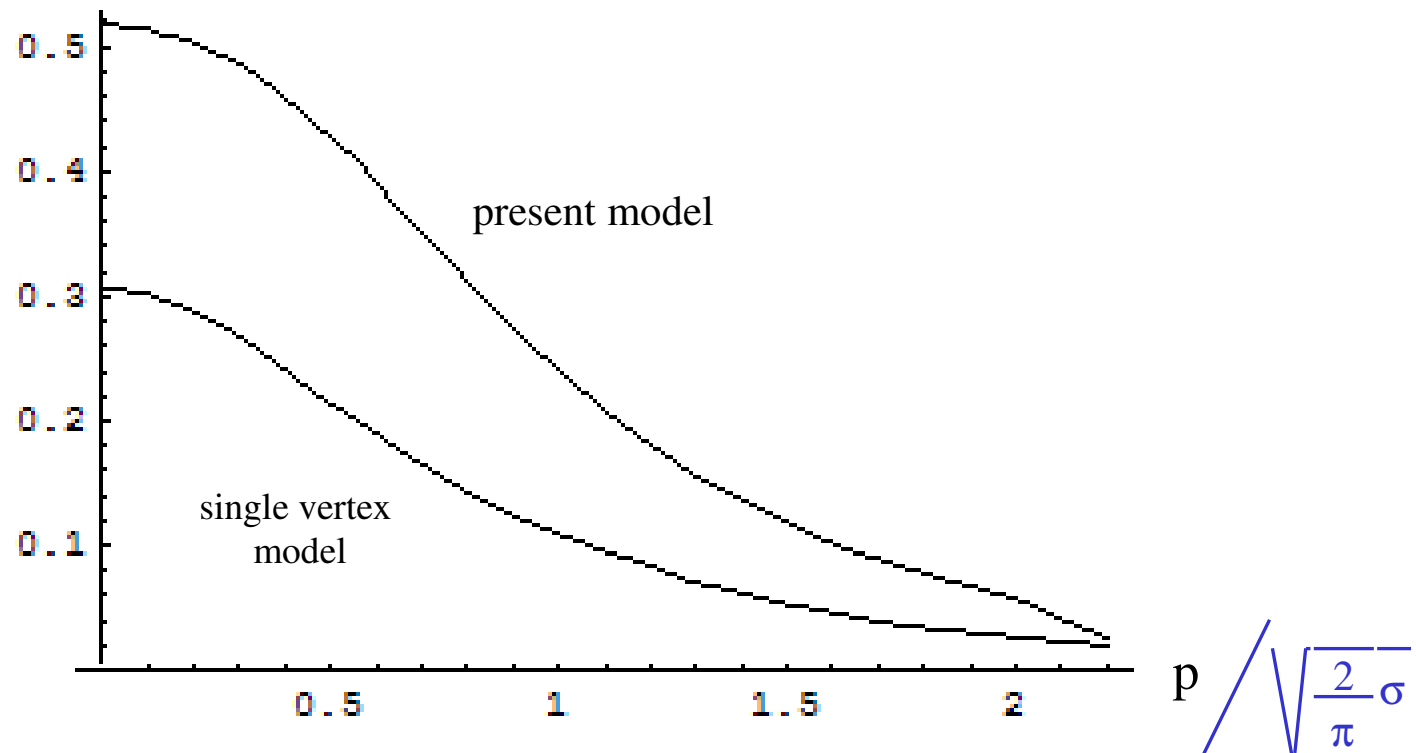
0.16 GeV

Scalar confinement in Schwinger Dyson Equations

We find the solution to the mass gap equation,

P. Bicudo, G. Marques
Phys.Rev. D70, 094047 (2004)

$$m_p \left/ \sqrt{\frac{2}{\pi} \sigma} \right.$$



Partial conclusion and Outlook

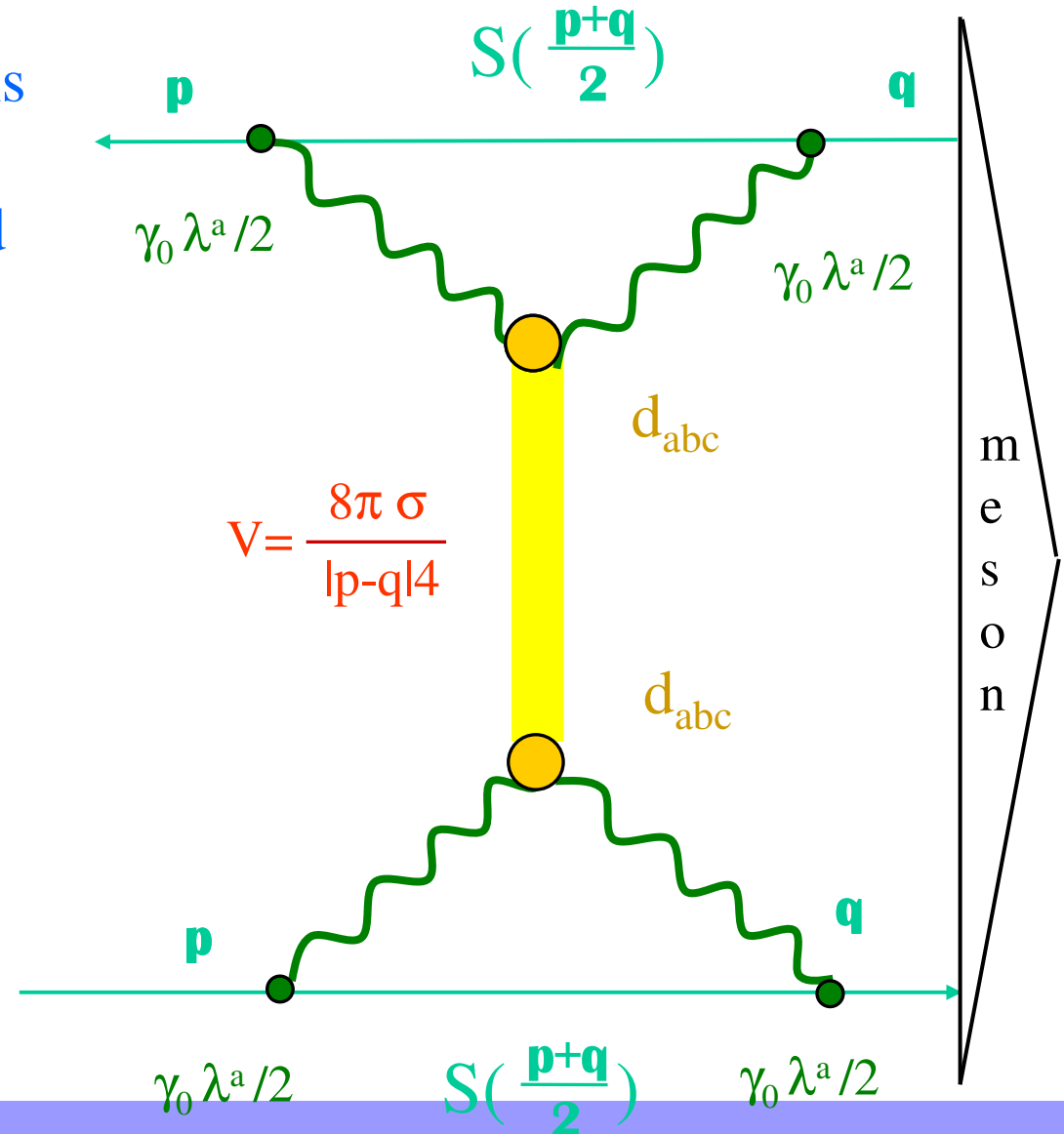
Partial conclusion and Outlook

The large M limit of our toy model remains to be checked

In the Salpeter equation for hadrons in the large m_q limit, which is relevant for charmed and bottomed bound states of quarks, we expand the double vertex potential in spin-tensor potentials,

$$1, \quad (S_1 + S_2) \cdot L_{12}, \\ S_1 \cdot S_2, \quad T_2(S_1, S_2) \cdot T_2(r_{12})$$

and we check that the spin-orbit potential is actually suppressed.



Partial conclusion and Outlook

- The GQQ and GGG are confined by **fundamental** strings, as in a **Type-II** superconductors. We also confirm a scale of $\sim 2 M_{\text{gluon}}$ in the transverse direction of the confining string.
- although simple, this result matters for constituent quark-gluon models, and for our understanding of confinement, where **fundamental strings are scalar objects**.
- In the Schwinger Dyson approach, the One Gluon Exchange, even with dressed vertices and propagator, will not reproduce the confinement as we see in the lattice. So the **SDE still has some way to go** before explaining the static quark confining potential. We illustrate this with a toy model.
- A different way for the SD approach would be to derive **the confining scale** (with the nexus, or the monopole?), and **the gluon mass scale**.